University of Alberta

Parametric Resonance Decay of a Complex Inflaton Field

by

Robert Heath Andrew David Shaw

A thesis submitted to the Faculty of Graduate Studies and Research in partial fulfillment of the requirements for the degree of Master of Science

Department of Physics

Edmonton, Alberta

Fall 1999

National Library of Canada
Acquisitions and Bibliographic Services
395 Wellington Street
Ottawa ON K1A 0N4
Canada

Bibliothèque nationale du Canada
Acquisitions et services bibliographiques
395, rue Wellington
Ottawa ON K1A 0N4
Canada

Your file Votre référence

Our file Notre référence

The author has granted a non-exclusive licence allowing the National Library of Canada to reproduce, loan, distribute or sell copies of this thesis in microform, paper or electronic formats.

L'auteur a accordé une licence non exclusive permettant à la Bibliothèque nationale du Canada de reproduire, prêter, distribuer ou vendre des copies de cette thèse sous la forme de microfiche/film, de reproduction sur papier ou sur format électronique.

The author retains ownership of the copyright in this thesis. Neither the thesis nor substantial extracts from it may be printed or otherwise reproduced without the author's permission.

L'auteur conserve la propriété du droit d'auteur qui protège cette thèse. Ni la thèse ni des extraits substantiels de celle-ci ne doivent être imprimés ou autrement reproduits sans son autorisation.

0-612-47092-X

Canada

University of Alberta

Library Release Form

NAME OF AUTHOR:	Robert Heath Andrew David Shaw
TITLE OF THESIS:	Parametric Resonance Decay of a Complex Inflaton Field
DEGREE:	Master of Science
YEAR THIS DEGREE GRANTED:	1999

Permission is hereby granted to the University of Alberta Library to reproduce single copies of this thesis and to lend or sell such copies for private, scholarly or scientific research purposes only.

The author reserves all other publication and other rights in association with the copyright in the thesis, and except as hereinbefore provided neither the thesis nor any substantial portion thereof may be printed or otherwise reproduced in any material form whatever without the author's prior written permission.

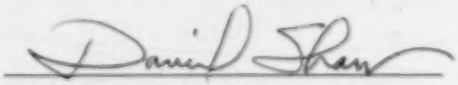

Robert Heath Andrew David Shaw
Apartment 104
10615 81st Avenue NW
Edmonton Alberta T6E 1Y1
CANADA

September 30, 1999

I did not have sexual relations with that woman...

William Jefferson Clinton

University of Alberta

Faculty of Graduate Studies and Research

The undersigned certify that they have read, and recommend to the Faculty of Graduate Studies and Research for acceptance, a thesis entitled **Parametric Resonance Decay of a Complex Inflaton Field** submitted by **Robert Heath Andrew David Shaw** in partial fulfillment of the requirements for the degree of Master of Science

B. A. Campbell (Supervisor)

M. Legaré (External)

D. N. Page

H. S. Sherif

DATE: 29/09/99

To

Don, Janis, and Meredith Shaw

Abstract

There have been many recent studies of parametric resonance decay of oscillating real homogeneous cosmological scalar fields, primarily within the context of inflaton decay and (p)reheating. However, many realistic models of particle cosmology, such as supersymmetric ones, inherently involve complex scalar fields. In this thesis, a treatment of parametric resonance for the decay of homogeneous complex scalar fields is given, analyzing properties of the resonance in the presence of out of phase oscillations of the real and imaginary components. For phase-invariant coupling of the driving parameter field to the decay field, and Mathieu type resonance, an explicit mapping from the complex resonance case to an equivalent real case with shifted resonance parameters is derived. In addition, the consequences of the complex field case as they apply to "instant preheating," the explosive decay of non-convex potentials, and resonance in an expanding Friedman-Robertson-Walker universe are considered.

Preface

The results in this thesis were obtained over the course of the author's M.Sc. program at the University of Alberta between 1997 and 1999. The presentation of this work given here is in accordance with the "Paper Format" regulations of the Faculty of Graduate Studies and Research of the University of Alberta, and is based on the following submitted paper:

- Rouzbeh Allahverdi, R. H. A. David Shaw, and Bruce Campbell, *Parametric Resonance for Complex Fields*, submitted to Physics Letters B, preprints: Alberta-Thy 14-99, CERN-TH-99-182, hep-ph/9909256.

Acknowledgements

Mark Twain once said: "I have never let my schooling interfere with my education." I have taken these words to heart—the past two years have been a time of significant personal growth in my life. I have learned many lessons; most were learned outside of the classroom, often from the most unlikely of teachers. In what follows, I will try to single out those who have had the greatest impact on me.

First and foremost, I wish to thank my supervisor, Bruce Campbell. Over the course of my program, he has provided invaluable career advice and guidance. Bruce tailored my M.Sc. thesis topic to my particular interests and strengths, while at the same time retaining its topicality and relevance. I have learned a great deal in courses which I have taken from him; he has time and again proven himself to be an excellent lecturer. Finally, he encouraged me to develop an ability to work independently, which will serve me well in my future endeavours.

I would also like to thank the other members of my committee: Helmy Sherif, Don Page, and Martin Legaré, especially for the patience which they have displayed in taking on a thesis defence on such short notice. I have learned much from these gentlemen in various courses over the years. Helmy, in particular, is recognized for his advice and wisdom.

Bruce's other graduate students, Rouzbeh Allahverdi and Kirk Kaminsky, also deserve special recognition. Rouzbeh has been a great source of information and insight, and I have benefitted much from my collaborations with him. The debates I have had with Kirk regarding the relative merits of our respective research topics has been a very useful process—I greatly appreciate his sober judgment and his realism.

The Natural Sciences and Engineering Research Council of Canada is recognized for its financial support throughout the course of my Master's program

here at the University of Alberta—research is so much easier on a full stomach.

By "coincidence," if you will, both my mother and my father will also receive M.Sc. degrees at Fall Convocation. I thank my parents for setting the challenge of this simultaneous convocation—it has proved to be a tremendous motivator in the past few weeks.

There are many other graduate students who have influenced my stay in one way or another. Special thanks to Adam Baig, Kristen Beaty, Ian Blokland, Andrew Brown, Norm Buchanan, Kipp Cannon, Jim Fuite, Jeremy Gallop, Kamran Kaveh, Philip Kayal, Charlie Kirkby, Eugene Kotik, Marko Mah, Dinesh Singh, and Patrick Sutton. They have helped to keep me sane through the ups and downs of my program.

Life after the inevitable all-nighters was made much more bearable by the Undergraduate Physics Society and the Mathematical Sciences Society, who maintain lounges with comfortable couches and quasi-nutritious food. I have enjoyed my interactions with the undergraduate student members of both clubs, and extend my gratitude.

In closing, I would like to thank Gail Daily. In my brief encounters with her, I have learned much about my own personal biases and the human condition. In the process, I have been forced to rethink or overthrow many of the convenient stereotypes which allow society to insulate itself from the sometimes bitter reality of our world. I believe I am much the better for it as a result.

I look forward to the challenges which the Ph.D. program will bring.

Thanks again to one and all.

Dave

Table of Contents

Abstract

Preface

Acknowledgements

Table of Contents

List of Tables

List of Figures

1 Why Inflation? 1

1.1 Introduction 1

1.2 The "Standard Model" of Cosmology 2

1.2.1 Introduction 2

1.2.2 A Tour of the FRW Universe 2

1.2.3 Three Problems 7

1.3 Inflation 13

1.3.1 Introduction 13

1.3.2 Historical Overview 13

1.3.3 Chaotic Inflation in a Nutshell 17

1.3.4 Three Problems Revisited 22
1.4 Conclusion 23
References 24

2 Preheating for Dummies **28**
2.1 Introduction 28
2.2 The Perturbative Case: Reheating 29
2.2.1 The Decay of the Inflaton 29
2.2.2 Particle Production 32
2.3 Elementary Preheating—$m^2\phi^2$ Models 36
2.3.1 Introduction 36
2.3.2 Breakdown of Perturbation Theory 36
2.3.3 Narrow- versus Broad-Band Resonance 42
2.3.4 Stochastic Resonance 48
2.3.5 Backreaction and Rescattering 60
2.3.6 Superheavy Particle Production 61
2.4 Conformal $\lambda\phi^4$ Models 63
2.4.1 Introduction 63
2.4.2 Evolution of the Inflaton Field 63
2.4.3 Conformal Variables 64
2.4.4 Quantum Fluctuations of the ϕ and χ Fields 67
2.4.5 The Stability Diagram in Conformal Theories 70
2.5 "Instant Preheating" 75
2.5.1 Introduction 75
2.5.2 Instant Preheating: The Basic Concept 75
2.5.3 A Simple Model 77
2.5.4 Quintessence and Instant Preheating 82
2.6 Preheating for Fermions 84

2.6.1 Introduction 84
2.6.2 Quantum Fluctuations for a Fermion Field ψ 84
2.6.3 Fermionic Resonance 87
2.7 Conclusion 93
References 95

3 Parametric Resonance for Complex Fields **99**
3.1 Introduction 99
3.2 Complex Mathieu Resonance 104
3.3 Parameter Domain For Broad-Band Resonance 110
3.4 Complex Resonance in "Instant Preheat" 112
3.5 Non-Convex Potentials 113
3.6 Other Couplings 114
3.7 Cosmic Expansion and Complex Resonance 115
3.8 Conclusions 117
References 120

4 Conclusions **123**

A Notation and Sign Conventions **125**

B Source Code **126**
B.1 Introduction 126
B.2 A Typical Program 126
B.2.1 Libraries 128
B.2.2 Parameters and Macros 128
B.2.3 Function Prototypes 131
B.2.4 Global Variables 133
B.2.5 Error Handling 134

B.2.6 Memory Allocation and Deallocation 134
B.2.7 The Main Routine 136
B.2.8 ODE Integration Routines 139
B.2.9 Matrix Algebra 152
B.2.10 Root Finding Algorithms 155
B.2.11 User-Defined System Equations 158
B.2.12 Output Routines 161
References 162

List of Tables

2.1 Typical values of various system variables for a system undergoing stochastic resonance. 55

List of Figures

2.1 Oscillations of the scalar field ϕ after inflation in the theory $\frac{m^2\phi^2}{2}$. 30

2.2 The Mathieu equation stability diagram, showing the first seven instability bands. 38

2.3 Narrow parametric resonance for the field χ in the theory $\frac{m^2\phi^2}{2}$ in Minkowski space for $q \sim 0.1$. 46

2.4 Broad parametric resonance for the field χ in Minkowski space for $q \sim 2 \times 10^2$ in the theory $\frac{m^2\phi^2}{2}$. 47

2.5 Early stages of parametric resonance in the theory $\frac{m^2\phi^2}{2}$ in an expanding universe with scale factor $a \sim t^{2/3}$ for $g = 5 \times 10^{-4}$, $m = 10^{-6} M_P$. 57

2.6 The same process as in Figure 2.5 over a longer period of time. . . 58

2.7 The same process as in Figures 2.5 and 2.6 over a longer period of time. 59

2.8 Oscillations of the field ϕ after inflation in the theory $\frac{\lambda\phi^4}{4}$. 65

2.9 Resonant production of particles in the conformal $\frac{\lambda}{4}\phi^4$ theory. . . 73

2.10 The stability diagram for the Lamé equation. 74

2.11 The occupation number n_k for fermions in $\lambda\phi^4$-inflation as a function of time τ. 87

2.12 The envelope functions F_k for the occupation number n_k, showing bands of fermion excitation in $\lambda\phi^4$-inflation 89

2.13 The resonance excitation band of fermions in $\lambda\phi^4$-inflation for $q \equiv \frac{h^2}{\lambda} = 1.0$. 91

2.14 As in Figure 2.13, the resonance excitation band in $\lambda\phi^4$-inflation for $q \equiv \frac{h^2}{\lambda} = 100.0$. 92

2.15 The log of the period of modulation $\frac{\pi}{\nu_k}$ (in units of T) as a function of κ^2 93

3.1 Distortion of the first resonance band on the Mathieu equation stability diagram with increasing f. 118

3.2 Distortion of the first seven bands on the Mathieu equation stability diagram with increasing f. 119

Chapter 1

Why Inflation?

1.1 Introduction

The idea that our current hot Friedman-Robertson-Walker universe was preceded by an inflationary phase, in which the universe was dominated by scalar field dynamics, is very popular with cosmologists. In most inflationary models, inflation is driven by a single real scalar field, ϕ, called an inflaton. In this thesis, we will investigate the ramifications of replacing the conventionally real scalar inflaton field with a complex one, examining in particular the manifestations of out of phase oscillations in the real and imaginary components of the field on the parametric resonance decay of the inflaton field. Before beginning, however, it may be instructive to consider why inflationary cosmology is of interest in the first place; therefore, this chapter shall give a brief overview of our current cosmological models and our motivations for studying them.

1.2 The "Standard Model" of Cosmology

1.2.1 Introduction

The most successful cosmological model to date is generally agreed to be the hot big bang model; indeed, it has been so successful that it has been dubbed the "standard model of cosmology" by Weinberg [1], after the similarly named Standard Model in particle physics. The standard cosmological model is built upon the fundamental assumption of the cosmological principle [1], which states that the universe is both homogeneous and isotropic. The dynamics of universes which possess both these qualities were initially studied in the 1920s and 1930s by A. Friedman [2], H. P. Robertson [3], and A. G. Walker [4]. Let us therefore review the dynamics of Friedmann-Robertson-Walker (or FRW) universes and some of the problems associated with these models.

1.2.2 A Tour of the FRW Universe

Basic Dynamics

Let us begin with the spatially maximally symmetric FRW metric in co-moving coordinates,

$$ds^2 = dt^2 - a^2(t)\left[\frac{dr^2}{1-kr^2} + r^2\left(d\theta^2 + \sin^2\theta d\phi^2\right)\right], \tag{1.1}$$

where $a(t)$ is the cosmological scale factor and k is the three-space curvature constant ($k = +1,\ 0,\ -1$ for a closed, spatially flat, or open universe, respectively.) Let us also assume that the energy-momentum tensor takes the form of a perfect fluid,

$$T_{\mu\nu} = -pg_{\mu\nu} + (p+\rho)u_\mu u_\nu, \tag{1.2}$$

where $g_{\mu\nu}$ is the FRW metric (1.1), p is the isotropic pressure, ρ is the energy density, and $u_\mu = (1,0,0,0)$ is the velocity vector for the isotropic fluid. Then

Einstein's equation (see Appendix A for sign conventions) takes the form

$$R_{\mu\nu} - \frac{1}{2}g_{\mu\nu}\mathcal{R} = \kappa^2 T_{\mu\nu} + \Lambda g_{\mu\nu}, \tag{1.3}$$

where $\mathcal{R} = R^{\mu}_{\mu}$ is the curvature scalar, Λ is the cosmological constant, and $\kappa^2 = 8\pi G_N = 8\pi/M_P^2$ ($M_P = 1.22 \times 10^{19}$ GeV is the Planck mass).

Let us examine (1.3) in more detail. From the 0-0 component, we obtain the Friedmann equation, which expresses the Hubble parameter H as

$$H^2 \equiv \left(\frac{\dot{a}}{a}\right)^2 = \frac{1}{3}\kappa^2\rho - \frac{k}{a^2} + \frac{1}{3}\Lambda, \tag{1.4}$$

while the i-i components, along with (1.4), give us

$$\left(\frac{\ddot{a}}{a}\right) = \frac{1}{3}\Lambda - \frac{1}{6}\kappa^2(\rho + 3p). \tag{1.5}$$

Using (1.4) and (1.5) together, or, alternatively, from the fact that $T^{\mu\nu}{}_{;\nu} = 0$, we have

$$\dot{\rho} = -3H(\rho + p). \tag{1.6}$$

The preceding three equations form the basis of the FRW model.

Equations of State

Many different scenarios for the evolution of the universe may be represented by equations of state of the form

$$p = (\gamma - 1)\rho \tag{1.7}$$

for various choices of the parameter γ. Assuming this simple form for the equation of state allows us to determine two very important results. First, let us substitute (1.7) into (1.6)—we see immediately that

$$\rho \sim a^{-3\gamma}. \tag{1.8}$$

Next, we substitute this result into (1.4). For a small enough and $\gamma > \frac{2}{3}$, we may neglect the contributions to H from k and Λ, giving

$$a(t) \sim t^{\frac{2}{3\gamma}}, \tag{1.9}$$

except, of course, for the special case where $\gamma = 0$.

Let us now consider a few special cases of the equation of state. For example, at early times, the universe was dominated by radiation. In this case, we have the equation of state $p = \frac{\rho}{3}$, so $\gamma = \frac{4}{3}$, and from (1.7) we have

$$\rho \sim a^{-4}, \tag{1.10}$$

$$a(t) \sim t^{\frac{1}{2}}. \tag{1.11}$$

We may also consider the behaviour of a matter (dust) dominated universe. In this case, the equation of state is $p = 0$, meaning $\gamma = 1$, leading to

$$\rho \sim a^{-3}, \tag{1.12}$$

$$a(t) \sim t^{\frac{2}{3}}. \tag{1.13}$$

Finally, let us consider the case of a universe dominated by vacuum energy. In this case, we have $\gamma = 0$, giving $p = -\rho$ for the equation of state, and

$$\rho \sim \text{constant}, \tag{1.14}$$

$$a(t) \sim \exp(H_0 t). \tag{1.15}$$

This particular behaviour will play an important role in the formulation of our inflationary models in the next section.

The Critical Density

In the special case where $\Lambda = 0$, we may define a critical energy density ρ_c,

$$\rho_c = \frac{3H^2}{\kappa^2}, \tag{1.16}$$

such that when $k = 0$, we have $\rho = \rho_c$. In terms of the present value of the Hubble parameter H_0, we have

$$\rho_c = 1.88 \times 10^{-29} h_0 \text{ g cm}^{-3}, \tag{1.17}$$

where

$$h_0 = \frac{H_0}{100 \text{ km Mpc}^{-1} \text{ s}^{-1}}. \tag{1.18}$$

Then we may define the cosmological density parameter,

$$\Omega \equiv \frac{\rho}{\rho_c}, \tag{1.19}$$

allowing us to rewrite the Friedman equation (1.4) as

$$(\Omega - 1)H^2 = \frac{k}{a^2}, \tag{1.20}$$

such that $k = 0, +1, -1$ corresponds to $\Omega = 1$, $\Omega > 1$, and $\Omega < 1$, respectively. Equation (1.5) may also be rewritten in terms of a deceleration parameter q,

$$q \equiv -\frac{\ddot{a}/a}{H^2} = \frac{1}{2}\Omega\left(1 + \frac{3p}{\rho}\right) = \frac{1}{2}\Omega(3\gamma - 2). \tag{1.21}$$

Generally accepted observational limits on h_0 and Ω_0 (subscripts denote the present values) are [5]

$$0.4 \leq h_0 \leq 1, \quad 0.1 \lesssim \Omega_0 \leq 4, \tag{1.22}$$

although recent supernova observations [6] tend to suggest much more stringent limits (and the existence of a significant positive cosmological constant Λ.)

An additional constraint arises when one considers the age of the universe. Let us consider the time elapsed as a function of the scale function $t(a)$. Then the age of the universe t_u is given by

$$t_u \equiv \int_0^{a_0} \frac{dt}{da} da = \int_0^{a_0} \frac{da}{\dot{a}}. \tag{1.23}$$

We therefore wish to obtain an expression for $\dot{a}$ in terms of the present day values of the cosmological parameters H_0 and Ω_0. To this end, taking $\Lambda = 0$, we multiply the Friedman equation (1.4) by a factor of $\frac{a^2}{a_0^2}$, obtaining

$$\frac{\dot{a}^2}{a_0^2} = \frac{\kappa^2}{3}\rho\left(\frac{a^2}{a_0^2}\right) - \frac{k}{a_0^2}. \tag{1.24}$$

Using (1.8), we may rewrite ρ in terms of ρ_0, yielding

$$\frac{\dot{a}^2}{a_0^2} = -\frac{k}{a_0^2} + \frac{\kappa^2}{3}\rho_0\left(\frac{a}{a_0}\right)^{-3\gamma+2}. \tag{1.25}$$

Replacing $\frac{k}{a_0^2}$ via (1.20) gives

$$\frac{\dot{a}^2}{a_0^2} = -H_0^2(\Omega_0 - 1) + \frac{\kappa^2}{3}\rho_0\left(\frac{a}{a_0}\right)^{-3\gamma+2}. \tag{1.26}$$

We now express the density ρ_0 in terms of the density paramter Ω_0 and collect terms:

$$\dot{a} = a_0 H_0\left[1 - \Omega_0 + \Omega_0\left(\frac{a}{a_0}\right)^{-3\gamma+2}\right]^{\frac{1}{2}}. \tag{1.27}$$

Therefore, following a change of variables $x = \frac{a}{a_0}$, we find that the age of the universe is given by

$$t_u = \frac{1}{H_0}\int_0^1 \frac{dx}{(1 - \Omega_0 + \Omega_0 x^{-3\gamma+2})^{-\frac{1}{2}}}, \tag{1.28}$$

which gives a reasonable estimate provided $\gamma > \frac{2}{3}$. If we set the requirement that $t_u \geq 10$ Gyr, then we are constrained to have $\Omega_0 h_0^2 \leq 1.1$.

Time vs. Temperature

Recall that the energy density of a black body (in units where $\hbar = c = k_B = 1$) is given by

$$\rho_\gamma = \frac{\pi^2}{15}T^4. \tag{1.29}$$

Now, the early universe was radiation dominated, so the total density in radiation must include contributions from all relativistic particle species, giving

$$\rho = \frac{\pi^2}{30} N(T) T^4, \tag{1.30}$$

where

$$N(T) = \sum_B g_B \left(\frac{T_B}{T}\right)^4 + \frac{7}{8} \sum_F g_F \left(\frac{T_F}{T}\right)^4. \tag{1.31}$$

In the latter expression, the sums are taken over all relativistic boson (fermion) degrees of freedom $g_{B(F)}$ with temperature $T_{B(F)}$ relative to the photon temperature T. (Such a distinction between different temperatures is necessary, as neutrinos or other particles can drop out of equilibrium [7], i.e., $T_{B(F)} < T$.)

It can be shown that during this early radiation dominated epoch, one can relate the age of the universe, t, to its temperature, T, by the expression

$$t = \left[\frac{45}{2\pi^2 \kappa^2 N(T)}\right]^{\frac{1}{2}} T^{-2}, \tag{1.32}$$

which simplifies to

$$tT^2 = \frac{2.4}{\sqrt{N(T)}}, \tag{1.33}$$

where T is in units of MeV and t is in seconds.

1.2.3 Three Problems

The standard model of cosmology is very successful in explaining many of the features observed in the universe. Examples of these successes include the observation [8] of the 2.73 K cosmic microwave background radiation (CMBR) and agreement with observations on the primordial abundances of the light elements [9].

Unfortunately, the theory is not without its shortcomings. In this subsection, we will examine three of the most well-known problems with the standard

cosmological picture. While these problems do not invalidate the model per se, their "solution" within the model requires in general either a high degree of fine-tuning or a good deal of lucky coincidences, neither of which appeals to most cosmologists.

The Flatness Problem

It is strange that we have a fairly restrictive bound on Ω_0 despite the fact that we are still unaware of the sign of the curvature term k in the Friedman equation (1.4). In fact, unless $k = 0$ exactly, then for $\rho \gg \Lambda$ and $\gamma > \frac{2}{3}$, Ω evolves away from the point $\Omega = 1$ with time [10]. For $\Lambda = 0$, we may rewrite (1.20) as

$$\Omega = \frac{k}{a^2 H^2} + 1. \tag{1.34}$$

Recalling our earlier discussions on equations of state, let us take our energy density to be

$$\rho = A a^{-3\gamma}, \tag{1.35}$$

giving

$$a^2 H^2 = \frac{1}{3}\kappa^2 A a^{2-3\gamma} - k; \tag{1.36}$$

hence,

$$\Omega = \frac{k}{\frac{1}{3}\kappa^2 A a^{2-3\gamma} - k} + 1. \tag{1.37}$$

Whenever $\gamma > \frac{2}{3}$, $\Omega = 1$ is an instability point of (1.37). It is clear from the above expression that $\Omega \to 1$ for small a. As a increases, however, there are two distinct possibilities. If $k = -1$, $\Omega \to 0$ and $a \to \infty$; if $k = +1$, on the other hand, $\Omega \to \infty$ as $a \to a_{\max} = \left(\frac{3}{\kappa^2 A}\right)^{\frac{1}{2-3\gamma}}$.

This all seems innocuous enough, but let's look a little closer. Let us rewrite (1.6) as

$$a^3 \frac{dp}{dt} = \frac{d}{dt}[a^3(\rho + p)]. \tag{1.38}$$

Introducing the entropy density $s = \frac{\rho+p}{T} = \frac{dp}{dT}$, then for $\gamma \neq 0$, we may rewrite this as

$$\frac{d}{dt}(a^3 s) = 0. \tag{1.39}$$

Now, for a radiation dominated gas, we have $s \sim T^3$ and $a \propto T^{-1}$. Therefore, for an adiabatically expanding universe, the quantity $\hat{k} = \frac{k}{a^2T^2}$ is a dimensionless constant. Taking the limit in (1.22) and applying it to the Friedman equation (1.20), we obtain the constraint

$$\hat{k} = \frac{k}{a^2T^2} = (\Omega_0 - 1)\frac{H_0^2}{T_0^2} < 2 \times 10^{-58}. \tag{1.40}$$

This limit on $\hat{k}$ gives us an initial condition for our model. The question is, what physical processes restricted $\hat{k}$ to such an extremely small value?

Naively reasoning, we might argue from naturalness that $\hat{k} \sim \mathrm{O}(1)$. However, a universe started off with these conditions becomes curvature dominated at $T \sim 0.1 M_{\bar{P}}$. If $k = +1$, the universe would recollapse at this point. Even setting $\hat{k}$ as small as $\mathrm{O}(10^{-40})$ is insufficient—the universe becomes curvature dominated at the ripe old age of $\mathrm{O}(10^{-2})$ s. As can be seen, (1.40) imposes a very tight constraint on our initial conditions.

Alternatively, one may express the problem in terms of the proximity of Ω to 1 at any given time. At early times, the dominant contribution to H is the thermal energy density. Therefore, we may write $H^2 \simeq \frac{1}{3}\kappa^2\rho = \frac{1}{90}\kappa^2\pi^2 N T^4$. This gives us the result

$$|\Omega - 1| \simeq \frac{90 M_P^2}{8\pi^3 N T^2}\hat{k}. \tag{1.41}$$

Once again, we are forced to require very special initial conditions—for $T \simeq$ 1 MeV, $|\Omega - 1| \lesssim 10^{-15}$, while at the GUT scale $T \simeq 10^{15}$ GeV, $|\Omega - 1| \lesssim 10^{-52}$.

In essence, the fact that Ω is so close to 1 is only a problem because the universe is so old. Simply speaking, the natural time scale for cosmology is the Planck time, 10^{-43} s, but the initial parameters of our model were so precisely

fine-tuned that the universe has survived on the order of 10^{60} Planck times without recollapsing or becoming curvature dominated.

The Horizon Problem

Because we are working with a homogeneous and isotropic universe, we have seen that all physical length scales grow as the scale factor $a(t) \sim t^{\frac{2}{3\gamma}}$. However, causality implies the existence of particle horizons $d_H \sim t$, where $d_H(t) \sim t$ is the maximal distance that light can travel from the co-moving position of some observer from some initial time to the time t. The fact that $\gamma > \frac{2}{3}$ means that length scales originally outside of our horizon eventually become part of our observable universe; therefore, we expect to see anisotropies on large scales [11], unless some mechanism exists which forces these anisotropies to be small.

For example, consider the microwave background. The photons we observe today have been decoupled since recombination (the formation of atomic hydrogen, which rendered the universe approximately electrically neutral), which occured at about $T_d \sim 4000$ K. At that point, the horizon volume of the universe was $V_d \propto t_d^3$, where t_d is the age of the universe at recombination. Taking the present age of the universe to be $t_0 = 15$ Gyr, we can calculate

$$t_d = t_0 \left(\frac{T_0}{T_d}\right)^{\frac{3}{2}} \sim 3 \times 10^5 \text{ yr}. \tag{1.42}$$

Let us now determine the portion of the universe at decoupling, $V_0(t_d)$, which has expanded to the present visible universe today. Our present horizon volume $V_0 \propto t_0^3$ scales back in time as $V_0(t_d) \propto V_0(T_0/T_d)^3$. We can now compute the ratio

$$\frac{V_0(t_d)}{V_d} \propto \frac{V_0}{V_d}\frac{T_0^3}{T_d^3} \propto \frac{t_0^3}{t_d^3}\frac{T_0^3}{T_d^3} \sim 4 \times 10^4, \tag{1.43}$$

which corresponds to the number of regions which were causally distinct at decoupling and are now included within our horizon volume.

However, the CMBR is highly isotropic on large scales, with COBE measurements giving $\Delta T/T \lesssim \mathrm{O}(10^{-5})$ [12]. Thus, the horizon problem deals with the question of how 10^5 causally disconnected regions at recombination somehow all conspired with each other to have the same temperature to within one part in 10^5.

Rampaging Monopoles

The monopole problem arises when one considers the implications of certain grand unified theories (or GUTs) on cosmologies. GUTs are extremely attractive from a theoretical standpoint [13], as they provide a viable method for producing a baryon asymmetry; however, they also lead to the production of magnetic monopoles.

Monopoles are produced [14] when a simple group—$SU(5)$, for example—is broken down to a gauge group containing a $U(1)$ factor—such as the Standard Model's $SU(3) \otimes SU(2) \otimes U(1)$). The mass of a monopole produced in this manner will be

$$M_m \sim \frac{M_X}{\alpha_G} \sim 10^{16}\ \mathrm{GeV}, \tag{1.44}$$

where M_X is the mass of the X leptoquark and α_G is the unified coupling constant. Essentially, monopoles are produced because when $SU(5)$ breaks, the adjoint cannot align itself over all space [15]. Therefore, on super-horizon length scales, the direction of the Higgs field is randomly aligned. Topological knots result—these are the magnetic monopoles. This allows for an estimate of the minimum number of monopoles produced [16]; we should have at least one monopole in each horizon volume at the time of the $SU(5)$ phase transition t_c, giving

$$n_m \sim (2t_c)^{-3}. \tag{1.45}$$

Using (1.33), we may rewrite t_c in terms of T_c as

$$t_c \simeq 0.3 M_P N(T_c)^{-\frac{1}{2}} T_c^{-2}, \tag{1.46}$$

allowing us to express the monopole to photon ratio as

$$\frac{n_m}{n_\gamma} \sim \left(\frac{10T_c}{M_P}\right)^3. \tag{1.47}$$

We can use the overall mass density of the universe to place an upper bound on the density of monopoles. For the mass density we write

$$\rho_m = M_m n_m, \tag{1.48}$$

where for the remainder of this argument M_m is in GeV and n_m is the number density, expressed in cm^{-3}. Then the fraction of critical density in monopoles can be written as

$$\Omega_m h_0^2 = 9.5 \times 10^4 \rho_m. \tag{1.49}$$

Taking $M_m \sim 10^{16}$ GeV and $\Omega h_0^2 < 1$, we have

$$n_m/n_\gamma < \mathrm{O}(10^{-25}). \tag{1.50}$$

However, we see from (1.47) that for $T_c \sim M_X \sim 10^{15}$ GeV, we have

$$n_m/n_\gamma \sim 10^{-9}. \tag{1.51}$$

Moreover, any particle species with large mass typically has a very small annihilation cross section, implying that any monopoles will not annihilate away as the universe cools. Therefore, we are faced with the fact that the marriage of GUTs and the standard cosmological picture ends up grossly overproducing magnetic monopoles.

1.3 Inflation

1.3.1 Introduction

Inflationary theory evolved in part through attempts to find a solution to the three problems mentioned above. As its central premise, the inflation scenario states that at some very early point in its evolution, the universe was dominated by a very high energy density vacuum state. This then leads to a phase of quasi-exponential growth (or a quasi-de Sitter phase). At the end of this inflationary epoch, the energy stored in the vacuum is transformed into thermal energy, and the universe then evolves as in the standard cosmological picture. The advantage offered here is that the initial conditions for the hot FRW universe are now dependent solely upon those processes which occurred during the inflationary epoch—little or no information about the structure of the universe prior to inflation remains. Through this mechanism, inflation solves many of the problems associated with the standard cosmological model.

In this section, I provide a brief overview of the history of the development of models of inflation, along with an introduction to the fundamental concepts of the theory. A detailed study of the (p)reheating era is deferred until Chapter 2.

1.3.2 Historical Overview

De Sitter's 1917 work [17] on the space-time which bears his name actually predates that of Friedmann, Robertson, and Walker. However, the advantages of de Sitter space as a cosmological model were not recognized for a long time—cosmology proceeded within the FRW paradigm, while de Sitter space was used as a staging ground for developing techniques in general relativity and quantum field theory in curved space-times.

The idea that the universe might expand exponentially at some point early

in its development, being filled with superdense matter governed by the equation of state $p = -\rho$, was first suggested by Gliner [18]. However, this work did not arouse much interest; Gliner had considered superdense baryonic matter, which we now believe to be described by an equation of state close to $p = \frac{\rho}{3}$.

Somewhat later, it was realised that a constant scalar field ϕ, such as those appearing in GUTs, could act as a vacuum state with energy density given by $V(\phi)$ [19]. If a phase transition should change the value of ϕ, the energy which is stored within the field can be released in the form of thermal energy [20–23]. Sometimes, the phase transition can take place when ϕ is in a supercooled metastable vacuum state—in such cases, the total entropy of the universe can increase significantly [22–24].

In 1976, Dowker and Critchley [25] found that the de Sitter metric is a solution of the Einstein equations with quantum corrections. Three years later, Starobinsky [26] introduced a model of the early universe based on these findings. The solution turns out to be unstable—the initial vacuum-like state decays, transforming de Sitter space into a hot FRW universe.

While Starobinsky's model was a significant milestone in the development of the inflationary universe scenario, the advantages of this de Sitter epoch were not recognised at that time. Indeed, the model was pursued in the hopes of solving the problem of the initial cosmological singularity [26], and in this regard it was unsuccessful. In addition, the density inhomogeneities which arose from the decay of de Sitter space were too large to be consistent with our universe [27]. Solving these problems required significant modifications to the original model [28–30]. Over time, however, the Starobinsky model has evolved into the chaotic inflation scenario.

Guth [31] was the first to realise that a period of exponential expansion in the early universe could be used to solve the flatness, horizon, and monopole

problems. In his model, Guth proposes that the universe is initially in a state with very high temperatures and restored symmetry $\phi_{(T)} = 0$. The potential $V(\phi)$ is chosen in such a way to ensure that there is a local minimum at $\phi = 0$ over a wide range of temperatures. This allows the universe to remain in a supercooled metastable state for a long time. As the temperature drops, the energy-momentum tensor eventually becomes $T_{\mu\nu} = g_{\mu\nu}V(0)$, causing the universe to expand exponentially for a long period of time. This "inflation" of the universe continues until the universe eventually undergoes a phase transition to a stable state $\phi_0 \neq 0$. This is a first order phase transition, which involves nucleation of bubbles containing the new phase $\phi = \phi_0$. The universe then heats up due to bubble wall collisions, and the subsequent evolution of the universe is described by the standard cosmological picture.

The phase of exponential expansion takes care of the flatness, horizon and monopole problems. In the Friedman equation (1.4), the curvature terms $\frac{k}{a^2}$ is swamped by the $\kappa^2\frac{\rho}{3}$ term, making the universe flatter and flatter. Because of the tremendous expansion, it is possible to ensure that the entire visible universe came from some very small patch of space-time which was originally causally connected. Finally, in Guth's scheme, monopoles arise where walls of exponentially large bubbles collide with each other; consequently, they have exponentially low density.

Unfortunately, despite its simplicity and its success in dealing with the various weaknesses of the standard cosmological picture, Guth's model is fundamentally flawed. Guth himself pointed out [31] that collisions of very large bubbles will result in the destruction of the homogeneity and isotropy desired in the universe after inflation. Moreover, Sato [32] showed that the inflationary phase never ends because the nucleation rate is too slow—regions which have stopped inflation grow more slowly than they move apart. While many attempts were made to

rectify this situation [33, 34], none met with success.

The "new inflationary universe scenario" was developed independently by Linde [35] and by Albrecht and Steinhardt [36]. They abandon the idea of a supercooled state undergoing a phase transition; instead, inflation occurs as the ϕ field increases to its equilibrium value ϕ_0 over a period of time t very large in comparison to H^{-1}. If the epoch where ϕ is rolling downhill is long enough, then inflation ensures that any bubbles of the new phase which do form are seperated from each other by distances far greater than our current horizon, preventing any inhomogeneities from forming. Indeed, in this scenario, the universe is not heated after inflation by collisions of bubbles, but instead by the decay of the field ϕ as it oscillates about the minimum of its potential $V(\phi)$.

Once again, the period of enormous quasi-exponential expansion of the universe provides solutions to the flatness, horizon, and monopole problems. However, while the new inflation scenario is not beset by the problems which affected Guth's model, it is still faced with a few shortcomings.

First, the scenario requires a realistic theory of elementary particles in which the effective potential must satisfy a number of constraints which are somewhat unnatural. For example, the potential $V(\phi)$ must be sufficiently flat for $\phi \approx 0$. Suppose we take a potential where $V(\phi) = V(0) - \frac{\lambda}{4}\phi^4$ for small ϕ. In order for the density inhomogeneities generated through inflation to have the required amplitude

$$\frac{\delta\rho}{\rho} \sim 10^{-5}, \tag{1.52}$$

we are forced to take an extremely small value for λ, namely [37]

$$\lambda \sim 10^{-12} \text{ to } 10^{-14}. \tag{1.53}$$

However, to ensure that the universe reheats to a high enough temperature T, the curvature of the effective potential $V(\phi)$ near its minimum must be very

large, so that the field oscillates with very high frequency. Finding a natural, realistic theory which satisfies both of these requirements is rather difficult.

Moreover, a weakly interacting (as λ is very small) field ϕ is unlikely to be in thermal equilibrium with the other fields in the universe. Even if it were in equilibrium, for λ small, high-temperature corrections to $V(\phi)$ of order $\lambda T^2\phi^2$ cannot alter the initial value of the ϕ field and make it zero between the birth of the universe and the assumed start of inflation [38, 39].

In both Guth's model and the new inflation scenario, inflation only begins when the temperature has dropped to the point where $T^4 \lesssim V(0)$. However, the condition (1.52), in addition to the constraint on λ (1.53), also sets a constraint in most models on the value of $V(\phi)$ in the last stages of inflation, which, due to the flatness of the potential, is practically equal to $V(0)$ [39, 40]:

$$V(0) \lesssim 10^{-13} M_P^4. \tag{1.54}$$

Hence, inflation will start when $T^2 \lesssim 10^{-7} M_P^2$. In other words, inflation begins at a time t which exceeds the Planck time $t_P \sim M_P^{-1}$ by six orders of magnitude. In order for a hot, closed, FRW universe to survive that long, its total entropy must be greater than $S = 10^9$. Therefore, in the case of a closed universe, the flatness problem has once again reared its ugly head.

These shortcomings meet their match in Linde's chaotic inflation scenario [41, 42]. Instead of being based on high-temperature phase transitions, it focusses on the evolution of a universe filled with a chaotically distributed scalar field ϕ. Chaotic inflation is one of the most promising inflationary models for the early universe.

1.3.3 Chaotic Inflation in a Nutshell

In this section, we will provide an overview of the main ideas of the chaotic inflation scenario. We begin with a scalar field ϕ which is minimally coupled to

gravity and described by the Lagrangian

$$\mathcal{L} = \frac{1}{2}\partial_\mu\phi\partial^\mu\phi - V(\phi). \tag{1.55}$$

We also assume that when $\phi \gtrsim M_P$, the potential $V(\phi)$ rises more slowly than (approximately) $\exp(\frac{6\phi}{M_P})$. This requirement is satisfied by any potential of the form

$$V(\phi) = \frac{\lambda\phi^n}{nM_P^{n-4}}, \tag{1.56}$$

where $n > 0$ and $0 < \lambda \ll 1$.

Let us begin with a region which is homogeneous and isotropic and is described by the FRW metric (1.1). While such an assumption may seem strange to the reader, it can be demonstrated that it is possible, with reasonable initial conditions on $(\partial_\mu\phi)^2$, $V(\phi)$, a^2, and the smoothness of the metric at $t \sim t_P$, to find a region of size $O(M_P^{-1})$ which satisfies these conditions [43]. The behaviour of such a patch obeys the Friedman equation (1.4)

$$H^2 \equiv \left(\frac{\dot{a}}{a}\right)^2 = \frac{\kappa^2}{3}\left(\frac{\dot{\phi}^2}{2} + \frac{(\nabla\phi)^2}{2} + V(\phi)\right) - \frac{k}{a^2}. \tag{1.57}$$

We also have that the field ϕ obeys the Klein-Gordon equation

$$\Box\phi + \frac{dV}{d\phi} = \ddot{\phi} + 3H\dot{\phi} - \frac{\Delta\phi}{a^2} + \frac{dV}{d\phi} = 0, \tag{1.58}$$

where $\Box$ is the d'Albembertian operator and Δ is the Laplacian in the three-dimensional space with time-independent metric given by

$$dl^2 = \frac{dr^2}{1-kr^2} + r^2\left(d\theta^2 + \sin^2\theta d\phi^2\right). \tag{1.59}$$

If we impose the following conditions requiring the field ϕ to be uniform and slowly varying, respectively,

$$\dot{\phi}^2,\ (\nabla\phi)^2 \ll V(\phi), \tag{1.60}$$

$$\ddot{\phi} \ll \frac{dV}{d\phi}, \tag{1.61}$$

then (1.57) and (1.58) can be reduced to

$$\left(\frac{\dot{a}}{a}\right)^2 = \frac{\kappa^2}{3}V(\phi) - \frac{k}{a^2}, \tag{1.62}$$

$$3H\dot{\phi} = -\frac{dV}{d\phi}. \tag{1.63}$$

If we take an expanding universe, with $\dot{a} > 0$, and require that the initial value of the field ϕ satisfy the initial condition

$$\phi_0(x) \sim \lambda^{-\frac{1}{4}} M_P \gg M_P, \tag{1.64}$$

then the solution of the system of equations (1.62) and (1.63) rapidly evolves towards an asymptotic limit of quasiexponential expansion. This is readily seen from (1.62), as when a^2 is large, $H^2 = \frac{\kappa^2}{3}V(\phi) = \frac{8\pi V(\phi)}{3M_P^2}$. We may now use (1.63) to obtain the result

$$\frac{1}{2}\dot{\phi}^2 = \frac{M_P^2}{48\pi V}\left(\frac{dV}{d\phi}\right)^2. \tag{1.65}$$

As we wish to deal with potentials of the form $V(\phi) \sim \phi^n$, we see

$$\frac{1}{2}\dot{\phi}^2 = \frac{n^2 M_P^2}{48\pi\phi^2}V(\phi), \tag{1.66}$$

so that we have $\frac{1}{2}\dot{\phi}^2 \ll V(\phi)$ when

$$\phi \gg \frac{n}{4\sqrt{3\pi}}M_P. \tag{1.67}$$

Therefore, for large ϕ, the energy-momentum tensor $T_{\mu\nu}$ of the inflaton field is dominated by the quantity $g_{\mu\nu}V(\phi)$, which corresponds to an equation of state of the form $p = -\rho$, and, as we have seen earlier, the universe expands quasiexponentially. While the field value $\phi \gg M_P$, the field ϕ and the potential $V(\phi)$ vary on time scales substantially longer than the rate of expansion of the universe ($\frac{\dot{\phi}}{\phi} \ll H$ and $\dot{H} \ll H^2$), so over intervals of time $\Delta t \lesssim \frac{H}{\dot{H}} \gg H^{-1}$, the universe behaves approximately like de Sitter space with

$$a(t) \sim e^{Ht}, \tag{1.68}$$

where

$$H(\phi(t)) = \sqrt{\frac{8\pi V(\phi)}{3M_P^2}} \tag{1.69}$$

decreases slowly with time [41].

In light of all of the above, the behaviour of the field $\phi(t)$ is

$$\phi(t) = \phi_0 \exp\left(-\sqrt{\frac{\lambda}{6\pi}} M_P t\right) \tag{1.70}$$

for a theory with $V(\phi) = \frac{\lambda}{4}\phi^4$, while for $V(\phi) \sim \phi^n$, for $n \neq 4$, we have

$$\phi(t)^{2-\frac{n}{2}} = \phi_0^{2-\frac{n}{2}} + t\left(2 - \frac{n}{2}\right)\sqrt{\frac{n\lambda}{24\pi}} M_P^{3-\frac{n}{2}}. \tag{1.71}$$

In particular, for a theory with $V(\phi) = \frac{m^2\phi^2}{2}$, substituting $n = 2$ and $\lambda M_P^2 = m^2$ into the above relation gives

$$\phi(t) = \phi_0 - \frac{mM_P}{2\sqrt{3\pi}} t. \tag{1.72}$$

The behaviour of the scale factor $a(t)$ is given by

$$a(t) = a_0 \exp\left\{\frac{4\pi}{nM_P^2}[\phi_0^2 - \phi^2(t)]\right\}, \tag{1.73}$$

which reduces to (1.68) for t small. Using (1.66), one can show that the inflation regime ends when $\phi \lesssim \frac{n}{12} M_P$. For $\phi \gg M_P$, we may use (1.72) to obtain the overall inflation factor $P \equiv \frac{a(t)}{a_0}$ for the universe at the end of the slow-rolling phase:

$$P \sim \exp\left(\frac{4\pi}{nM_P^2}\phi_0^2\right). \tag{1.74}$$

The above result tells us that the degree of inflation grows exponentially with increasing values of the initial value of the field ϕ_0. Consequently, most of the physical volume of the universe evolves as the result of the inflation of regions of a size larger than the event horizon $H^{-1}(\phi)$ which were initially filled with a very homogeneous, slowly varying, extremely large field $\phi = \phi_0$.

Let us assume an initial state of the form

$$V(\phi_0) \sim \frac{\lambda \phi_0^n}{n M_P^{n-4}} \sim M_P^4, \tag{1.75}$$

then the inflation factor of the corresponding region is given by

$$P \sim \exp\left[\frac{4\pi}{n}\left(\frac{\lambda}{n}\right)^{-\frac{2}{n}}\right]. \tag{1.76}$$

Hence, for a $\frac{\lambda}{4}\phi^4$ theory, we have

$$P \sim \exp\left(\frac{\pi}{\sqrt{\lambda}}\right), \tag{1.77}$$

while for a $\frac{m^2\phi^2}{2}$ theory,

$$P \sim \exp\frac{\pi\sqrt{2}M_P^2}{m^2}. \tag{1.78}$$

When the inflaton field ϕ decreases to a value of order M_P (1.66), the friction term $3H\dot{\phi}$ in (1.58) is no longer large enough to enforce the slow-rolling condition, and the ϕ field rapidly rolls to the minimum of the potential. The field begins oscillating about the minimum of the $V(\phi)$, transferring energy to new particles which are created due to the oscillations of the field—the subsequent collisions of these created particles heats up the universe [31, 44, 45].

If we assume that the reheating phase occurs over a very short interval $\Delta t \lesssim H^{-1}(\phi \sim M_P)$, then almost all of the energy from the oscillating field will be transformed into thermal energy and we can obtain an estimate for the temperature of the universe after reheating:

$$\frac{\pi^2 N(T_R)}{30} T_R^4 \sim V\left(\phi \sim \frac{n}{12} M_P\right). \tag{1.79}$$

For a $V(\phi) = \frac{\lambda}{4}\phi^4$ theory with $N(T) \sim 10^3$, we have $T_R = c\lambda^{\frac{1}{4}} M_P$, where $c = \mathrm{O}(10^{-1})$. (This is a rather simplistic treatment of the reheating epoch—we will examine various mechanisms of reheating in detail in the next chapter.)

1.3.4 Three Problems Revisited

We are now in a position to consider what has been accomplished through the process of inflation. In the chaotic inflation scenario considered above, the initial temperature of the universe after reheating ends is essentially independent of the initial conditions for or the duration of the inflationary phase. Only the scale factor changes, growing exponentially as shown in (1.73,1.76–1.78). It is this exponential growth which solves the flatness, horizon, and monopole problems associated with the standard cosmological picture. The exact number of e-folds required to ameliorate these difficulties can be computed (see, e.g., [46]); however, 60 e-folds represents a general lower bound for a wide range of models.

Let us begin by discussing the flatness and horizon problems. During the quasiexponential expansion of the universe, the $\frac{k}{a^2}$ term in the Friedman equation (1.57) is exponentially suppressed, while all other terms only decrease very slowly. Therefore, the three-dimensional geometry of the universe becomes exponentially close to the geometry of flat space while the global topology of the space remains the same. With 60 e-folds (or more) of inflation, it is possible to inflate a patch with size originally on the order of the Planck length to scales well beyond our current horizon. Additionally, in chaotic inflation, the universe can begin inflating at arbitrarily high energy densities and arbitrarily soon after the universe begins expanding. Hence, chaotic inflation does not suffer from problems in the case of a closed universe, as both the old and new inflationary schemes did.

Finally, through the stretching of all scales of inhomogeneities, there results an exponential decrease in the density of any monopoles, domain walls, gravitinos, or other undersirable entities which may be produced before or during inflation. Provided that the reheat temperature T_R is not high enough to produce these relics again, the monopole problem is solved.

1.4 Conclusion

It is hoped that this chapter has provided the reader with some idea of why it is of interest to study realistic models of inflation. While the reader must be cautioned that inflation is not the only proposed solution to the problems mentioned above—for example, recent works [47, 48] have explored the effects of a time-varying value for the speed of light on the above problems. However, inflation remains the most promising model for pre-FRW dynamics.

Before we can proceed with our studies of particular complex inflation models, we must first learn in detail the theory behind the reheating epoch. In the following chapter, we will study the work to date on parametric resonance decay of the inflaton.

References

[1] S. Weinberg, *Gravitation and Cosmology*, (Wiley, New York, 1972).

[2] A. Friedmann, Z. Phys. **10** (1922), 377;
A. Friedmann, Z. Phys. **21** (1924), 326.

[3] H. P. Robertson, Ap. J. **82** (1935), 284;
H. P. Robertson, Ap. J. **83** (1936), 187, 257.

[4] A. G. Walker, Proc. Lond. Math. Soc. (2) **42** (1936), 90.

[5] A. Sandage and G. A. Tammann, in: *Inner Space/Outer Space*, eds E. Kolb et al., (Univ. of Chicago Press, Chicago, 1986), 41;
J. P. Huchra, in: *Inner Space/Outer Space*, eds E. Kolb et al., (Univ. of Chicago Press, Chicago, 1986), 65.

[6] see, for example: S. Perlmutter et al., Ap. J. **517** (1999), 565.

[7] G. Steigman, K. A. Olive, and D. N. Schramm, Phys. Rev. Lett. **43** (1979), 239;
K. A. Olive, D. N. Schramm, and G. Steigman, Nucl. Phys. **B180** (1981), 497.

[8] A. A. Penzias and R. W. Wilson, Astrophys. J. **142** (1965), 419.

[9] G. Gamow, Phys. Rev. **70** (1946), 572;
R. A. Alpher, H. Bethe, and G. Gamow, Phys. Rev. **73** (1948), 803.

[10] B. Carter, in: *The Conformation of Cosmological Theories with Observational Data; IAU Symp. 63*, ed. M. Longair (Reidel, Dordrecht, 1974);
C. B. Collins and S. W. Hawking, Astrophys. J. **181** (1973), 317;

R. H. Dicke and P. J. E. Peebles, in *General Relativity: An Einstein Centenary Survey*, eds. S. W. Hawking and W. Israel, (Cambridge Univ. Press, Cambridge, 1979).

[11] W. Rindler, Mon. Not. R. Astron. Soc. **116** (1956), 663;
G. F. R. Ellis and W. Stoeger, Class. Quantum Grav. **5** (1988), 207.

[12] G. F. Smoot, et al., Astrophys. J. Lett. **396** (1992), L1.

[13] For a review see: P. Langacker, Phys. Rep. **C72** (1981), 185.

[14] G. 't Hooft, Nucl. Phys. **B79** (1974), 276;
A. M. Polyakov, JETP Lett. **20** (1974), 194.

[15] T. W. B. Kibble, J. Phys. **A9** (1976), 1387.

[16] Ya. B. Zeldovich and M. Y. Khopolov, Phys. Lett. **B79** (1979), 239;
J. P. Preskill, Phys. Rev. Lett. **43** (1979), 1365.

[17] W. de Sitter, Proc. Kon. Ned. Akad. Wet. **19** (1917), 1217;
W. de Sitter, Proc. Kon. Ned. Akad. Wet. **20** (1917), 229.

[18] E. B. Gliner, Sov. Phys. JETP **22** (1965), 378;
E. B. Gliner, Dokl. Akad. Nauk SSSR **192** (1970), 771;
E. B. Gliner and I. G. Dymnikova, Sov. Astron. Lett. **1** (1975), 93.

[19] A. D. Linde, JETP Lett. **19** (1974), 183;
M. Veltman, Rockefeller University Preprint (1974);
M. Veltman, Phys. Rev. Lett. **34** (1975), 77;
J. Dreitlein, Phys. Rev. Lett. **33** (1975), 1243.

[20] D. A. Kirzhnits and A. D. Linde, Sov. Phys. JETP **40** (1974), 628.

[21] D. A. Kirzhnits and A. D. Linde, Lebedev Phys. Inst. Preprint Number 101 (1974).

[22] D. A. Kirzhnits and A. D. Linde, Ann. Phys. **101** (1976), 195.

[23] A. D. Linde, Rep. Prog. Phys. **42** (1979), 389.

[24] A. D. Linde, Phys. Lett. **B99** (1981), 391.

[25] J. S. Dowker and R. Critchley, Phys. Rev. **D13** (1976), 3224.

[26] A. A. Starobinsky, JETP Lett. **30** (1979), 682;
A. A. Starobinsky, Phys. Lett. **B91** (1980), 99.

[27] V. F. Mukhanov and G. V. Chibisov, JETP Lett. **33** (1981), 523;
V. F. Mukhanov and G. V. Chibisov, Sov. Phys. JETP **56** (1982), 258.

[28] J. D. Barrow and A. Ottewill, J. Phys. **A16** (1983), 2757.

[29] A. A. Starobinsky, Sov. Astron. Lett. **9** (1983), 302.

[30] L. A. Kofman, A. D. Linde, and A. A. Starobinsky, Phys. Lett. **B157** (1985), 36.

[31] A. H. Guth, Phys. Rev. **D23** (1981), 347.

[32] K. Sato, Mon. Not. Roy. Astron. Soc. **195** (1981), 467.

[33] S. W. Hawking, I. G. Moss, and J. M. Stewart, Phys. Rev. **D26** (1982), 2681.

[34] A. H. Guth and E. J. Weinberg, Nucl. Phys. **B212** (1983), 321.

[35] A. D. Linde, Phys. Lett. **B108** (1982), 389.

[36] A. A. Albrecht and P. J. Steinhardt, Phys. Rev. Lett. **48** (1982), 1220.

[37] S. W. Hawking, Phys. Lett. **B115** (1982), 295;
A. A. Starobinsky, Phys. Lett. **B117** (1982), 175;
A. H. Guth and S. Y. Pi, Phys. Rev. Lett. **49** (1982), 1110;
J. M. Bardeen, P. J. Steinhardt, and M. S. Turner, Phys. Rev. **D28** (1983), 679.

[38] A. D. Linde, Phys. Lett. **B132** (1983), 317.

[39] A. D. Linde, Rep. Prog. Phys. **47** (1984), 925.

[40] V. A. Rubakov, M. V. Sazhin, and A. V. Veryaskin, Phys. Lett. **B115** (1982), 189.

[41] A. D. Linde, JETP Lett. **38** (1983), 149;
A. D. Linde, Phys. Lett. **B129** (1983), 177.

[42] A. D. Linde, Mod. Phys. Lett. **A1** (1986), 81;
A. D. Linde, Phys. Lett. **B175** (1986), 395;
A. D. Linde, Physica Scripta **T15** (1987), 169.

[43] A. D. Linde, *Particle Physics and Inflationary Cosmology*, (Harwood, New York, 1990).

[44] A. D. Dolgov and A. D. Linde, Phys. Lett. **B116** (1982), 329.

[45] L. F. Abbott, E. Farhi, and M. B. Wise, Phys. Lett. **B117** (1982), 29.

[46] E. W. Kolb and M. S. Turner, *The Early Universe*, 2nd ed., (Addison Wesley, New York, 1994), Ch. 8.

[47] A. Albrecht and J. Magueijo, preprint: astro-ph/9811018.

[48] P. P. Avelino and C. J. A. P. Martins, Phys. Lett. **B449** (1999), 468.

Chapter 2

Preheating for Dummies

2.1 Introduction

In the previous chapter, we reviewed the standard cosmological model, the hot FRW universe, along with some of its associated problems. We subsequently detailed the historical development of inflationary cosmology, demonstrated how inflation solves the flatness, horizon, and monopole problems, and reviewed Linde's chaotic inflation scenario in some detail.

Let us now turn to the key element within the inflationary paradigm which remains to be addressed, namely the reheating process after the rapid expansionary phase. This is the epoch during which the elementary particles of the universe are produced due to oscillations of the inflaton ϕ about the minimum of some potential well $V(\phi)$, and subsequently thermalize with some reheating temperature T_r. For a long time, it was believed that a perturbative treatment was sufficient to obtain a reasonable understanding of reheating; however, several recent papers have shown that non-perturbative effects can play a very significant role in some cases. In particular, the inflaton field ϕ can undergo parametric resonance decay, during which there is a coherent enhancement of the transition to

various decay products. The stage where the universe reheats due to mechanisms following this pattern has been named *preheating*.

Therefore, in this chapter, we examine in detail four of the most significant papers [1–4] on parametric resonance. After a brief review section on the standard perturbative treatment of reheating, we proceed with sections on narrow-band, broad-band, and stochastic resonance in $m^2\phi^2$ theories [1]; parametric resonance in conformal theories [2]; instant preheating [3]; and preheating for fermions [4].

2.2 The Perturbative Case: Reheating

2.2.1 The Decay of the Inflaton

Let us begin by considering the evolution of a non-decaying inflaton ϕ. During inflation the leading contribution to the energy-momentum tensor is given by the inflaton scalar field with the Lagrangian

$$\mathcal{L}(\phi) = \frac{1}{2}(\partial_\mu\phi)^2 - V(\phi), \tag{2.1}$$

where $V(\phi)$ is the effective potential of the scalar field ϕ. Let us further assume that the field is sufficiently homogenous and isotropic to allow any spatial dependence in the equations of motion to be dropped. Then as we saw in (1.57), the evolution of a flat FRW universe is described by the Friedman equation

$$H^2 = \frac{8\pi}{3M_P^2}\left(\frac{1}{2}\dot{\phi}^2 + V(\phi)\right), \tag{2.2}$$

while (1.58) tells us that the Klein-Gordon equation for $\phi(t)$ is

$$\ddot{\phi} + 3H\dot{\phi} + V_{,\phi} = 0, \tag{2.3}$$

where $\dot{}$ denotes a time derivative and $_{,\phi}$ denotes differentiation with respect to ϕ. In the inflationary stage, where the universe expands quasi-exponentially with

$a(t) \sim a_0 \exp\left[\int dt H(t)\right]$, $\ddot{\phi}$ is dominated by the "friction" term $3H\dot{\phi}$ in (2.3), while in (2.2), the kinetic term is dominated by the the potential term.

Consider the simplest model of chaotic inflation: $V(\phi) = \frac{1}{2}m^2\phi^2$ [5]. As we saw in the previous chapter, inflation occurs at $\phi \gtrsim M_P$. As ϕ decreases below M_P the "friction" term $3H\dot{\phi}$ becomes less and less important, with inflation terminating at $\phi \sim M_P/2$.

Figure 2.1: Oscillations of the field ϕ after inflation in the theory $\frac{m^2\phi^2}{2}$. The value of the scalar field in this and all other figures in this chapter is measured in units of M_P, while time is measured in units of m^{-1}. Adapted from [1].

As can be seen in Figure 2.1, the amplitude of the inflaton field after the first oscillation is reduced by a factor of ten from its value at the end of inflation, becoming $0.04M_P$. The asymptotic solution for ϕ tends towards that of a damped harmonic oscillator, taking on the form

$$\phi(t) = \Phi(t) \sin mt, \tag{2.4}$$

where the amplitude of oscillations $\Phi(t)$ is given by

$$\Phi(t) = \frac{M_P}{\sqrt{3\pi}mt} \sim \frac{M_P}{\sqrt{3\pi}(2\pi N)} \approx \frac{M_P}{20N}, \tag{2.5}$$

where N is the number of oscillations after inflation has ended.

If we average the scale factor over several oscillations, we see that $a(t) \approx a_0(\frac{t}{t_0})^{2/3}$. Oscillations of ϕ in this theory are approximately sinusoidal, with the amplitude decreasing as $\Phi(t) = \frac{M_P}{3}(\frac{a_0}{a(t)})^{3/2}$. Consequently, the energy density of the field decreases as it would for nonrelativistic particles of mass m: $\rho_\phi = \frac{1}{2}\dot{\phi}^2 + \frac{1}{2}m^2\phi^2 \sim a^{-3}$. Therefore, the coherent oscillations of the inflation behave in accordance with a matter dominated effective equation of state with vanishing pressure.

We now allow the inflaton to couple to other fields, opening up possible decay channels. The universe reheats as the inflaton energy density is transferred to the energy density of other particles and fields. As a result of this energy loss, the amplitude of ϕ oscillations decreases much faster than computed in (2.5). The decay of the inflaton as it oscillates about the minimum of its effective potential $V(\phi)$ is the underlying concept of the elementary theory of reheating developed in [6, 7]; see also [5].

Consider a basic model in which the inflaton scalar field ϕ interacts with another scalar field χ and a spinor field ψ:

$$\begin{aligned}\mathcal{L} &= \tfrac{1}{2}(\partial_\mu\phi)^2 - V(\phi) + \tfrac{1}{2}(\partial_\mu\chi)^2 - \tfrac{1}{2}m_\chi^2(0)\chi^2 - \tfrac{1}{2}\xi\mathcal{R}\chi^2 \\ &\quad + \bar{\psi}\left(i\gamma^\mu\partial_\mu - m_\psi(0)\right)\psi - \tfrac{1}{2}g^2\phi^2\chi^2 - h\bar{\psi}\psi\phi,\end{aligned} \tag{2.6}$$

where g, h and ξ are small coupling constants, $\mathcal{R}$ is the Ricci curvature scalar, and $V(\phi)$ is the effective potential for the field ϕ. Without loss of generality we may take an effective potential which has a minimum at $\phi = \sigma$, and require that near its minimum, $V(\phi)$ is quadratic in ϕ:

$$V(\phi) \sim \frac{1}{2}m^2(\phi - \sigma)^2, \tag{2.7}$$

where m^2 is the effective mass squared of the ϕ field.

If we shift the field $\phi - \sigma \to \phi$, the effective potential becomes $\frac{1}{2}m^2\phi^2$, and the Lagrangian acquires an interaction term $\delta\mathcal{L} = -g^2\sigma\phi\chi^2$. Therefore, after spontaneous symmetry breaking, the χ and ψ particles acquire masses $m_\chi = \sqrt{m_\chi^2(0) + g^2\sigma^2}$ and $m_\psi = m_\psi(0) + h\sigma$, respectively.

Consider the oscillation of the scalar field near the minimum of its effective potential. In the arguments that follow, we consider the case $m \gg m_\chi, m_\psi$. We also take $H \ll m$, which is a valid assumption during the last, most important stages of reheating. The energy density of the (shifted) oscillating field is $\rho_\phi = \frac{1}{2}\dot{\phi}^2 + \frac{1}{2}m^2\phi^2$. Ignoring particle creation, the field ϕ oscillates with frequency $k_0 = m$ about $\phi = 0$. The amplitude of oscillations is redshifted as $a^{-\frac{3}{2}}$, while the energy density ρ_ϕ is redshifted as a^{-3}. We can treat a homogeneous scalar field oscillating with frequency m as a coherent wave of ϕ-particles with zero momenta and particle density $n_\phi = \rho_\phi/m$. Therefore, provided that we consider time intervals larger than m^{-1}, both the energy density of the oscillating field and the number density of the particles will be related to the field amplitude Φ in a simple way:

$$\begin{aligned} \rho_\phi &= \tfrac{1}{2}m^2\Phi^2, \\ n_\phi &= \tfrac{1}{2}m\Phi^2. \end{aligned} \tag{2.8}$$

2.2.2 Particle Production

We now include effects related to the expansion of the universe and particle production in our considerations. Taking into account all non-gravitational quantum corrections, a homogeneous scalar field in an expanding FRW universe satisfies the equation of motion

$$\ddot{\phi} + 3H(t)\dot{\phi} + \left(m^2 + \Pi(\omega)\right)\phi = 0, \tag{2.9}$$

where $\Pi(\omega)$ is the flat space polarization operator for the ϕ field with four-momentum $k_\mu = (\omega, 0, 0, 0)$ and $\omega = m$.

While the real part of $\Pi(\omega)$ only introduces a small correction to m^2, as ω becomes larger than $\min(2m_\chi, 2m_\psi)$, the polarization operator $\Pi(\omega)$ acquires an imaginary part $\mathrm{Im}\,\Pi(\omega)$. Assuming $m^2 \gg \mathrm{Im}\,\Pi$, which holds in most situations, we have $\Phi(t) = \Phi_0 a^{-3/2}(t) = \Phi_0 \exp(-\frac{3}{2}\int dt H(t))$. As we have already assumed $H \ll m$, we may ignore the time-dependence of H and $\mathrm{Im}\,\Pi$ due to the expansion of the universe, obtaining a solution of (2.9) that describes the motion of the field near the point $\phi = 0$:

$$\begin{aligned} \phi &= \Phi(t)\exp(imt) \\ &\approx \phi_0 \exp(imt) \times \exp\left[-\frac{1}{2}\left(3H + \frac{\mathrm{Im}\,\Pi(m)}{m}\right)t\right]. \end{aligned} \tag{2.10}$$

Continuing on, unitarity implies that [8]

$$\mathrm{Im}\,\Pi = m\Gamma, \tag{2.11}$$

where $\Gamma = \Gamma(\phi \to \chi\chi) + \Gamma(\phi \to \psi\psi)$ is the total decay rate of ϕ-particles. Therefore, using (2.10), we see that particle production due to the decay of the inflaton field causes the amplitude ϕ oscillations to decrease as $\exp\left[-\frac{1}{2}(3H + \Gamma)t\right]$.

As we have taken the polarization operator Π and the decay rates Γ to be essentially independent of time (and thus on the curvature of the universe), they are well-approximated by their flat-space limits. At tree level, the decay widths of a ϕ-particle into pairs of scalar χ's or spin-$\frac{1}{2}$ ψ's is given by [5]:

$$\Gamma(\phi \to \chi\chi) = \frac{g^4\sigma^2}{8\pi m}, \qquad \Gamma(\phi \to \psi\psi) = \frac{h^2 m}{8\pi}. \tag{2.12}$$

To obtain a phenomenological description of the damping of oscillations of the scalar field ϕ (2.10), one may replace the term proportional to the imaginary part of the polarization operator with an extra friction term $\Gamma\dot{\phi}$ in the classical

equation of motion of the field ϕ,

$$\ddot{\phi} + (3H(t) + \Gamma)\dot{\phi} + m^2\phi = 0\ . \tag{2.13}$$

This result, when combined with (2.11), reproduces the damped oscillator solution we obtained in (2.10). Attempts to use various friction terms in the equation of motion to obtain a description of reheating effects originated in one of the first papers on reheating [9]. However, as is clear from the assumptions used in the derivation of (2.11), equations of the form of (2.13) are valid only as the field ϕ rapidly oscillates near the minimum of $V(\phi)$—they cannot be used to investigate the slow rolling phase.

From the damped oscillator solution (2.10), we see that the field amplitude $\Phi(t)$ obeys the equation

$$\frac{1}{a^3}\frac{d}{dt}(a^3\Phi^2) = -\Gamma\Phi^2. \tag{2.14}$$

Multiplying through by m, we see that the number density (2.8) of the coherently oscillating ϕ-particles is given by

$$\frac{d}{dt}(a^3 n_\phi) = -\Gamma \cdot a^3\, n_\phi, \tag{2.15}$$

implying that the total comoving number density of particles $\sim a^3 n_\phi$ decreases exponentially with the decay rate Γ. In an analogous manner, one may show that the total energy density of the oscillating field ϕ is given by

$$\frac{d}{dt}(a^3\rho_\phi) = -\Gamma \cdot a^3\, \rho_\phi. \tag{2.16}$$

It is clear that the decay products of the scalar field ϕ are ultrarelativistic (as we have assumed that $m \gg m_\chi, m_\psi$), and we have seen above that their energy density redshifts much faster than that of the oscillating field ϕ. As a result, reheating in our model can terminate only when the Hubble constant $H \sim \frac{2}{3t}$ becomes smaller than Γ; otherwise, the ϕ retains the majority of the energy.

Therefore, we must have that when reheating ends, the age of the universe is given by $t_r \sim \frac{2}{3}\Gamma^{-1}$. At that stage the main part of the matter in the universe becomes ultrarelativistic. Since the age of the universe as a function of energy density ρ is given by $t(\rho) = \sqrt{M}_P/\sqrt{6\pi\rho}$ [5] we can combining this result with the condition $t_r \sim \frac{2}{3}\Gamma^{-1}$ to obtain the energy density at time t_r:

$$\rho(t_r) \simeq \frac{3\Gamma^2 M_P^2}{8\pi}. \tag{2.17}$$

Provided that the universe reaches thermodynamic equilibrium quickly after the inflaton decays, we have that the matter acquires a temperature T_r given by

$$T_r^4 \simeq \frac{30\rho(t_r)}{\pi^2 N(T_r)} \tag{2.18}$$

where $N(T)$ is the number of relativistic degrees of freedom at the temperature T; e.g., 1 for each scalar, 2 for each massless vector particle, etc. [5]. In realistic particle models of the early universe, one typically has $N(T_r) \sim 10^2$–10^3, allowing us to estimate the reheating temperature:

$$T_r \simeq 0.2\sqrt{\Gamma M_P}. \tag{2.19}$$

It is important to note that T_r does not depend on the initial value of ϕ; instead, it is completely determined by the microphysics of the underlying elementary particle theory.

The elementary perturbative theory of reheating described above is rather elegant, and has proven to be very successful in describing reheating after inflation in many realistic inflationary models. However, as we shall explore in the next section, in some cases where the amplitude of the oscillating field is sufficiently large, reheating occurs via a non-perturbative mechanism—parametric resonance, or *preheating*.

2.3 Elementary Preheating—$m^2\phi^2$ Models

2.3.1 Introduction

The "breakthrough" paper concerning the parametric resonance decay of the inflaton was written by Kofman, Linde, and Starobinsky [1]. They correctly realized that the ordinary methods of quantum field theory describing the decay of the inflaton ϕ to another scalar χ, $\phi \to \chi\chi$, were misleading in cases where many χ-particles had already been produced (i.e., $n_k > 1$), as the probability of decay becomes greatly enhanced due to effects related to Bose-Einstein statistics, potentially leading to explosive particle production. In this section, we review several of their most important results.

2.3.2 Breakdown of Perturbation Theory

Consider the interaction between a *classical* inflaton field ϕ and a *quantum* scalar field $\hat{\chi}$ as specified by the Lagrangian (2.6). In the Heisenberg representation, we may write the quantum scalar field $\hat{\chi}$ as

$$\hat{\chi}(t,\mathbf{x}) = \frac{1}{(2\pi)^{3/2}} \int d^3k \left(\hat{a}_k \chi_k(t)\, e^{-i\mathbf{k}\cdot\mathbf{x}} + \hat{a}_k^+ \chi_k^*(t)\, e^{i\mathbf{k}\cdot\mathbf{x}} \right), \tag{2.20}$$

where $\hat{a}_k$ and $\hat{a}_k^+$ are annihilation and creation operators, respectively. In a flat FRW spacetime with scale factor $a(t)$, the mode eigenfunctions χ_k satisfy the equation

$$\ddot{\chi}_k + 3\frac{\dot{a}}{a}\dot{\chi}_k + \left(\frac{\mathbf{k}^2}{a^2} + m_\chi^2(0) - \xi\mathcal{R} + g^2\phi^2 \right) \chi_k = 0, \tag{2.21}$$

where the physical momentum $\mathbf{p} = \frac{\mathbf{k}}{a(t)}$ coincides with the comoving momentum $\mathbf{k}$ in Minkowski space, where $a = 1$. The above equation describes an oscillator with a variable frequency ω due to the time-dependence of both the scale factor $a(t)$ and the background field $\phi(t)$. For the time being, we will assume $m_\chi(0) = 0$ for $\phi = 0$. In Section 2.3.6 we will investigate the opposite case, namely $m_\chi(0) \gg m$.

Once again, we simulate spontaneous symmetry breaking through the choice of the potential $V(\phi) \sim \frac{1}{2}m^2(\phi - \sigma)^2$; under the field redefinition $\phi - \sigma \to \phi$, the effective potential becomes $\frac{1}{2}m^2\phi^2$, and the interaction term $-\frac{1}{2}g^2\phi^2\chi^2$ transforms to $-\frac{1}{2}g^2\phi^2\chi^2 - g^2\sigma\phi\chi^2 - \frac{1}{2}g^2\sigma^2\chi^2$. We wish to study various aspects of the equation (2.21).

For the time being, we shall drop the $\xi\mathcal{R}$ term and neglect the expansion of the universe by setting $a = 1$ in (2.21). We further assume that the amplitude of oscillations ϕ is much smaller than σ, allowing us to write the equation for the mode eigenfunctions (quantum fluctuations) corresponding to the physical momentum $\mathbf{k}$ of the field χ as

$$\ddot{\chi}_k + \left(k^2 + g^2\sigma^2 + 2g^2\sigma\Phi \sin mt\right)\chi_k = 0, \tag{2.22}$$

where $k = \sqrt{\mathbf{k}^2}$ and Φ represents the amplitude of oscillations of the inflaton field. The above equation is of a form similar to that of a harmonic oscillator, with the exception that it has a periodically changing frequency $\omega_k^2(t) = k^2 + g^2\sigma^2 + 2g^2\sigma\Phi\sin(mt)$, which can lead to parametric resonance in certain modes. Through a change of variables $mt = 2z - \pi/2$, we may cast (2.22) into the canonical form of the Mathieu equation [10]

$$\chi_k'' + (A_k - 2q\cos 2z)\,\chi_k = 0, \tag{2.23}$$

where prime denotes differentiation with respect to z, and, in our case, we have

$$A_k = 4\frac{k^2 + g^2\sigma^2}{m^2}, \tag{2.24}$$

$$q = \frac{4g^2\sigma\Phi}{m^2}, \tag{2.25}$$

$$z = \frac{mt}{2}. \tag{2.26}$$

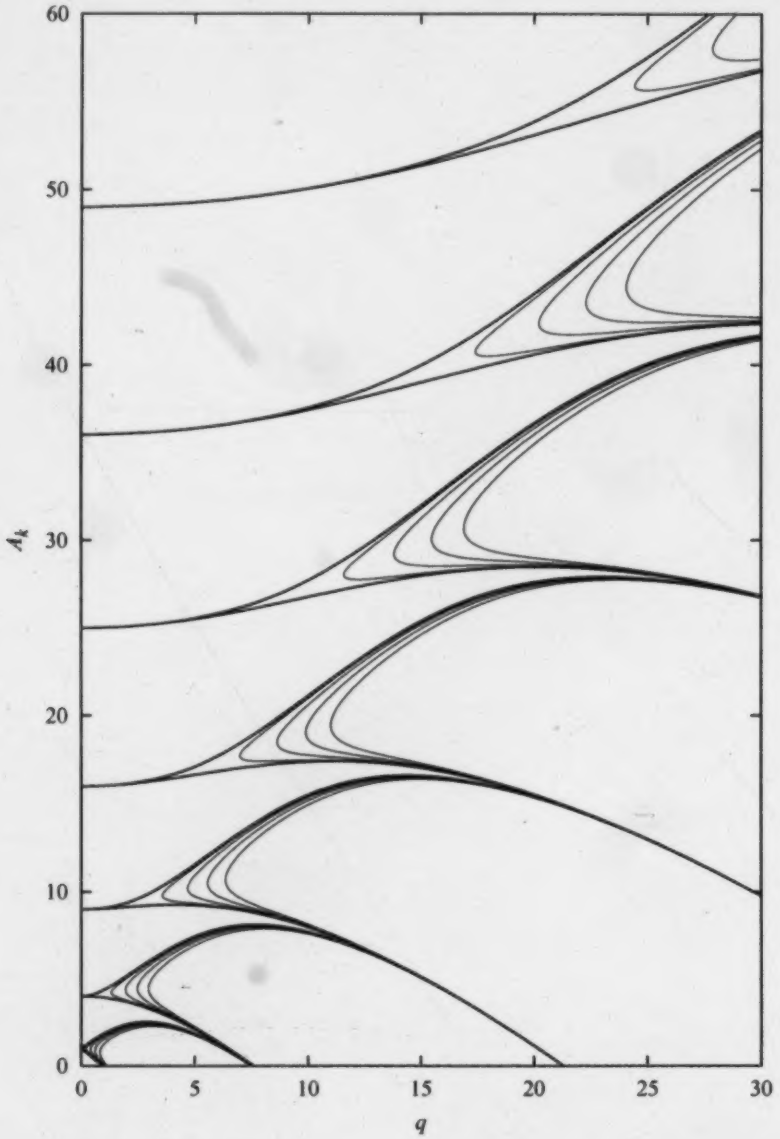

Figure 2.2: The Mathieu equation stability diagram, showing the first seven instability bands. The heavy contour represents $\mu = 0$, the band boundary, and the contour interval is 0.1.

The stability diagram of the Mathieu equation, which can be found in Figure 2.2, allows for easy visualization of the properties of its solutions. Perhaps the most important aspect of solutions of (2.23) is the existence of exponential instabilities $\chi_k \propto \exp(\mu_k^{(n)} z)$ within a set of resonance bands of frequencies $\Delta k^{(n)}$, where n denotes the order of the resonance band. These instabilities can be viewed as corresponding to regions where particle production occurs, as one observes an exponential growth of occupation numbers $n_k(t) \propto \exp(2\mu_k^{(n)} z)$.

For now, we shall consider the case where $g\Phi \ll g\sigma \ll m$, for which the theory of parametric resonance is well understood [11]; in this case, we see $q \ll 1$, and the resonance occurs only in narrow bands near $A_k \simeq l^2$, where $l = 1, 2, \ldots$. The width of each band in momentum space is of order $\Delta k \sim q^l$, so for $q < 1$ the widest, and therefore the most important, instability band is the first one, for which we have $A_k \sim 1 \pm q = 1 \pm \frac{4g^2\sigma\Phi}{m^2}$.

The critical exponent μ_k for the first instability band is given by [10]

$$\mu_k = \sqrt{\left(\frac{q}{2}\right)^2 - \left(\frac{2k}{m} - 1\right)^2}, \tag{2.27}$$

so we see that resonance occurs for $k = \frac{m}{2}(1 \pm \frac{q}{2})$. At the boundaries of the resonance band, $\mu_k = 0$, while for $k = \frac{m}{2}$, $\mu_k = \frac{q}{2} = \frac{2g^2\sigma\Phi}{m^2}$, its maximal value. The corresponding maximally growing modes grow as $\exp(\frac{qz}{2})$, or, in terms of the parameters of our system, $\exp(\frac{g^2\sigma\Phi t}{m})$.

As the modes χ_k grow, so do the corresponding occupation numbers of the created particles $n_k(t)$. The number density n_k of particles with momentum $\mathbf{k}$ can be evaluated by dividing the energy of that mode $\frac{1}{2}|\dot{\chi}_k|^2 + \frac{1}{2}\omega_k^2|\chi_k|^2$ by the energy ω_k of each particle:

$$n_k = \frac{\omega_k}{2}\left(\frac{|\dot{\chi}_k|^2}{\omega_k^2} + |\chi_k|^2\right) - \frac{1}{2}. \tag{2.28}$$

From the above result, we can demonstrate that for χ_k modes growing as $\exp(\frac{qz}{2})$, the corresponding occupation number grows as $\exp(qz) = \exp(\frac{2g^2\sigma\Phi t}{m})$.

In the limit where $g\sigma \ll m$, the effective mass of the χ particles is very much smaller than m. Therefore, the resonance occurs near $k = \frac{m}{2}$, with each ϕ-particle decaying to two χ-particles with momentum $k \sim m/2$. While this mechanism bears some similarity to the process of decay $\phi \to \chi\chi$ discussed in the previous section, we get completely different results. In perturbation theory, particle production is independent of the number of particles produced earlier; instead, particles are produces at a fixed rate $\Gamma(\phi \to \chi\chi) = \frac{g^4\sigma^2}{8\pi m}$. As Γ^{-1} is suppressed by the factor g^4, the decay proceeds very slowly in the weak coupling limit. With parametric resonance, however, the rate of production of χ-particles is proportional to the amount of particles produced earlier, resulting in exponential growth where the rate of the process is given by $\mu_k m \sim \frac{g^2\sigma\Phi}{m}$, which exceeds Γ when $\Phi > \frac{g^2}{8\pi}\sigma$.

All our considerations to this point have dealt with a static universe. When we turn the expansion back on, it turns out that the expansion provides mechanisms by which the universe can evolve from parametric resonance to perturbative decay. For example, as the universe expands, the "friction term" $3H\dot{\phi}$ in the ϕ equation of motion causes an additional decrease in the ϕ field over and above that due to its decay. Therefore, we must compare qm with the effective decay rate $3H + \Gamma$, as parametric resonance occurs only for $qm \gtrsim 3H + \Gamma$. Since when $\Gamma > H$, perturbative decay leads to efficient reheating by itself, we are only interested in seeing whether parametric resonance can arise when perturbative decay is inefficient, i.e. for $\Gamma < H$. To this end, we consider the case where $qm \gtrsim 3H$.

The redshift of momenta k away from the resonance band is another mechanism which can prevent parametric resonance from being efficient. The width of the portion of the first resonance band for which the resonance is efficient is approximately $\frac{qm}{2}$. The interval Δt for which any given mode remains within

the first order band, while dependent on the equation of state of matter, can be estimated by qH^{-1}. Since the number of particles in growing modes increases as $\exp\left(\frac{q^2 m}{2H}\right)$ during this time, we see that we will have efficient decay of inflatons only if $q^2 m \gtrsim H$. For narrow-band resonance, with $q \ll 1$, this enforces a stronger bound than $qm \gtrsim 3H$.

Therefore, we can typically formulate the set of conditions which are required in order for the resonance to be efficient as

$$qm \gtrsim \Gamma, \tag{2.29}$$

$$q^2 m \gtrsim H. \tag{2.30}$$

For our model, we may reexpress these conditions as

$$\Phi > \frac{g^2}{32\pi}\sigma, \tag{2.31}$$

$$\Phi \gtrsim \frac{m\sqrt{mH}}{4g^2\sigma}. \tag{2.32}$$

While we have seen that parametric resonance can be efficient for Φ sufficiently large, it is important to note that reheating never ends in the regime of parametric resonance. As the amplitude of ϕ oscillations becomes smaller and smaller, parametric resonance terminates, and we find ourselves back in the perturbative regime of [6, 7]. Since the reheating temperature is still typically determined by this final perturbative stage, it is insufficient to calculate the reheating temperature at the end of parametric resonance; preheating merely changes the initial conditions for the last stage of reheating.

The expansion of the universe and the decay of the inflaton are only two of many possible mechanisms which can prevent the onset of preheating. Other possibilities include the backreaction of created particles, which can change the parameters A_k and q in such a way as to prevent resonance from occuring. Additionally, no resonance can begin if the χ-particles decay very quickly, with decay

rate $\Gamma > \mu_k m$, or if some interaction takes them away from the resonance band within a time $\sim (\mu_k m)^{-1}$.

As mentioned above, reheating never ends in a state of narrow parametric resonance. One might wonder whether it is possible for reheating to begin in the narrow-band regime. As we shall see in the next subsection, in most cases inflation will begin in the broad-band regime and evolve into the narrow-band regime, where it quickly ceases to exist.

2.3.3 Narrow- versus Broad-Band Resonance

In the remainder of this section we will concentrate on the simplest chaotic inflation model without symmetry breaking, which has the effective potential $V(\phi) = \frac{m^2}{2}\phi^2$ and an interaction term given by $-\frac{1}{2}g^2\phi^2\chi^2$. As a result, we must replace (2.22) with

$$\ddot{\chi}_k + \left(k^2 + g^2\Phi^2 \sin^2(mt)\right)\chi_k = 0, \tag{2.33}$$

which, again, describes an oscillator with a periodically changing frequency $\omega_k^2(t) = k^2 + g^2\Phi^2 \sin^2 mt$. As above, we can rewrite this equation in the form of the Mathieu equation (2.23), with

$$A_k = \frac{k^2}{m^2} + 2q, \tag{2.34}$$

$$q = \frac{g^2\Phi^2}{4m^2}, \tag{2.35}$$

$$z = mt. \tag{2.36}$$

In close analogy with the results of the previous subsection, when $g\Phi < m$ we have narrow-band resonance for $q \ll 1$. In this regime, resonance is most effective in the first resonance band, which affects modes with $k^2 \sim m^2(1 - 2q \pm q)$. The fastest growing modes χ_k have momenta $k \sim m$ and grow as $e^{qz/2} = e^{\mu_k mt} \sim \exp\left(\frac{g^2\Phi^2 t}{8m}\right)$; the corresponding number of χ-particles grows as

$e^{2\mu_k z} \sim e^{qz} \sim \exp\left(\frac{g^2\Phi^2 t}{4m}\right)$. We intepret this process as a resonant decay of two ϕ-particles with mass m to two χ-particles with momenta $k \sim m$. The numerical solution of (2.33) for the fastest growing mode χ_k in the narrow-band regime is given in Figure 2.3. As we can see, with each oscillation of the field $\phi(t)$, the growing modes of the field χ oscillate one time, the number of particles grows exponentially, and $\ln n_k$ is an approximately straight line with a constant slope—this slope divided by 4π gives the value of the characteristic exponent μ_k. As we have taken $q = 0.1$, we see that as $\mu_k \sim \frac{q}{2}$, we have $\mu_k \sim 0.05$, which agrees with the numerically obtained value. As a rule of thumb, the rate at which parametric resonance develops is very close to the rate of growth for the leading mode χ_k.

Up to this point, we have always taken $q \ll 1$. It is clear, however, that for oscillations with a large amplitude Φ, the parameter $q = \frac{g^2\Phi^2}{4m^2}$ can be very large. The resulting broad-band resonance is characterized by very wide resonance bands, correspondingly large critical exponents μ_k, and extremely efficient reheating. We are restricted by the condition $\frac{k^2}{m^2} = A - 2q$, which tells us that the physical region lies above the line $A = 2q$ on the stability diagram for the Mathieu equation [12]. Unfortunately, the techniques which we developed for narrow parametric resonance do not work in the broad-band case. The difference between these two regimes can readily be seen by comparing solutions of (2.33) for small and for large q; this is done in Figures 2.3 and 2.4, respectively.

In Figure 2.4, the time evolution is shown in units $m/2\pi$, which corresponds to the number of oscillations N of the inflaton field. The oscillating field $\phi(t) \sim \Phi \sin mt$ is zero at integer and half-integer values of the variable $mt/2\pi$; therefore, it is clear that particle production occurs at time intervals when $\phi(t)$ is very small. At these points, the occupation number n_k is not well defined, but shortly after that time it stabilizes at a new, higher level, and remains constant until the next jump. A comparison of the two parts of Figure 2.4 demonstrates the importance

of choosing the correct variables when describing preheating. We see that χ_k (and its integrated dispersion $\langle\chi^2\rangle$) oscillate wildly in the process of parametric resonance; n_k, on the other hand, is an adiabatic invariant. As a result, n_k behaves in a relatively simple and predictable manner everywhere except during those short intervals of time when particle production occurs.

The product field χ oscillates many times during each oscillation of the inflaton field. Indeed, for the majority of the period of oscillation of ϕ in the broad-band regime with $q^{1/2} = \frac{g\Phi}{2m} \gg 1$, the effective mass $m_\chi(t) = g\phi(t)$ is much greater than the inflaton mass m. Consequentially, the typical frequency of oscillation of the χ field, $\omega(t) = \sqrt{k^2 + g^2\phi^2(t)}$, is substantially larger than that of the ϕ field. For this reason, we are able to talk about an adiabatically changing effective mass $m_\chi(t)$ during the most of this interval.

For $\phi(t)$ sufficiently small, however, the change in the frequency of oscillations $\omega(t)$ is no longer adiabatic. Adiabaticity is violated for

$$\frac{d\omega}{dt} \gtrsim \omega^2, \tag{2.37}$$

which is a required condition for particle production. It is interesting to note that for narrow-band resonance this condition is not necessary, as small variations of $\omega(t)$ can be exponentially accumulated over several oscillations. For broad-band resonance, on the other hand, we expect a large change each oscillation, which can only occur if (2.37) is satisfied. In order to find the time interval Δt_* and the *physical* momenta k_* for which adiabaticity may be violated, we recall that for small ϕ we have $\dot{\phi} \approx m\Phi$. Our condition (2.37) therefore requires

$$k^2 \lesssim (g^2\phi m\Phi)^{2/3} - g^2\phi^2. \tag{2.38}$$

This condition is satisfied for small k when the field $\phi(t)$ is less than $\sqrt{\frac{m\Phi}{g}}$. We are also able to determine that the maximal range of momenta for which particle

production occurs corresponds to $\phi(t) = \phi_*$, where

$$\phi_* \approx \frac{1}{2}\sqrt{\frac{m\Phi}{g}} \approx \frac{1}{3}\Phi q^{-1/4}. \tag{2.39}$$

Particles produced during this epoch have a maximal value of momentum which can be estimated as $k_{\max} = \sqrt{\frac{gm\Phi}{2}}$. Throughout the majority of the interval $|\phi| \lesssim 2\phi_*$ the range of momentum is somewhat smaller, but remains on approximately the same order of magnitude as $k_{\max}$. A reasonable estimate of the typical value of momentum of particles produced during this stage is $\frac{k_*}{2}$, where

$$k_* = \sqrt{gm\Phi} = \sqrt{2}\, mq^{1/4}. \tag{2.40}$$

This result implies that for broad-band resonance, $m \ll k_* \ll g\Phi$.

As the field ϕ approaches the zero, there is an interval of time

$$\Delta t_* \sim \frac{2\phi_*}{\dot{\phi}} \sim \frac{1}{\sqrt{gm\Phi}} \sim k_*^{-1} \tag{2.41}$$

where $|\phi| \lesssim \phi_*$. During this interval $k_* \sim m_\chi = g\phi_*$, which gives $\omega \sim k_*$. We therefore have that particle production in the broad-band regime occurs within short intervals of time on the order of the period of one oscillation of the field χ, $\Delta t_* \sim \omega^{-1}$, as we might have expected from the uncertainty principle. These short intervals are readily apparent in Figure 2.4.

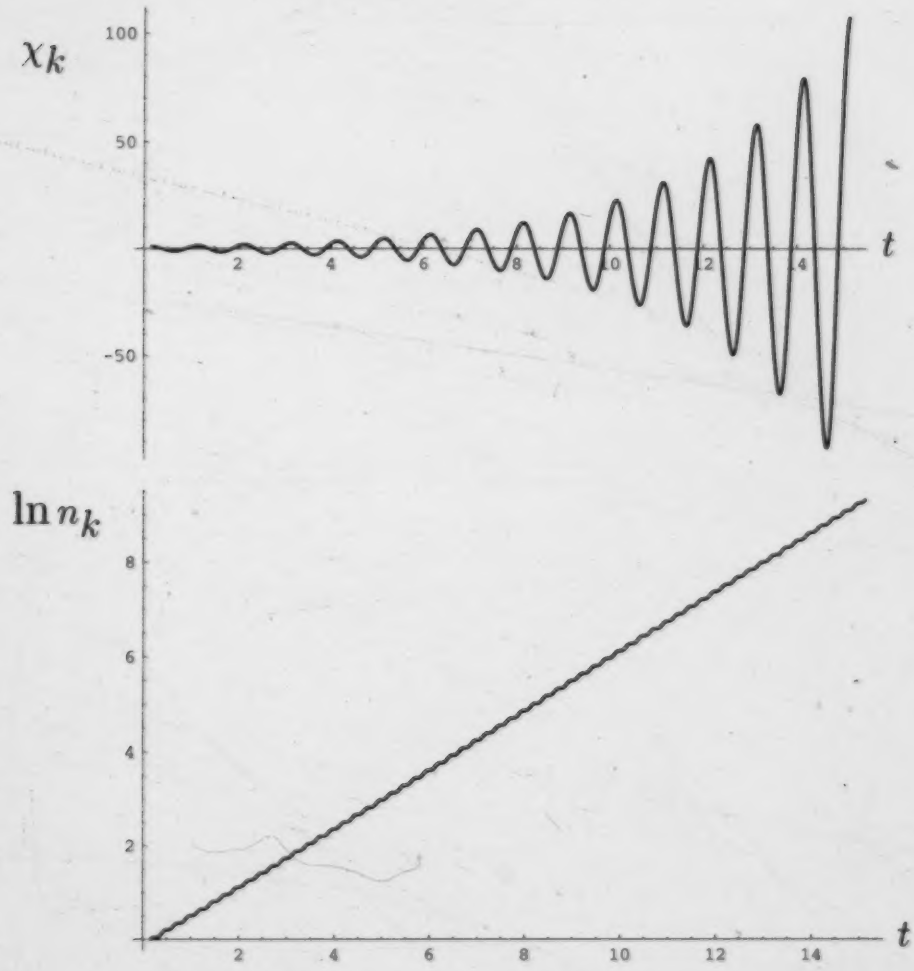

Figure 2.3: Narrow parametric resonance for the field χ in the theory $\frac{m^2\phi^2}{2}$ in Minkowski space for $q \sim 0.1$. Time is shown in units of $m/2\pi$. The upper figure shows the growth of the mode χ_k for the momentum k corresponding to the maximal speed of growth. The lower figure shows the logarithm of the occupation number of particles n_k in this mode, see Eq. (2.28). Adapted from [1].

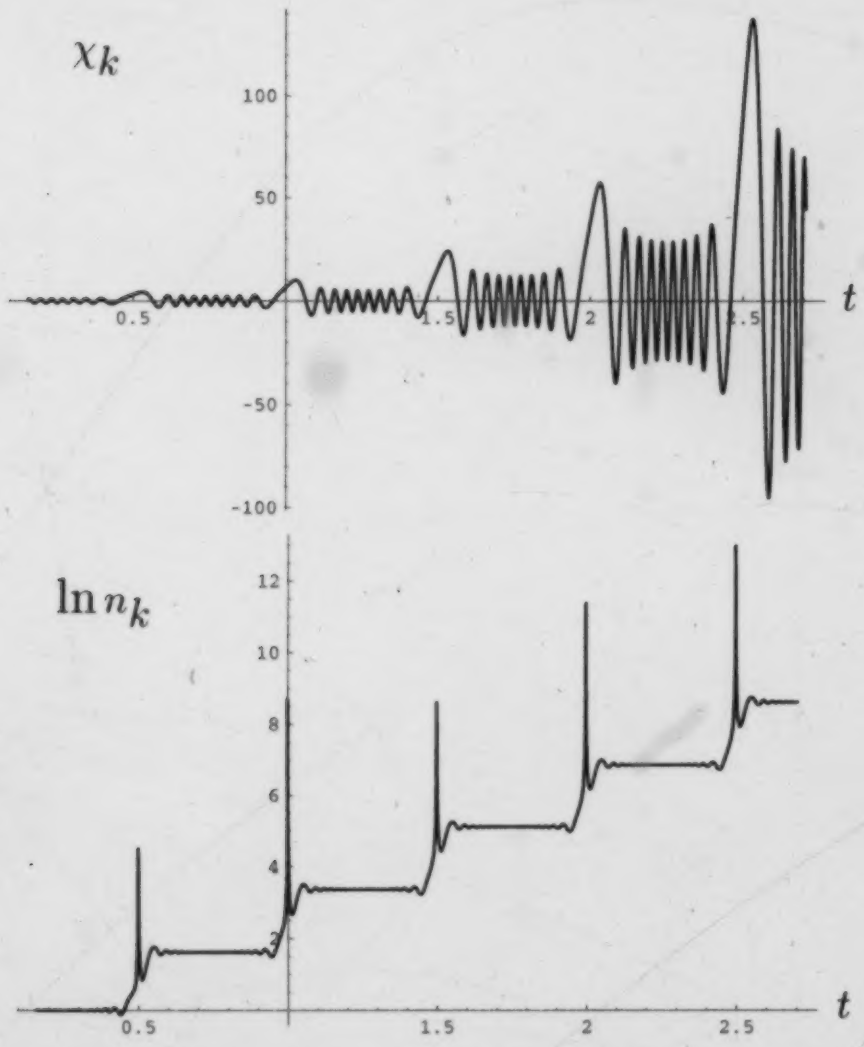

Figure 2.4: Broad parametric resonance for the field χ in Minkowski space for $q \sim 2 \times 10^2$ in the theory $\frac{m^2\phi^2}{2}$. The average rate of growth of the occupation number n_k is close to the maximal possible rate for our model, $\mu_k \sim 0.3$. Adapted from [1].

2.3.4 Stochastic Resonance

The first analytical investigations of the broad-band resonance regime were carried out by Kofman, Linde, and Starobinsky [1, 12], see also [13]. In this subsection, we shall examine in detail the broad-band resonance regime in an expanding universe.

Recall that resonance in an expanding universe arises only when we satisfy the condition $q^2 m \gtrsim H$, which in our case reads

$$g\Phi \gtrsim 2m \left(\frac{H}{m}\right)^{1/4}. \tag{2.42}$$

In various simple models of inflation, at the end of inflation, the Hubble constant H satisfies the condition $H \lesssim m$, where m is the inflaton mass. Since the amplitude Φ of the inflaton field is about $M_P/20$ during the first oscillation (see Figure 2.1), we have that the Hubble constant is $H \sim \sqrt{\frac{2\pi}{3}}\frac{m\Phi}{M_P} \sim 0.1m$. As the resonance condition only depends on H as $H^{1/4}$, we see that the regime of explosive reheating after inflation occurs only for $\Phi > m/g$; therefore, explosive decay ends at $\Phi \lesssim m/g$, which corresponds to $q \lesssim 1/4$.

Consequently, in this model preheating cannot begin for $\Phi < m/g$, which corresponds to the narrow resonance regime. While narrow resonance might be important during the very late stages of preheating [12], at that point one must also take into account the backreaction of the particles produced during broad-band resonance. It is readily apparent that in the theory of narrow-band resonance which we examine here, the end of preheating is substantially more complex than the one we discussed in the previous subsection.

In fact, extremely large initial values of q are often required for efficient preheating. Since the amplitude of the scalar field decreases much faster than $H^{1/4}$ as the universe expands, for moderate values of q, we violate (2.42) before the resonance has sufficient time to transfer any substantial amount of energy of

the oscillating field ϕ into χ-particles. It can be shown that in the model under consideration here, preheating is efficient only if the initial value of q is very large, $q_0 \gtrsim 10^3$ [1].

When we do build models with extremely large initial values of q, the expansion of the universe affects preheating in a rather peculiar manner—the resulting behaviour was dubbed *stochastic resonance* by Kofman, Linde, and Starobinsky [1]. For the time being, we shall continue to ignore the effects of backreaction and rescattering of particles. Instead, we will examine and interpret the results of numerical studies of the development of broad-band resonance in an expanding universe.

Let us begin with an expanding universe in the asymptotic regime where $a = (\frac{t}{t_0})^{2/3}$ and $\Phi(t) = \frac{M_P}{\sqrt{3\pi}mt}$. While these conditions are strictly speaking, only satisfied for sufficiently large t, if we begin counting time from the end of inflation, setting $t_0 = \frac{\pi}{2m}$, the approximation turns out to be good enough for our purposes. If we further stipulate that $m_\chi^2 = 0$, $\xi = 0$, then, considering (2.21) for a given mode χ_k, we have that the initial values of the field ϕ and the parameter q in our calculations are given by

$$\phi_0 = \frac{2M_P}{\pi\sqrt{3\pi}} \sim \frac{M_P}{5}, \qquad q_0^{1/2} = \frac{gM_P}{\pi\sqrt{3\pi}m} \sim \frac{gM_P}{10m}. \tag{2.43}$$

We now introduce the function $X_k(t) = a^{3/2}(t)\chi_k(t)$, which is given by $\frac{t}{t_0}\,\chi_k(t)$ in our case. This allows us to rewrite (2.21) in the simpler form

$$\ddot{X}_k + \omega_k^2 X_k = 0, \tag{2.44}$$

where

$$\omega_k^2 = \frac{k^2}{a^2(t)} + g^2\Phi^2 \sin^2 mt + \Delta, \tag{2.45}$$

with $\Delta = m_\chi^2 - \frac{3}{4}\left(\frac{\dot{a}}{a}\right)^2 - \frac{3}{2}\frac{\ddot{a}}{a} - \xi\mathcal{R}$. We wish to consider the case of light χ particles, such that $m_\chi \ll k_*$, so we will simply neglect m_χ. In addition, $H^2 = \left(\frac{\dot{a}}{a}\right)^2 \sim$

$\frac{\ddot{a}}{a} \ll m^2$ shortly after the end of inflation, so we are able to neglect the Δ term altogether, reducing (2.44) to the form of an oscillator with variable frequency $\omega_k^2(t)$ due to the time-dependence of the background field $\phi(t)$ and $a(t)$. We are interested in the positive-frequency solution $X_k(t) \simeq e^{-i\omega_k t}/\sqrt{2\omega_k}$.

Figures 2.5, 2.6, and 2.7 depict different stages of development of the fastest growing mode χ_k in the broad-band resonance regime in an expanding universe, where we are working in the theory $\frac{m^2\phi^2}{2}$, and have taken $q_0 \sim 3 \times 10^3$. As the amplitude of scalar field oscillations decreases as t^{-1} during the expansion of the universe, the figures illustrate the *relative* growth of the fluctuations of the field χ with respect to the ϕ amplitude through the use of the rescaled field $X_k = \chi_k \frac{t}{t_0}$, where t_0 denotes the beginning of the calculation. We may also construct an adiabatic invariant for (2.44), which can interpreted as *comoving* occupation number of particles n_k in the k-th mode in an expanding universe

$$n_k = \frac{\omega_k}{2}\left(\frac{|\dot{X}_k|^2}{\omega_k^2} + |X_k|^2\right) - \frac{1}{2}\,. \tag{2.46}$$

As preheating begins, we see that we have parametric resonance analogous to that studied in the previous subsection—Figures 2.4 and Figure 2.5 depict very similar behaviour. In both figures, we are able to identify the periods when χ-particle production is most efficient with the intervals when the field ϕ becomes small.

Some major differences are also evident, however. For example, because the ϕ amplitude gradually decreases as the universe expands, we observe a corresponding decrease in both the effective mass of the field χ and the frequency of its oscillations. Another difference lies in the fact that while the number of particles n_k typically increases, there are also times when it decreases. This is a distinctive feature of stochastic resonance. A decrease in the number of particles is a non-equilibrium effect which would be impossible if these particles were in a state of thermal equilibrium. In order to better understand the strange be-

havior of X_k and n_k evident in the figures, let us study the resonance band in which our process arises. Recall that the order n of a resonance band of the Mathieu equation is given by $n = \sqrt{A}$. Since the most important contribution to reheating occurs for those modes with $A \sim 2q$, we have $n \sim \sqrt{2q} \sim \frac{g\Phi}{\sqrt{2m}}$. In our case, we have an inflationary theory with $m \sim 10^{-6} M_P$, and we assume, for example $g \sim 10^{-1}$. Recall that after the first oscillation of the field, we have $\Phi(t) \sim M_P/20$, so we have $q \sim \frac{10^8}{16}$. We therefore begin in a band with $n \sim 3 \times 10^3$. During the next oscillation, the amplitude of the field drops by an additional factor of two, meaning that the band number also decreases by a factor of two, so we now find ourselves in the $n \sim 1.5 \times 10^3$ band.

Simply put, during a single oscillation of ϕ, the χ field has jumped over 10^3 different instability bands! In this situation, the standard method of investigating broad-band resonance, which describes the behaviour of the Mathieu equation in a single resonance band, is completely inadequate.

All is not lost, however. As we saw in the previous subsection, in broad-band resonance, particle production occurs in a small vicinity of $\phi = 0$. The process is completely independent of the behaviour of the field ϕ at any other point. Therefore, the description of the process of particle production at $\phi = 0$ is remarkably invariant with respect to change in the shape of the potential $V(\phi)$ or of the equation describing the field χ, so long as the small ϕ behavior of either field is left unchanged. This allows us to utilize some of the results related to the Mathieu equation in investigating stochastic resonance.

Inspection of the phase of the functions χ_k near the points where $\phi(t) = 0$ reveals one of the most important differences between broad-band resonance in Minkowski space and in an expanding universe. In the case of Minkowski space, we see that the phases of χ_k near where $\phi = 0$ are all equal. It is useful to think of this in terms of a useful anaolgy: in order to open a swinging door by a small

force, one must apply it periodically, "in resonance" with the motion of the door.

Such a regime is impossible in an expanding universe, however, because the frequency of χ_k oscillations is proportional to Φ, which decreases in time. As a result, the frequency of oscillations of the modes χ_k decreases significantly with each ϕ oscillation. When q is large, therefore, the phases of the field χ_k at successive moments when $\phi(t) = 0$ are essentially uncorrelated. Returning to our previous analogy, our door is vibrating with a large and ever changing frequency, so it is very difficult to push it at the proper moment once, let alone many times in a row. Qualitatively speaking, this is why the amplitude of the field χ_k experiences an occasional decrease or two.

While in light of this one might believe that broad parametric resonance in an expanding universe is impossible, this is not the case. To help visualize why, consider the following example: at each instant of particle production, let us assume that there is a 50–50 chance of either increasing or decreasing the number of particles by a factor of 10. We begin with 10 particles in each of two modes, and consider the evolution—we get 1 particle in the first mode and 100 particles in the second. In other words, the total number of particles in this example increases by a factor of 5, so parametric resonance does take place.

The stochastic resonance regime only occurs in the early stages of preheating, when the effective parameter q is very large and the resonance is very broad. As the amplitude of the field ϕ gradually decreases, q becomes smaller. The expansion of the universe also slows down, such that the field stays in each resonance band for progressively longer and longer times; eventually, the standard methods of investigation based on the Mathieu equation become useful again. It can be shown that stochastic resonance ends and the analytic techniques of this subsection may be replaced by the standard methods for the Mathieu equation after the first $q_0^{1/4}/\sqrt{2\pi}$ oscillations [1]; this many oscillations can take place before

q decreases from $q_0 \gg 1$ to $q \sim 1$. The transition from stochastic to regular broad-band resonance is manifested by a short plateau in the ln n_k versus t plot, which appears for $10 \lesssim t \lesssim 15$ in Figure 2.6. The system lies within this plateau when the mode X_k lies within the region of stability which divides the first and second instability bands of the Mathieu equation, and the resonance is no longer stochastic

In order to obtain a better understanding of this effect, Figure 2.7 displays the results of the same numerical simulation, but over a longer period of time. At $t > 15$, the amplitude still grows exponentially; however, the process does not look like a broad resonance. Exponential growth continues until the ϕ amplitude becomes smaller than m/g, which corresponds to $q \sim \frac{1}{3} - \frac{1}{4}$. Soon afterwards, for $t \approx 25$, resonance ceases and the amplitude stabilizes at some constant value.

By considering the moment when $g\Phi \approx \frac{gM_P}{3mt}$ is equal to m, we can estimate the time, t_f, and the number of oscillations, N_f, at the end of parametric resonance in an expanding universe:

$$t_f \approx \frac{gM_P}{3m^2}, \qquad N_f \approx \frac{gM_P}{6\pi m}. \tag{2.47}$$

For our particular simulation, with $m = 10^{-6}M_P$ and $g = 5 \times 10^{-4}$, this estimate gives $N_f \sim 26.5$, which is in good agreement with the numerical results displayed in Figure 2.7. There is about a 10% discrepancy between the results because our criterion for the end of the resonance $g\Phi \sim m$ was not quite precise: it turns out that the resonance ends somewhat earlier, at $g\Phi \sim 1.1m$.

One has $q \sim 1$, when $t \sim t_f/2$. As the system continues to evolve from $t_f/2$ to t_f, all resonance occurs in the first resonance band. This is narrow-band resonance, so there are no stochastic jumps from one resonance band to another. For times just prior to $t_f/2$ there was no resonance, as the field was in the stable region between the first and second instability bands.

It can be seen in Figure 2.7 that the amplitude X_k continues to grow slowly,

even after the resonance terminates and n_k becomes constant. We can understand this by noting that as the universe expands, the momentum of each mode is gradually redshifted, which leads to a growth of χ_k even though n_k does not change. This further illustrates the importance of the proper choice of variables used to describe parametric resonance.

Apart from a small stable region near $t \sim 12$, the slope of the curve ln n_k remains almost constant up to $t \sim 25$. For the case depicted in Figures 2.5–2.7, we have that the occupation number n_k grows exponentially with characteristic exponent $\mu_k \sim 0.13$.

Table 2.1 presents a sampling of results for several different values of the coupling constant g over the interval from 0.9×10^{-4} to 10^{-3} as an illustration of the stochastic nature of the resonance in this theory

As can be seen from the table, over this range of g, the initial momentum is comparable to m but slightly smaller than the typical initial width of the resonance $k_*/2$, which increases from $2m$ to about $5m$ as g increases throughout the interval. The reason why k is usually somewhat smaller than $k_*/2$ is very simple. The resonance is in the broad-band regime for the first half of preheating; the second half of preheating occurs in the narrow-band regime. Narrow-band resonance is typically more efficient for smaller k. As an aside, we note that for $g \gtrsim 3 \times 10^{-4}$, the backreaction of produced particles becomes an important factor, tending to shorten the narrow-band stage [1].

Investigation of the leading mode is, in general, insufficient; in order to obtain the full picture, we must integrate over all possible modes. However, as the number of particles n_k is exponentially sensitive to k, the mode integral will be dominated by those trajectories which are close to the leading one. An anaologous situation exists in the theory of tunneling, where one finds the trajectory corresponding to the minimum of action, then calculates e^{-S} along this

g	k	μ	t_f	$\ln n_k$
0.9×10^{-4}	1.5	0.1	5	6
10^{-4}	2	0.14	5	9
1.1×10^{-4}	0.5	0.17	5.5	12
1.2×10^{-4}	1.5	0.12	6	9
1.3×10^{-4}	1	0.13	6.5	11
1.4×10^{-4}	2	0.12	7	11
1.5×10^{-4}	0.5	0.18	7	17
2×10^{-4}	3.5	0.12	11	16
3×10^{-4}	0.5	0.14	14	27
5×10^{-4}	4	0.13	24	40
10^{-3}	6	0.12	48	75

Table 2.1: The initial momentum k (in units of m) corresponding to the fastest growing mode, the total increase of the number of particles $\ln n_k$ at the end of the resonance for this mode, the average value μ for this mode, and the time t_f (the number of oscillations of the field ϕ) at the end of the resonance over a range of values of the interaction strength g. Adapted from [1].

trajectory. Similarly, one can calculate the rate of growth of the total number of χ-particles by finding the leading trajectory and calculating the average value of μ along the trajectory.

Table 2.1 demonstrates that the effective values of μ_k and the final number of particles n_k produced by the resonance are very sensitive to small variations in g. The process is called stochastic resonance because of the chaotic manner in which these parameters change with small perturbations of g. Moreover, we see that for $g \sim 10^{-3}$, the occupation numbers n_k are extremely large. It can be shown that for $g \sim 10^{-4}$ backreaction of created particles is insignificant, but when $g \gtrsim 3 \times 10^{-4}$, backreaction becomes very significant, as it prevents the resonance from producing an indefinitely large number of particles [1].

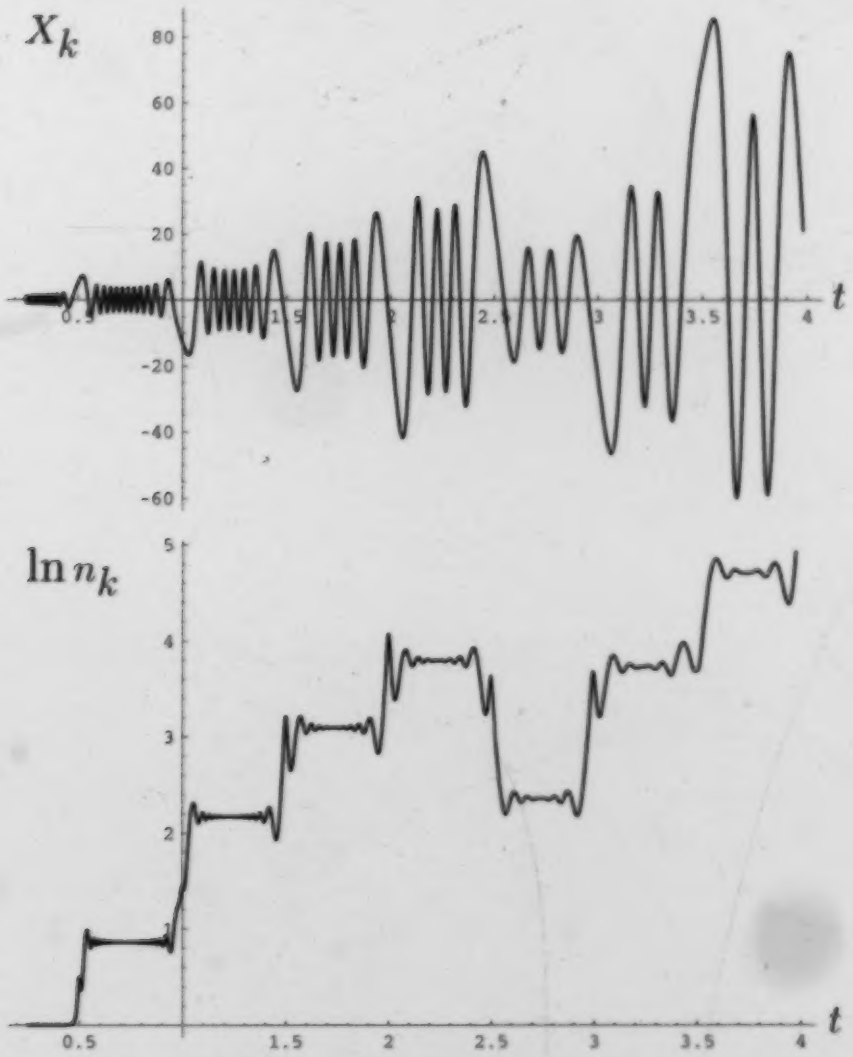

Figure 2.5: Early stages of parametric resonance in the theory $\frac{m^2\phi^2}{2}$ in an expanding universe with scale factor $a \sim t^{2/3}$ for $g = 5 \times 10^{-4}$, $m = 10^{-6} M_P$. According to our conventions (2.43), the initial value of the parameter q in this process is $q_0 \sim 3 \times 10^3$. Adapted from [1].

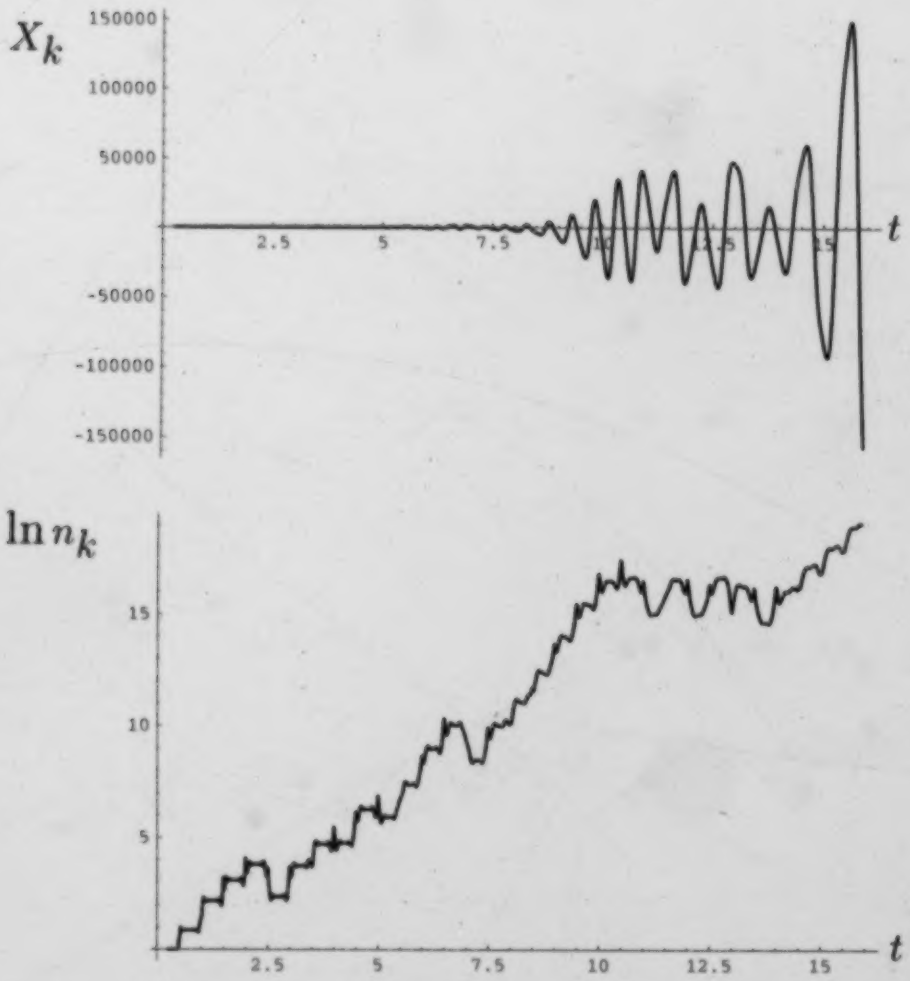

Figure 2.6: The same process as in Figure 2.5 over a longer period of time. The parameter $q = \frac{g^2\Phi^2}{4m^2}$ decreases as t^{-2} during this process, which gradually makes the broad resonance more and more narrow. As before, we show time t in units of $\frac{2\pi}{m}$, which corresponds to the number of oscillations of the inflaton field. Adapted from [1].

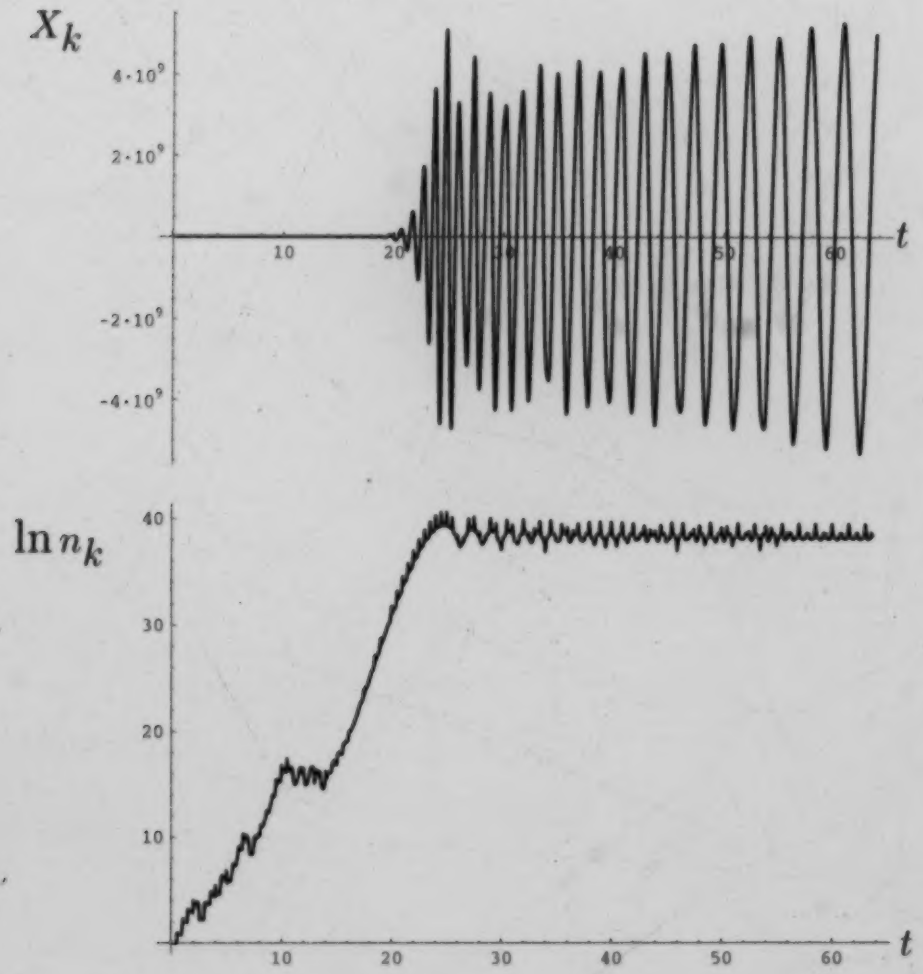

Figure 2.7: The same process as in Figures 2.5 and 2.6 over a longer period of time, which is shown in the units $\frac{mt}{2\pi}$, corresponding to the number of oscillations N. The figures show the growth of the mode X_k for the momentum k corresponding to the maximal speed of growth of n_k. In this particular case $k \sim 4m$. Adapted from [1].

2.3.5 Backreaction and Rescattering

Up to this point, we have treated χ as a test field which exists alongside two independent background fields $\phi(t)$ and $a(t)$. In certain situations, there is a resonant amplification of $\chi_k(t)$, which can be interpreted as an exponentially fast creation of χ particles. As we saw in the previous subsection, resonance in an expanding universe begins, in general, in the broad-band regime, becomes narrow, and eventually disappears.

Because the χ field is exponentially unstable, the effects of its backreaction on the background dynamics should accumulate slowly until it affects the resonance itself. We therefore must consider two distinct stages. In the first stage of the process, we are able to neglect the backreaction of the created particles. This stage is, in general, rather long; if q was initially small enough ($q_0 \lesssim 10^3$), then preheating may end before backreaction can significantly affect the resonance [14]. However, when $q_0 \gtrsim 10^3$, then at some point in time, we enter the second stage of preheating, where the backreaction effects must be considered.

Backreaction can affect the resonance in several ways. For example, the effective masses of all particles and the frequency of inflaton oscillations are influenced by interactions with particles created by parametric resonance. Moreover, scattering of χ particles, both off each other and off the oscillating field $\phi(t)$, or "rescattering," can remove previously produced particles from the resonance.

In our model we have two important effects. To begin with, χ-particles can alter the frequency (m) of oscillations of the field $\phi(t)$. If m increases in the mode equation, the resonance becomes narrow and is eventually terminated. In addition, ϕ particles could be produced via the interaction of χ-particles with the oscillating field $\phi(t)$—in effect χ-particles scatter off of the oscillating field $\phi(t)$. With each interaction, a χ-particle knocks a ϕ-particle out of the zero-momentum condensate. Over a sufficiently long period of time, this scattering

destroys the oscillating field $\phi(t)$ by decomposing it into separate ϕ-particles.

2.3.6 Superheavy Particle Production

Preheating is particularly attractive as it provides the possibility for the copious production of particles with mass greater than the inflaton mass m. The production of superheavy particles with mass M a few times heavier than m is essential for various models of GUT baryogenesis [15]. While no such processes exist in either perturbation theory or the narrow-band regime, it is possible to produce superheavy χ-particles with mass $M \gg m$ in the broad-band regime.

To study this effect, we return to our considerations in Section 2.3.3, in particular to our derivation of the width of the resonance band (2.38). We proceed by adding a ϕ-independent mass $m_\chi(0) \equiv M$ to k^2 on the LHS of the equation

$$k^2 + M^2 \lesssim (g^2 \phi m_\phi \Phi)^{2/3} - g^2\phi^2. \tag{2.48}$$

As in our previous considerations, the maximal range of momenta over which particle production can occur corresponds to $\phi(t) = \phi_*$, where $\phi_* \approx \frac{1}{2}\sqrt{\frac{m_\phi \Phi}{g}}$. Particles produced at that epoch have a maximal value of momentum which we estimate as $k_{\rm max}^2 + M^2 = \frac{g m_\phi \Phi}{2}$. Therefore, our resonance becomes efficient for

$$g m_\phi \Phi \gtrsim 4M^2. \tag{2.49}$$

It is clear that when this condition is satisfied, the resonance decay of the allows for copious production of superheavy particles with $M \gg m$.

In an expanding universe, however, Φ and m_ϕ are time-dependent. In order for this mechanism of particle production to work, it is insufficient to only have $gm\Phi \gtrsim 4M^2$ at the very beginning of the process; the condition must be satisfied until close to the end of preheating.

As backreaction becomes more and more important, both m_ϕ and Φ change very rapidly, but their product remains almost constant, as the energy density of the field ϕ, which is proportional to $m_\phi^2\Phi^2/2$, is essentially constant until the very end of preheating. We are therefore only required to check that $gm\Phi \gtrsim 4M^2$ before backreaction begins to significantly affect our system. Essentially, we require

$$M \lesssim \frac{m}{\sqrt{2}} q_1^{1/4} \approx m \left(\frac{g\mu M_P}{3m} \ln^{-1} \frac{10^{12} m}{g^5 M_P} \right)^{1/2}. \tag{2.50}$$

As an example, we consider the case where $M = 2m$ and $g \approx 0.007$, which, in the normalization of [16], corresponds to $q_0 = 10^6$. Then (2.50) is satisfied, and considering both backreaction and rescattering, we observe $\langle \chi^2 \rangle$ is suppressed by about a factor of 3, which is relatively insignificant. Further investigation [1] indicates that for $g \gg 10^{-2}$ the process is completely unsuppressed. For g sufficiently large, (2.50) tells us that superheavy particles with $M \gg m$ can be produced. In particular, for $g \gtrsim 0.065$, we can produce χ-particles with $M = 10m$.

We may have overestimated the significance of the suppression of superheavy particle production, however. The resonance only becomes strongly suppressed for $k^2 \ll \frac{k_*^2}{4} \sim \frac{gm_\phi\Phi}{4}$. We can therefore relax the condition for the efficient preheating (2.49) slightly: $gm_\phi\Phi \gtrsim 2M^2$. This in turn gives us that significant suppression of superheavy particle production is not a factor for

$$M \lesssim m\, q_1^{1/4} \approx m \left(\frac{2g\mu M_P}{3m} \ln^{-1} \frac{10^{12} m}{g^5 M_P} \right)^{1/2}. \tag{2.51}$$

Returning to our earlier example, for $M = 10m$ we now have a weaker requirement, namely $g \gtrsim 0.036$.

Therefore, in our simple model at least, the production of superheavy particles during preheating is possible.

2.4 Conformal $\lambda\phi^4$ Models

2.4.1 Introduction

While the $\frac{m^2\phi^2}{2}$ model of the previous section is useful in qualitatively understanding many of the features common to all models of parametric resonance, each model has its own subtleties. Conformally invariant theories, such as chaotic inflation with $V(\phi) = \frac{\lambda}{4}\phi^4$ are of particular theoretical interest. Greene, Kofman, Linde, and Starobinsky [2] examined the structure of resonance in the conformally invariant $\frac{\lambda}{4}\phi^4$ theory; in this section, we survey their results.

2.4.2 Evolution of the Inflaton Field

Throughout this section, we will consider chaotic inflation based on the potential $V(\phi) = \frac{1}{4}\lambda\phi^4$, and which couples to the decay product bose fields χ as given in the conformally invariant Lagrangian

$$\mathcal{L} = \frac{1}{2}(\partial_\mu\phi)^2 - \frac{\lambda}{4}\phi^4 + \sum_m \left[\frac{1}{2}(\partial_\mu\chi_m)^2 - \frac{1}{2}g_m^2\phi^2\chi_m^2 - \frac{1}{2}\xi_m\mathcal{R}\chi_m^2\right], \qquad (2.52)$$

where χ_m stands for the m-th scalar field, which interacts with both the inflaton field through the coupling constant g_m and the scalar curvature $\mathcal{R}$ through the coupling constant ξ_m.

Strictly speaking, this model is conformally invariant only when $\xi_m = \frac{1}{6}$. However, as the average value of $\mathcal{R}$ vanishes when $\phi \ll M_p$, we obtain a reasonable approximation even if we take $\xi_m = 0$.

During inflation, the energy-momentum tensor is dominated by contributions from the inflaton field ϕ. Assuming that ϕ is sufficiently homogeneous and isotropic, we may write the Friedman equation for the flat FRW universe as

$$H^2 = \frac{8\pi}{3M_P^2}\left(\frac{1}{2}\dot{\phi}^2 + \frac{\lambda\phi^4}{4}\right), \qquad (2.53)$$

In addition, it follows from the Einstein equations that

$$\dot{H} = -\frac{4\pi\dot{\phi}^2}{M_P^2}. \tag{2.54}$$

The Klein Gordon equation of motion for the classical field $\phi(t)$ is

$$\ddot{\phi} + 3H\dot{\phi} + \lambda\phi^3 = 0. \tag{2.55}$$

As we have seen in preceding sections, when $\phi > M_P$, the friction term, $3H\dot{\phi}$, in (2.55) dominates $\ddot{\phi}$, while the potential term in (2.53) dominates the kinetic term, and inflation results, with the universe expanding as $a(t) = a_0 \exp(\int dt H(t))$. When ϕ decreases below M_P, the contributions from the friction term gradually becomes negligible and inflation terminates at $\phi \sim M_P/2$. The inflaton field then oscillates about the minimum of the effective potential with an initial amplitude $\Phi_0 \sim 0.1 M_P$.

The type of oscillations of the homogeneous scalar field depends on the shape of the effective potential. Unlike the results of the previous section, where we studied a $\frac{m^2\phi^2}{2}$ model, in the $\frac{\lambda}{4}\phi^4$ case, the inflaton oscillations are not sinusoidal. The amplitude Φ of oscillations of the scalar field ϕ asymptotically approaches

$$\Phi(t) \approx \frac{1}{\sqrt{t}}\left(\frac{3M_p^2}{8\pi\lambda}\right)^{1/4} \sim \frac{M_P}{10N} \tag{2.56}$$

as $t \to \infty$, where N is the number of oscillations after the end of inflation.

2.4.3 Conformal Variables

In order to find the form of the oscillations, we introduce a conformal transformation of the space-time metric and the fields. To this end, we define the conformal time

$$\eta = \int \frac{dt}{a(t)}, \tag{2.57}$$

and the conformal field,

$$\varphi = a\phi. \tag{2.58}$$

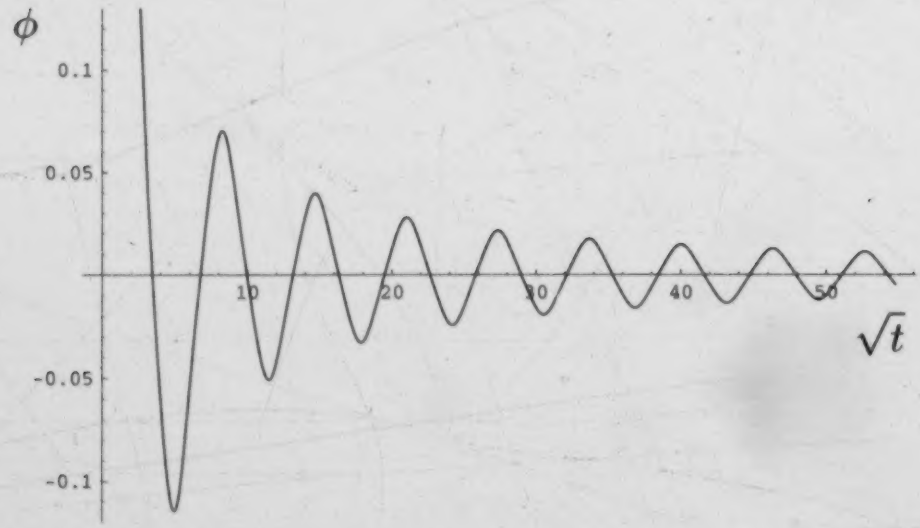

Figure 2.8: Oscillations of the field ϕ after inflation in the theory $\frac{\lambda\phi^4}{4}$. The value of the scalar field here and in all other figures in this section is measured in units of M_P, time is measured in units of $(\sqrt{\lambda}M_P)^{-1}$. Adapted from [2].

Expressed in these new coordinates $(\eta, \mathbf{x})$, the Klein-Gordon equation (2.55) for φ now takes on the form

$$\varphi'' + \lambda\varphi^3 - \frac{a''}{a}\varphi = 0, \tag{2.59}$$

where $'$ denotes differentiation with respect to the conformal time, $\frac{d}{d\eta}$. We may also reexpress the Friedmann equation (2.53) in terms of the conformal variables, obtaining

$$a'^2 = \frac{8\pi}{3M_P^2}\left[\frac{1}{2}\left(\varphi' - \varphi\frac{a'}{a}\right)^2 + \frac{\lambda\varphi^4}{4}\right]. \tag{2.60}$$

We note that the Klein-Gordon equation in conformal coordinates (2.59), is not of the same form as the equation for the theory $\frac{\lambda}{4}\varphi^4$ in Minkowski space; in order to obtain the Minkowski space form, we need to add the term $\frac{\phi^2}{12}\mathcal{R}$

to the Lagrangian. However, we will ignore this term for two reasons. First, shortly after the end of inflation, we have $\frac{\lambda}{4}\phi^4 \gg \frac{\phi^2}{12}\mathcal{R}$, and $\lambda\varphi^3 \gg \frac{a''}{a}\varphi$. Second, the energy-momentum tensor of the field ϕ in $\frac{\lambda}{4}\phi^4$ theory is effectively traceless ($p = \rho/3$) when averaged over several oscillations of the ϕ field [17]. Therefore, we are justified in taking $\mathcal{R} = 0$, $a(\eta) \sim \eta$, and $a'' = 0$, allowing us to cancel the last term in (2.59), obtaining

$$\varphi'' + \lambda\varphi^3 = 0\,. \tag{2.61}$$

If we also average the Friedmann equation (2.60) over several oscillations of the field, we may express it in a somewhat simpler form

$$a'^2 = \frac{8\pi}{3M_P^2}\left(\frac{1}{2}\varphi'^2 + \frac{\lambda\varphi^4}{4}\right) \equiv \frac{8\pi\rho_\varphi}{3M_P^2}, \tag{2.62}$$

where $\rho_\varphi = \frac{1}{2}\varphi'^2 + \frac{\lambda}{4}\varphi^4$ is the conformal energy density.

The conformal energy density ρ_φ can be expressed somewhat more simply as $\rho_\varphi = \frac{\lambda}{4}\tilde{\varphi}^4$, where $\tilde{\varphi}$ is the amplitude of the φ oscillations, which (2.61) tells us is constant. Then we have, considering (2.62),

$$a(\eta) = \sqrt{\frac{2\pi\lambda}{3}}\frac{\tilde{\varphi}^2}{M_P}\eta, \qquad t = \sqrt{\frac{\pi\lambda}{6}}\frac{\tilde{\varphi}^2}{M_P}\eta^2. \tag{2.63}$$

It is clear from the above result that $a'' = 0$, which is consistent with our earlier approximation.

We can reduce our Klein-Gordon equation (2.61) to the form of the canonical equation for an elliptic function. To do so, we introduce a dimensionless conformal time variable

$$x \equiv \sqrt{\lambda}\tilde{\varphi}\eta = \left(\frac{6\lambda M_P^2}{\pi}\right)^{1/4}\sqrt{t}. \tag{2.64}$$

This allows us to rescale the function $\varphi \equiv a\phi = \tilde{\varphi}f(x)$, where $f(x)$ is a function which satisfies the canonical equation for the elliptic function and is normalised

such that its amplitude is 1. The integral of the canonical equation for the elliptic function, $f'^2 = \frac{1}{2}(1 - f^4)$, is solved by an elliptic cosine

$$f(x) = \mathrm{cn}\Big(x - x_0, \frac{1}{\sqrt{2}}\Big). \tag{2.65}$$

It is quite clear that oscillations in this theory are not sinusoidal. Moreover, from our conformal transformation, we have that the energy density of the ϕ field decreases as a^{-4}.

The solution (2.65) has many interesting properties. For example, it can be matched to the solution describing the slow rolling of the field φ at the end of inflation with the choice $x_0 \approx 2.44$. The period of the oscillations, expressed in units of the conformal time x, is given by $T = 4K(\frac{1}{\sqrt{2}}) = \frac{\Gamma^2(1/4)}{\sqrt{\pi}} \approx 7.416$, where K is the complete elliptic integral of the first kind. Since the value of f^4 averaged over a period is $\frac{1}{3}$, we have that the potential energy density $\frac{1}{4}\lambda\varphi^4$ averaged over a period of oscillation is given by $\frac{\lambda}{12}\varphi^4 = \frac{1}{3}\rho_\varphi$, while the average kinetic energy $\frac{1}{2}\varphi'^2$ can be expressed as $\frac{2}{3}\rho_\varphi$.

The elliptic cosine can be written as an infinite series of cosine functions

$$f(x) = \frac{8\pi\sqrt{2}}{T}\sum_{n=1}^{\infty}\frac{e^{-\pi(n-1/2)}}{1+e^{-\pi(n-1/2)}}\cos\frac{2\pi(2n-1)x}{T}. \tag{2.66}$$

The series can be approximated by its leading term, $0.9550\cos 0.8472x$—all subsequent terms have very small amplitudes by comparison. However, while the first harmonic term is a good approximation of the actual form of oscillations, the small corrections resulting from higher order terms in (2.66) are crucial in determining the structure of the resonance for our theory.

2.4.4 Quantum Fluctuations of the ϕ and χ Fields

Once more, as in the previous section, we consider the interaction between a *classical* inflaton field, ϕ, and a massless, *quantum* scalar field, $\hat{\chi}$, as described

by the Lagrangian (2.52). In the Heisenberg representation of the quantum scalar field $\hat{\chi}$, the Fourier mode decomposition can be written as

$$\hat{\chi}(t,\mathbf{x}) = \frac{1}{(2\pi)^{3/2}} \int d^3k \left(\hat{a}_k \chi_k(t) e^{-i\mathbf{k}\cdot\mathbf{x}} + \hat{a}_k^+ \chi_k^*(t) e^{i\mathbf{k}\cdot\mathbf{x}} \right), \tag{2.67}$$

where $\hat{a}_k$ and $\hat{a}_k^+$ are annihilation and creation operators. In a flat FRW universe, the mode eigenfunction corresponding to comoving momentum $\mathbf{k}$ satisfies

$$\ddot{\chi}_k + 3\frac{\dot{a}}{a}\dot{\chi}_k + \left(\frac{k^2}{a^2} + g^2\phi^2 \right) \chi_k = 0, \tag{2.68}$$

where $k = \sqrt{\mathbf{k}^2}$ and we have neglected the interaction term $\sim \xi\phi^2\mathcal{R}$.

However, in contrast to our previous results, the self-interaction term $\frac{1}{4}\lambda\phi^4$ generates fluctuations of the inflaton field itself in an analogous manner. The eigenmodes of the inflaton field, $\phi_k(t)$, satisfy the equation

$$\ddot{\phi}_k + 3\frac{\dot{a}}{a}\dot{\phi}_k + \left(\frac{k^2}{a^2} + 3\lambda\phi^2 \right) \phi_k = 0. \tag{2.69}$$

The form of this equation is identical to that of (2.68) for the particular choice $g^2 = 3\lambda$. Therefore, the fluctuations ϕ_k due to the self interactions of the ϕ field in the $\frac{1}{4}\lambda\phi^4$ model is simply a special case of the general fluctuations described in (2.68).

Now, both the physical momentum, $\mathbf{p} = \frac{\mathbf{k}}{a(t)}$, and the background field, $\phi(t) = \frac{\varphi}{a(t)}$, experience equivalent redshifts. We are therefore able to eliminate the redshifting of momenta from the evolution of χ_k through the introducion of a conformal transformation of the mode function $X_k(t) = a(t)\chi_k(t)$. This allows us to rewrite the mode equation for $X_k(t)$ in terms of the dimensionless conformal time x defined in (2.64) as

$$X_k'' + \left(\kappa^2 + \frac{g^2}{\lambda} \mathrm{cn}^2\left(x, \frac{1}{\sqrt{2}} \right) \right) X_k = 0, \tag{2.70}$$

where we have dropped the initial value $x_0 = 2.44$ for the sake of simplicity. The above equation is completely independent of the expansion of the universe—we

have succeeded in reducing our problem to an analogous simpler problem in Minkowski space-time. Such simplifications are a special feature for conformally invariant theories.

In particular, setting $g^2 = 3\lambda$, we have for the fluctuations of the field $\varphi = a\phi$

$$\varphi_k'' + \left(\kappa^2 + 3\mathrm{cn}^2\left(x, \frac{1}{\sqrt{2}}\right)\right)\varphi_k = 0. \tag{2.71}$$

The mode equation (2.70) represents our master equation for the investigation of resonance in our $\frac{\lambda}{4}\phi^4 + \frac{1}{2}g^2\phi^2\chi^2$ theory. As the comoving momentum k enters into the mode through

$$\kappa^2 = \frac{k^2}{\lambda\bar{\varphi}^2}, \tag{2.72}$$

we see that the natural units of momenta k are $\sqrt{\lambda}\bar{\varphi}$. The master equation (2.70) describes an ensemble of oscillators, X_k, with frequencies

$$\omega_k^2 = \kappa^2 + \frac{g^2}{\lambda}\mathrm{cn}^2\left(x, \frac{1}{\sqrt{2}}\right), \tag{2.73}$$

which vary periodically with the conformal time x. By analogy with the Mathieu equation, we expect some of the solutions X_k to be exponentially unstable with $X_k(x) \propto e^{\mu_k x}$. Choosing the vacuum positive-frequency initial condition, $X_k(x) \simeq \frac{e^{-i\kappa x}}{\sqrt{2\kappa}}$, we anticipate that the oscillations of the background inflaton field will lead to exponentially fast creation of χ-particles $n_k \propto e^{2\mu_k x}$. The dimensionless coupling parameter g^2/λ determines the intensity of the dependence of ω_k on the oscillations $\mathrm{cn}^2(x, \frac{1}{\sqrt{2}})$. In our conformal theory, therefore, broad-band parametric resonance does not require a large initial amplitude of the inflaton field, ϕ_0, as it did for the toy $\frac{m^2\phi^2}{2}$ model [12] considered in the previous subsection. The structure of parametric resonance in our theory is ultimately dependent on the the combination of parameters g^2/λ.

The mode equation (2.70) is a variant of the Lamé equation [18]. Kofman, Linde, and Starobinsky [1] first noticed that this was the case for preheating;

in-depth studies of models with $g^2 = \lambda$ were conducted in [19] and [20]. Greene, Kofman, Linde, and Starobinsky [2] performed both numerical and analytical investigations of the Lamé equation in the conformally invariant theory $\frac{1}{4}\lambda\phi^4 + \frac{1}{2}g^2\phi^2\chi^2$ for arbitrary choices of the parameter $\frac{q^2}{\lambda}$. In the next subsection, we present the stability diagram for the Lamé equation (2.70) in terms of variables κ^2 and $\frac{q^2}{\lambda}$.

2.4.5 The Stability Diagram in Conformal Theories

In the previous subsection, we reduced the equation for interactions between vacuum fluctuations and the oscillating inflaton field ϕ in conformal theories to a simpler, but equivalent, problem in Minkowski space. The resulting equation (2.70) contains only two parameters: $\frac{q^2}{\lambda}$, which encodes the strength of the interaction, and the conformal vacuum fluctuation momentum, κ. The solutions X_k of this equation are either stable or unstable, depending on our choices of κ and $\frac{q^2}{\lambda}$. For the early stages of preheating, we may neglect backreaction, and the solutions of (2.70) give an accurate description of the behaviour of the induced unstable fluctuation by themselves. Now, as opposed to the stability for the Mathieu equation, which is well known and can be found in many textbooks, see e.g. [21], the stability diagram for the Lamé equation was apparently unpublished until its inclusion in Greene, Kofman, Linde, and Starobinsky [2]. Therefore, in this subsection we shall examine various features of the Lamé stability diagram in terms of the two parameters $\left(\kappa^2, \frac{q^2}{\lambda}\right)$.

A typical resonant solution of (2.70) is plotted in Figure 2.9. The upper plot compares the amplification of the real part of the eigenmode $X_k(x)$ (solid curve) with the evolution of the oscillating inflaton background (dotted curve).

As we saw in the previous section, a tremendous amount of information is encoded in the evolution of the comoving number density of created χ-particles

with comoving momentum k, n_k, as this is an adiabatic invariant. We can define n_k in terms of the comoving energy density and the energy per particle, ω_k, as follows

$$n_k = \frac{\omega_k}{2}\left(|X_k|^2 + \frac{|\dot{X}_k|^2}{\omega_k^2}\right) - \frac{1}{2}. \tag{2.74}$$

The lower plot of Figure 2.9 contrasts the evolution of the natural logarithm of n_k (solid curve) with that of the inflaton field (dotted curve). As we can see, after an initial period of transition, the solution settles down to an approximately linear trend with $\ln n_k \approx 2\mu_k x$, where μ_k is the characteristic exponent of the unstable solution.

We can construct the stability diagram for the Lamé equation through numerically solving (2.70) over a range of κ and $\frac{q^2}{\lambda}$ and exploiting the simple relation $\ln n_k \approx 2\mu_k x$ to extract the characteristic exponent. (Note that in regions of stability the characteristic exponent is imaginary, corresponding to oscillatory solutions of the mode equation.) The stability diagram is plotted in Figure 2.10, where shaded (unshaded) regions correspond to the instability (stability) bands. It is clear from Figure 2.10 that maximal values of the characteristic exponent occur where $\kappa^2 = 0$ and $\frac{q^2}{\lambda}$ lies between alternating values of $\frac{n(n+1)}{2}$, where n is an integer. (In other words, the first band lies between $n = 1 \Rightarrow \frac{q^2}{\lambda} = 1$ and $n = 2 \Rightarrow \frac{q^2}{\lambda} = 3$, the second band lies between $n = 3 \Rightarrow \frac{q^2}{\lambda} = 6$ and $n = 4 \Rightarrow \frac{q^2}{\lambda} = 10$, and so on.)

While this stability diagram shares some similarities with that of the Mathieu equation, there are important differences. For example, on the Mathieu equation stability diagram, there are infinitely many instability bands for every q, which is analogous to the parameter $\frac{q^2}{\lambda}$ in our theory. This is in sharp contrast to the case of the Lamé equation, where some of the instability bands shrink to points for particular values of $\frac{q^2}{\lambda}$. In particular, in Figure 2.10 there is only one non-trivial instability band, as all higher order bands shrink to nodes as $\frac{q^2}{\lambda}$ approaches 1

and 3.

In fact, there are only a finite number of instability bands for positive κ^2 when $\frac{g^2}{\lambda} = \frac{n(n+1)}{2}$, although all other values of $\frac{g^2}{\lambda}$ have an infinite number of instability bands, in close analogy with the Mathieu equation. In fact, for $\frac{g^2}{\lambda} \ll 1$, the Lamé equation may be mapped onto the Mathieu equation with the parameters $A \approx 1.3932\kappa^2$ and $q \approx 0.3464\frac{g^2}{\lambda} \ll 1$ [2].

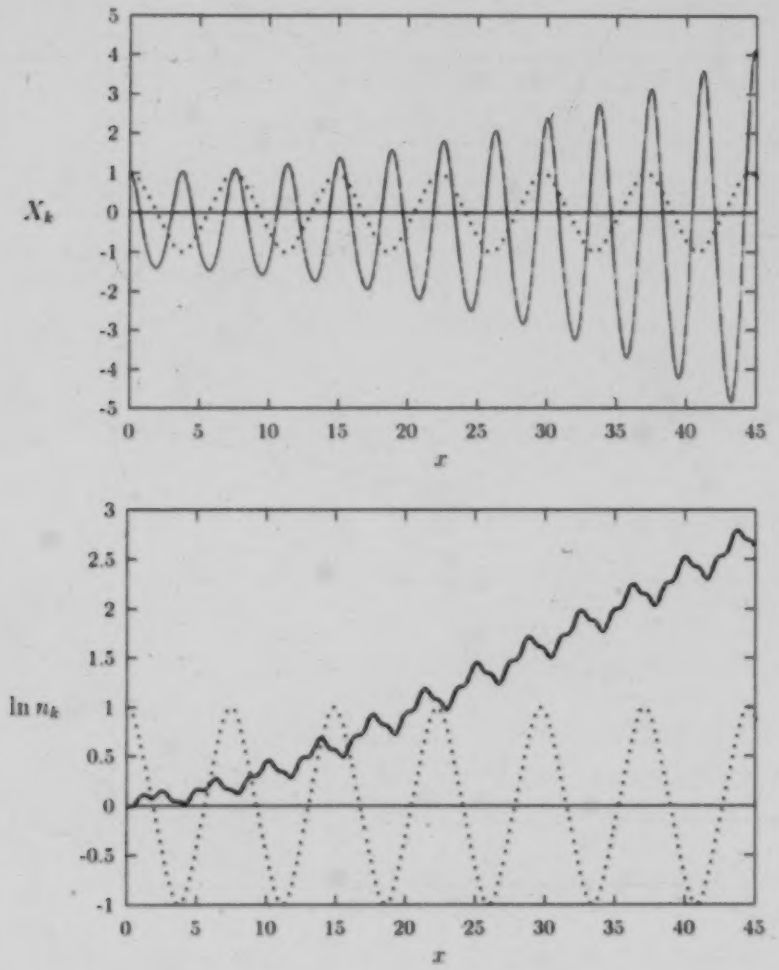

Figure 2.9: Resonant production of particles at the particular choice of rescaled comoving momentum $\kappa^2 = 1.6$, and the parameter $\frac{g^2}{\lambda} = 3$. The dotted curves show the oscillations of the background inflaton field. The upper plot shows the amplification of the real part of the eigenmode $X_k(x)$. The lower plot shows the logarithm of the comoving particle number density, n_k. In this case, $\mu_k \approx 0.035$. Adapted from [2].

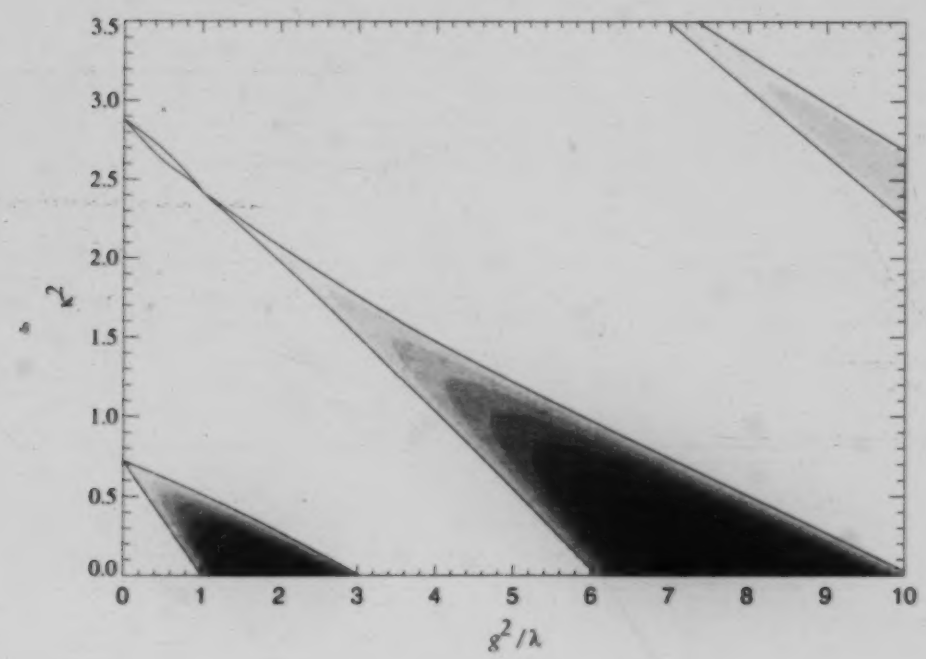

Figure 2.10: The stability diagram for the Lamé equation for fluctuations $X_k(x)$ in the variables $(\kappa^2, \frac{g^2}{\lambda})$, obtained from the numerical solution of equation (2.70). Shaded (unshaded) areas are regions of instability (stability). For instability bands, the darker shade implies a larger characteristic exponent μ_k. Altogether, there are 10 color steps. One color step corresponds to the increment $\Delta\mu_k = 0.0237$, so the darkest shade corresponds to maximal $\mu_k = 0.237$, the least dark shade in the instability bands corresponds to $\mu_k = 0.009$. For positive κ^2, there is only one instability band for the particular values of the parameter $\frac{g^2}{\lambda} = 1$ and 3, because the higher bands shrink into nodes as $\frac{g^2}{\lambda}$ approaches 1 and 3. Adapted from [2].

2.5 "Instant Preheating"

2.5.1 Introduction

As we have seen in the preceding sections, in both $\frac{m^2\phi^2}{2}$ and $\frac{\lambda}{4}\phi^4$ theories of inflation, it is possible to produce superheavy particles during preheating. These effects are of great theoretical interest, as interactions and decays of superheavy particles at the GUT scale can lead to baryogenesis. Unfortunately, in the standard preheating treatments, the production of particles with masses on order of the GUT scale is fraught with difficulties; in particular, backreaction and rescattering of the final state products often prevent sufficient parametric resonance from taking place.

In a recent paper, Felder, Kofman, and Linde [3] came up with a new non-perturbative mechanism for reheating, which they dubbed "instant preheating." It does not require any form of parametric resonance; indeed, it is even successful in non-oscillatory inflationary models. Therefore, we shall devote this section to an examination of the key features of models of "instant preheating."

2.5.2 Instant Preheating: The Basic Concept

Consider a chaotic inflation model with effective potential $\frac{m^2}{2}\phi^2$ or $\frac{\lambda}{4}\phi^4$ and interaction term $-\frac{1}{2}g^2\phi^2\chi^2$. In such models, we recall from Chapter 1 that inflation occurs for $|\phi| \gtrsim \frac{M_P}{3}$. We begin by assuming that inflation occurs for ϕ initially large and negative, with inflation ending at $\phi \sim -0.3M_P$. The field ϕ rolls to $\phi = 0$, overshoots, reaches a turning point around $10^{-1}M_P \sim 10^{18}$ GeV, then rolls back and begins to oscillate about $\phi = 0$, where the amplitude decreases over the course of many oscillations. In the broad-band regime, for a large enough coupling constant g ($g \gtrsim 10^{-4}$), χ particles are first produced when the scalar field ϕ crosses $\phi = 0$ after the end of inflation [1, 2, 12], and exponential growth

of occupation numbers occurs in some modes. As we shall see, in certain cases, efficient preheating can occur using only those particles which are produced when ϕ first passes through zero.

At each point in time where $\phi = 0$, a small fraction of the energy of the inflaton field $\sim 10^{-2}g^2$ is transferred to the χ particles. In the standard treatment of parametric resonance, we saw that this energy increases exponentially over several oscillations of the inflaton field. Unfortunately, parametric resonance can be either disrupted or prevented if the produced χ particles are taken out of the resonance bands through such mechanisms as backreaction, rescattering, or the decay of the χ's. If the χ particles decay (to fermions ψ via the coupling $h\bar{\psi}\psi\chi$, for example), however, parametric resonance may be replaced by another interesting effect, namely that the energy density of the χ particles, in the instant when they decay, has the potential to be substantially larger than their energy density when they were originally created.

Once created, as we have seen in the two previous subsections the number density of χ particles, n_χ, remains practically constant until they decay, as n_χ is an adiabatic invariant. The effective mass of each χ particle, on the other hand, grows as $m_\chi = g\phi$ as the field ϕ increases. In essence, the χ particles are being "fattened" by the energy of the ϕ field. The decay width for these fattened χ particles is largest when the χ's have the greatest mass, which corresponds to when ϕ is at or near the turning point of its oscillations $\phi \sim 10^{-1}M_P$.

At this point in time, the fattened χ particles can decay to two fermions with masses up to $m_\psi \sim \frac{g}{2}10^{-1}M_P$. For $g \sim 1$, we see that we may produce particles with masses which are two orders of magnitude larger than the maximum mass of the particles which can be produced by parametric resonance [1, 2, 12]. As we can see, the chain reaction $\phi \rightarrow \chi \rightarrow \psi$ is a remarkably efficient mechanism for transferring energy from the inflaton field to matter.

It is also possible that these superheavy ψ particles eventually dominate the total energy density of matter. In the previous subsection, we saw that the energy density of the oscillating inflaton field in $\frac{\lambda}{4}\phi^4$ theory decreases as a^{-4} in an expanding universe. On the other hand, the energy stored in the nonrelativistic ψ particles is only redshifted as a^{-3}, allowing their energy density to rapidly become dominant. When these ψ's subsequently decay, a complete reheating of the universe should result.

Instant preheating draws its name from the fact that the production of χ's and ψ's occurs within less than one oscillation of the inflaton field. Like parametric resonance, it is a completely nonperturbative effect, and allows for the production of particles with momenta and masses many orders of magnitude greater than the inflaton mass, an impossibility within the context of the elementary perturbative theory of reheating of [6, 7]. In the following subsection we will consider various aspects of the instant preheating scenario in considerably more detail.

2.5.3 A Simple Model

Within the chaotic inflation paradigm, we choose an effective potential $V(\phi) = \frac{m^2}{2}\phi^2$, and an interaction Lagrangian $-\frac{1}{2}g^2\phi^2\chi^2 - h\bar{\psi}\psi\chi$. In order to satisfy the microwave background anisotropy, we are required to take $m = 10^{-6}M_P$ [5]; for simplicity we will additionally assume that χ particles do not have a bare mass. As we only have efficient preheating in this model for $g \gtrsim 10^{-4}$ [1, 2, 12], we will have $gM_P \gtrsim 10^2 m$, where $m \sim 10^{-6}M_P$ is the inflaton mass. Since at the end of inflation, $\phi \sim M_P/3$, the effective mass $g|\phi|$ of the χ field is initially much greater than m. Although m_χ decreases proportionally to the ϕ field, the process remains adiabatic for a long period of time.

Particle production occurs when the adiabaticity condition is violated; we may express this condition as $|\dot{m}_\chi| > m_\chi^2$, or, in the language of the model

under consideration, as $g|\dot{\phi}| > g^2\phi^2$. If we treat the motion of the ϕ field as being analogous to that of a harmonic oscillator, we have that $|\dot{\phi}_0| = m\Phi$, where $|\dot{\phi}_0|$ is the velocity of the field at the minimum of the effective potential and $\Phi \sim 10^{-1}M_P$ is the amplitude of the first oscillation. Therefore, the process is nonadiabatic when $g\phi^2 \lesssim m\Phi$; in other words, adiabaticity is violated over a range $-\phi_* \lesssim \phi \lesssim \phi_*$, where $\phi_* \sim \sqrt{\frac{m\Phi}{g}}$ [1, 2, 12]. If we impose the condition $g \gg 10^{-4}$, requiring efficient preheating, then the interval $-\phi_* \lesssim \phi \lesssim \phi_*$ becomes very small in comparison to the amplitude of the oscillations Φ. Therefore, particle production must occur almost instantaneously, within an interval of time

$$\Delta t_* \sim \frac{\phi_*}{|\dot{\phi}_0|} \sim (gm\Phi)^{-1/2}. \tag{2.75}$$

During preheating, as this time interval is very small compared to the age of the universe, we are justified in neglecting all effects related to the expansion of the universe. Therefore, combining the above result with the uncertainty principle, we find that typical momenta for particles created in this manner are $k \sim (\Delta t_*)^{-1} \sim (gm\Phi)^{1/2}$.

Now, we have that the occupation number $n_k = 0$ until ϕ passes through a small region $-\phi_* \lesssim \phi \lesssim \phi_*$. At this point, the occupation number suddenly (within the time Δt_*) acquires the value [1, 2, 12]

$$n_k = \exp\left(-\frac{\pi k^2}{gm\Phi}\right), \tag{2.76}$$

which again remains constant until the inflaton field passes through the point $\phi = 0$ once again. For a more in-depth description of this process, see [1].

We can rewrite (2.76) in a more general form. Since χ particles are only produced when the ϕ field is very close to $\phi = 0$, we can express $\phi(t)$ in the region of particle production as $\phi(t) \approx \dot{\phi}_0(t - t_0)$; therefore, model-specific quantities such as $V(\phi)$, m, or Φ are unimportant in our considerations—we only need to know the maximum velocity of the field, $\dot{\phi}_0$. We therefore replace $m\Phi$ with $|\dot{\phi}_0|$

in (2.76). Moreover, the result continues to hold for massive particles χ with the substitution of $k^2 + m_\chi^2$ for k^2, where m_χ is the bare mass of the χ particles at $\phi = 0$. Therefore, the general form of (2.74) is

$$n_k = \exp\left(-\frac{\pi(k^2 + m_\chi^2)}{g|\dot{\phi}_0|}\right), \tag{2.77}$$

which we integrate to obtain the number density of χ particles

$$n_\chi = \frac{1}{2\pi^2}\int_0^\infty dk\, k^2 n_k = \frac{(g\dot{\phi}_0)^{3/2}}{8\pi^3}\exp\left(-\frac{\pi m_\chi^2}{g|\dot{\phi}_0|}\right). \tag{2.78}$$

It can be shown that for the $\frac{m^2\phi^2}{2}$ theory under consideration here, we have $|\dot{\phi}_0| = 10^{-7}M_P^2$; alternatively, with $V(\phi) = \frac{\lambda}{4}\phi^4$, where $\lambda = 10^{-13}$, the velocity is smaller, $|\dot{\phi}_0| = 6 \times 10^{-9}M_P^2$. In particular, for $g \sim 1$ in the theory $\frac{m^2}{2}\phi^2$, we may produce scalar particles with mass up to $m_\chi \sim 2 \times 10^{15}$ GeV, in agreement with the standard constraints found in the literature [1, 2, 12, 14, 15, 24].

We now turn our attention to the case $m_\chi^2 \lesssim g|\dot{\phi}_0|$. From the above result, we find that the number of particles produced is not exponentially suppressed

$$n_\chi \approx \frac{(g\dot{\phi}_0)^{3/2}}{8\pi^3}. \tag{2.79}$$

From (2.77), we know that when each χ particle is produced, they typically possess an energy $\sim (g|\dot{\phi}|/\pi)^{1/2}$, so we have that the total energy density is

$$\rho_\chi \sim \frac{(g\dot{\phi}_0)^2}{8\pi^{7/2}}, \tag{2.80}$$

which, in turn, gives us that the ratio of ρ_χ to the total energy density of the inflaton field $\rho_\phi = \dot{\phi}_0^2/2$ of the scalar field ϕ is

$$\frac{\rho_\chi}{\rho_\phi} \sim 5 \times 10^{-3}\, g^2. \tag{2.81}$$

Provided one has the interaction term $-\frac{1}{2}g^2\phi^2\chi^2$, the above result is practically model-independent.

Let us now consider implications of (2.78) when we have $m_\chi^2 \sim g|\dot{\phi}_0|$. While particle production of such particles is essentially unaffected during the first oscillation, it becomes exponentially suppressed during all subsequent oscillations, since $|\dot{\phi}|$ decreases as the universe expands, violating the condition $m_\chi^2 \lesssim g|\dot{\phi}|$. No new χ particles are created after the first oscillation. However, as we saw above, these new particles may be unnecessary, since the energy density of any χ's produced may redshift more slowly than that of the inflaton, eventually dominating the energy-momentum tensor $T_{\mu\nu}$. The subsequent decay of these χ particles completes the reheating of the universe.

Let us now consider the enhancement of preheating which occurs if we use the mechanism described in the previous subsection. Assume that the particles χ survive while the field ϕ rolls from $\phi = 0$ to the turning point ϕ_1. Now, for $\frac{m^2}{2}\phi^2$ theories, $\phi_1 \approx 0.07\, M_P$, while in $\frac{\lambda}{4}\phi^4$ theories, $\phi_1 \approx 0.12\, M_P$. At the turning point, the effective mass of the χ's is given by $g\phi_1 \sim 10^{-1} g M_P$, so they are nonrelativistic, with total energy density (for the case $V(\phi) = \frac{m^2}{2}\phi^2$)

$$\rho_\chi = m_\chi n_\chi \approx 10^{-1} g M_P \frac{(g\dot{\phi}_0)^{3/2}}{8\pi^3} \sim 10^{-14} g^{5/2} M_P^4. \tag{2.82}$$

Using the fact that $|\dot{\phi}_0| \sim 10^{-7} M_P^2$ in the theory under consideration, we compute the ratio of ρ_χ particles to the energy density of the inflaton field $\rho_\phi \sim \dot{\phi}_0^2/2$, obtaining

$$\frac{\rho_\chi}{\rho_\phi} \sim 10^{-3} |\dot{\phi}_0|^{-1/2} M_P g^{5/2} \sim 2\, g^{5/2}. \tag{2.83}$$

In the case where we have efficient preheating, we have $g \gtrsim 10^{-4}$ [1, 2, 12], forcing this ratio to be much larger than the one computed in (2.81).

Instant preheating is the most efficient if the majority of the χ's decay when the field ϕ reaches ϕ_1. We therefore wish to ensure that the lifetime of the created particles χ is close to $\Delta t \sim \pi m^{-1}/4$. At tree level, the decay rate of χ particles

into fermions ψ is given by [1, 2, 12]

$$\Gamma(\chi \to \psi\psi) = \frac{h^2 m_\chi}{8\pi} = \frac{h^2 g|\phi|}{8\pi}. \tag{2.84}$$

Since the decay rate is directly proportional to $|\phi|$, χ particles tend to decay for $|\phi|$ large. We can construct a model in which the χ particles decay when the field ϕ reaches $|\phi_1| \approx 0.07 M_P$ by setting

$$h^2 g \sim \frac{500m}{M_P} \sim 5 \times 10^{-4}. \tag{2.85}$$

When $|\phi|$ reaches $0.07M_P$, the particles χ have effective mass $m_\chi = g|\phi| \sim 0.07 g M_P$. These particles can, in turn, decay to two fermions ψ if $m_\psi < 0.035\, g M_P$. Therefore, after the first half of an oscillation, the scalar field ϕ can produce fermions with mass up to $0.035\, g M_P$. Let us illustrate the effectiveness of this scenario by considering two examples: for a theory with $g \sim 10^{-1}$, $h \sim 7 \times 10^{-2}$, fermions with mass $m_\psi \sim 4 \times 10^{16}$ GeV can be produced, while for the case of $g \sim 1$, $h \sim 2 \times 10^{-2}$, the maximal fermion mass is about 4×10^{17} GeV.

Now, (2.83) tells us that $\frac{\rho_\chi}{\rho_\phi}$ is initially suppressed as $2g^{5/2}$. In general, however, this suppression turns out to be rather weak, and we are still able to accomplish a complete reheating of the universe if ρ_ψ decays more slowly than ρ_ϕ, ρ_χ, etc., and eventually dominates the dynamics of the universe.

If we have $h^2 g \gg 5 \times 10^{-4}$, the χ particles tend to decay before ϕ reaches its maximal value $\phi_1 \sim 0.1 M_P$, which tends to reduce the efficiency of instant preheating. However, the χ's cannot decay unless $m_\chi = g|\phi| > 2m_\psi$ becomes greater than $2m_\psi$, so the efficiency of instant preheating is preserved to some extent, even for very large $h^2 g$.

Conversely, when $h^2 g \ll 5 \times 10^{-4}$, the particles χ survive for more than one oscillation. This is not entirely negative, as parametric resonance becomes viable, and we will have efficient preheating according to [1, 2, 12]. In addition,

since the oscillating field still spends some time at $\phi \sim \phi_1$, some production of superheavy fermions is still possible.

We should also note that since we have no need for exponential growth of occupation numbers within the instant preheating scenario, we can also have instant preheating of fermions [4, 27], as we merely require the violation of adiabaticity in the change of the mass of the produced particle. The efficiency of fermionic instant preheating can be further increased if the fermions ψ have decay channels to other fermions and bosons.

2.5.4 Quintessence and Instant Preheating

Instant preheating is even more effective for models with "quintessential" potentials, where $V(\phi)$ behaves as $\frac{m^2}{2}\phi^2$ or $\frac{\lambda}{4}\phi^4$ for $\phi < 0$, and slowly vanish when ϕ becomes positive. Ford and Spokoiny first proposed quintessential models of inflation, and there has been much recent work within this paradigm by several other authors [25].

In the previous subsection, we saw that instant preheating is essentially independent of our choice of $V(\phi)$—the number of particles produced depends only on g and $|\dot{\phi}_0|$. In quintessential-type theories where $V(\phi)$ gradually vanishes at large ϕ, ϕ increases to $\phi \sim M_P$ before it stops or is turned back by the $3H\dot{\phi}$ friction term. Therefore, the decay product χ's can acquire masses $m_\chi \sim gM_P$; for g sufficiently large ($g \sim 10^{-1}$), the subsequent decay of χ particles can produce superheavy particles ψ with masses $m_\chi \sim 10^{17}$–10^{18} GeV. As we can see, the value of the ϕ field can reach values an order of magnitude larger than in our $\frac{m^2\phi^2}{2}$ model. Therefore, as the energy density ρ_ϕ redshifts as the universe expands, we anticipate that ρ_χ will be much greater than the estimate $\rho_\chi = 2g^{5/2}\rho_\phi$ of the previous discussion.

In theories with quintessential potentials, the energy density of the inflaton

field ϕ decreases as a^{-6}—which is clearly *much* faster than the redshift of the energy density for any other matter in the universe, so preheating in these models is extremely efficient. In an extreme case where the χ's decay to relativistic particles immediately after they are produced, their energy density still dominates the dynamics of the universe after the universe has grown by a factor of $15g^{-1}$. If, instead, we consider the mechanism of the previous subsection, whereby χ particles "fatten" before decaying, we obtain a considerably larger energy density of produced particles, whose contributions are significantly larger than those of the inflaton field from a very early time, when the scale factor is given by $a \sim g^{-5/6}$.

Since backreaction of the χ's can force the field back to $\phi = 0$, we still require that the χ field rapidly decays to other particles. However, when g is small, both the number of produced particles and their interaction with the field ϕ are suppressed. Consequently, backreaction is only significant after a time interval $\Delta t \gg m^{-1}$ [31]. The constraints in this scenario are therefore much milder than those in scenarios where ϕ oscillates about a minimum of $V(\phi)$.

One can remove these constraints altogether if $V(\phi)$ only becomes flat for $\phi \gtrsim M_P$. For models of this form, backreaction never turns the scalar field ϕ back to $\phi = 0$, the decay of the particles χ may occur very late, and we have efficient preheating for any choice of g and h.

Consider a possible alternative scenario, in which χ's are stable with bare mass $m_\chi \sim 10^{16}$ GeV. Although the probability of particle production is exponentially suppressed in this case, the masses of these particles can still increase by as much as $g|\phi|$. This allows the production of superheavy weakly interacting massive particles (or WIMPS) with mass $m_\chi \gg 10^{16}$ GeV without requiring the decay of χ's to ψ's.

One other particularly interesting case arises if we consider stable χ particles

with bare masses $m_\chi \ll 10^{16}$ GeV. Since the χ's cannot decay, we could end up with the universe filled with too many superheavy WIMPS. However, in models where the potential only becomes flat for $\phi \gtrsim M_P$, ϕ rolls for a very long time, reaching values much greater than M_P, and driving the effective masses $g|\phi|$ of the χ's larger than M_P. Naively speaking, one might expect that as $m_\chi = g|\phi|$ becomes greater than M_P, each χ particle becomes a Planck-size black hole, which immediately evaporates and reheats the universe; however, this is likely an unwarranted extrapolation beyond reasonable limits for standard quantum field theory treatments.

2.6 Preheating for Fermions

2.6.1 Introduction

Up to this point, the resonant decay products considered have all been bosons. Indeed, this would seem reasonable—after all, for fermions, the Pauli exlusion principle prohibits the occupation number from exceeding 1. As a result, many assumed that the decay of the inflaton to fermions could be treated exclusively in the perturbative regime.

Recently, however, Greene and Kofman [4] demonstrated that fermions do, in fact, experience some form of preheating. In this section, therefore, we review the significant features of their results.

2.6.2 Quantum Fluctuations for a Fermion Field ψ

The Dirac equation for a massless Fermi field $\psi(t, \mathbf{x})$ in the theory described by the Lagrangian

$$\mathcal{L} = \tfrac{1}{2}(\partial_\mu \phi)^2 - V(\phi) + i\bar{\psi}\gamma^\mu \partial_\mu \psi - h\bar{\psi}\phi\psi, \tag{2.86}$$

is given by

$$[i\gamma^\mu\partial_\mu - h\phi(t)]\,\psi = 0. \tag{2.87}$$

As in the boson case, the inflatons producing fermions act as a coherently oscillating field $\phi(t)$ instead of as individual particles. We are interested in determining whether the coherent oscillations of inflatons gives the same results as the ensemble of individually decaying inflatons considered in perturbative treatments.

To this end, we consider the conformal model $\frac{1}{4}\lambda\phi^4 + h\bar{\psi}\phi\psi$. In a manner analogous to that used in the conformal model of bosonic resonance considered earlier in this chapter, the problem of fermion production by the inflaton ϕ in an expanding universe can be completely reduced to an equivalent simpler problem in Minkowski space. To this end, in complete analogy with our work in Section 2.4, we introduce a conformal transformation of the fields,

$$\varphi \equiv a\phi, \tag{2.88}$$

$$\Psi \equiv a^{3/2}\psi, \tag{2.89}$$

in addition to a (dimensionless) conformal time variable,

$$\tau \equiv \sqrt{\lambda\tilde{\varphi}^2}\int\frac{dt}{a(t)}. \tag{2.90}$$

Neglecting decay, the amplitude of the transformed field φ remains constant. Parallelling our earlier results, we see that the inflaton background inflaton solution evolves as an elliptic function $\varphi(\tau) \approx \tilde{\varphi}\,\mathrm{cn}\left(\tau, \frac{1}{\sqrt{2}}\right)$ with period $T \approx 7.416$.

The field Ψ can be written in terms of an auxillary field $X(\tau, \mathbf{x})$ as $\Psi = [i\gamma^\mu\partial_\mu + h\varphi]\,X$. The auxillary field eigenmodes take the form $X_k(\tau)e^{+i\mathbf{k}\cdot\mathbf{x}}R_\tau$, where the R_τ are eigenvectors corresponding to an eigenvalue $+1$ of the Dirac matrix γ^0. It can be demonstrated that the temporal component of the eigenmode, $X_k(\tau)$, obeys the equation

$$\ddot{X}_k + \left(\kappa^2 + qf^2 - i\sqrt{q}\dot{f}\right)X_k = 0, \tag{2.91}$$

where $\dot{}$ denotes differentiation with respect to the conformal time τ. The above equation describes an oscillator with a complex, time-dependent frequency. Continuing in a manner which is completely analogous to the discussion in Section 2.4, we have that since the comoving momentum k only appears in the above equations as $\kappa^2 \equiv \frac{k^2}{\lambda\tilde{\varphi}^2}$, the natural units for momentum are therefore $\sqrt{\lambda}\tilde{\varphi}$. The background oscillations enter the equation through a function $f(\tau) = \mathrm{cn}\left(\tau, \frac{1}{\sqrt{2}}\right)$ which has unit amplitude. The combination of the coupling parameters $\frac{h^2}{\lambda} \equiv q$, combined with κ^2, uniquely defines the solution to (2.91).

All the information about the preheating of fermions is encoded in our master equation (2.91). Comparison with the corresponding master equation (2.70) for the parametric resonance production of Bose particles χ in the theory $\frac{1}{4}\lambda\phi^4 + \frac{1}{2}g^2\phi^2\chi^2$ reveals distinct similarities; the major differences are that (2.70) is missing the imaginary part of the frequency and that h is replaced with g in the resonance parameter q.

We take the vacuum positive-frequency initial condition $X_k(\tau_0) = \mathcal{N}_k e^{-i\kappa\tau}$, with normalization factor $\mathcal{N}_k = \left(2\Omega_k(\Omega_k + \sqrt{q}f)\right)^{-1/2}$, where $\Omega_k^2 \equiv \kappa^2 + qf(\tau)^2$ is the real component of the effective frequency.

Through use of the standard Ψ-field operator expansion and (2.91), we may write the comoving occupation number of particles in a given spin state (see, e.g., [32] for details)

$$n_k(\tau) = \frac{1}{2} - \frac{\kappa^2}{\Omega_k}\mathrm{Im}\left(X_k\dot{X}_k^*\right) - \frac{\sqrt{q}f}{2\Omega_k}. \tag{2.92}$$

It can be demonstrated that $n_k \leq 1$, so we do not violate the Pauli exclusion principle. We can compute both the total comoving number density of particles and antiparticles in both spin states, in addition to the energy density of created fermions, obtaining

$$n_\psi = \frac{4}{(2\pi)^3}\int d^3k\, n_k, \tag{2.93}$$

$$\epsilon_\psi = \frac{1}{2\pi^3}\int d^3k\,\Omega_k\,n_k, \tag{2.94}$$

respectively.

2.6.3 Fermionic Resonance

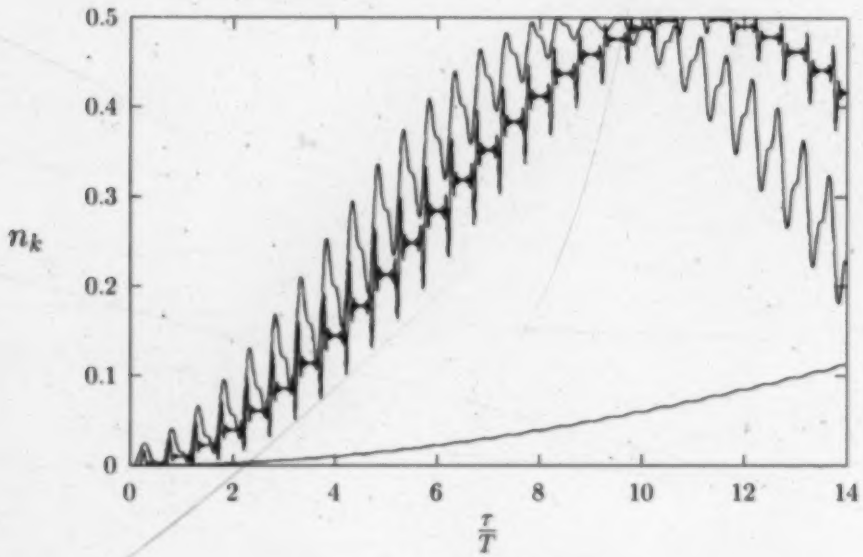

Figure 2.11: The occupation number n_k in $\lambda\phi^4$-inflation as a function of time τ (in units of T) for $q \equiv \frac{h^2}{\lambda} = 10^{-4}$ (lower), 1 (middle on right), and 100 (upper on right) and $\kappa^2 = 0.18, 1.11$, and 11.9, respectively. The period of the modulation $\frac{\pi}{\nu_k}$ (see Eq. (2.95)) is about 88, 20 and 22 (in units of T) accordingly. Adapted from [4]; note that n_k should be twice as large as that depicted above.

We can solve (2.91) numerically; using the results, the occupation number of particles can then be computed using (2.92). The occupation number, $n_k(\tau)$, for three different values of q is plotted in Figure 2.11.

Close examination of Figure 2.11 reveals that the occupation number, in general, exhibits high frequency oscillations about a slowly varying periodic solution. Averaging the occupation number over the high frequency oscillations using $\bar{n}_k(\tau) = \frac{1}{T}\int_{\tau}^{(\tau+T)} d\tau n_k(\tau)$, we can express the smoothed occupation number of fermions in a factorized form

$$\bar{n}_k(\tau) = F_k \sin^2 \nu_k \tau. \tag{2.95}$$

Therefore, for all q, the smoothed fermionic occupation number $\bar{n}_k(\tau)$ evolves *periodically* with time. In fact, (2.95) is an exact result when $\tau = NT$ is an integer number of background field oscillations. (For a derivation of this result, albeit in the context of external EM fields, see [33].) Both ν_k and the envelope function F_k are dependent on the parameter q. Typically, values of $\frac{\pi}{\nu_k}$ range from 10 to 100. Therefore, the fermionic modes are fully excited to their time-average value $\frac{F_k}{2}$ after O(10) inflaton oscillations. This result contrasts sharply with the results in the perturbative regime, which gives $\Gamma^{-1}_{\phi\to\psi\psi} \sim 10^{14}$ inflaton oscillations [1].

In Figure 2.11, we observe that for $q \gg 1$, n_k is essentially constant between points where the inflaton field passes through $\phi = 0$, at which point it undergoes a quasi-discontinuous increase to the new value. This behaviour recalls the broad-band resonance we discussed in Sections 2.3 and 2.4 for the bosonic case. However, as opposed to the unbounded bosonic resonance, in fermionic resonance the occupation number oscillates between its peak value $F_k \leq 1$ and zero with period $\frac{\pi}{\nu_k}$.

The computation of F_k and ν_k is greatly simplified by the existence of a semi-analytic shortcut.[1] It can be shown that the envelope function is given by the expression

$$F_k = \frac{1}{\sin^2 \nu_k T} \frac{\kappa^2}{2\Omega_k^2} \left(\mathrm{Im} X_k^{(1)}(T)\right)^2, \tag{2.96}$$

[1] To derive (2.96) for preheating, Greene and Kofman [4] significantly extended the method developed for pair production from the vacuum by an external electric field in [34].

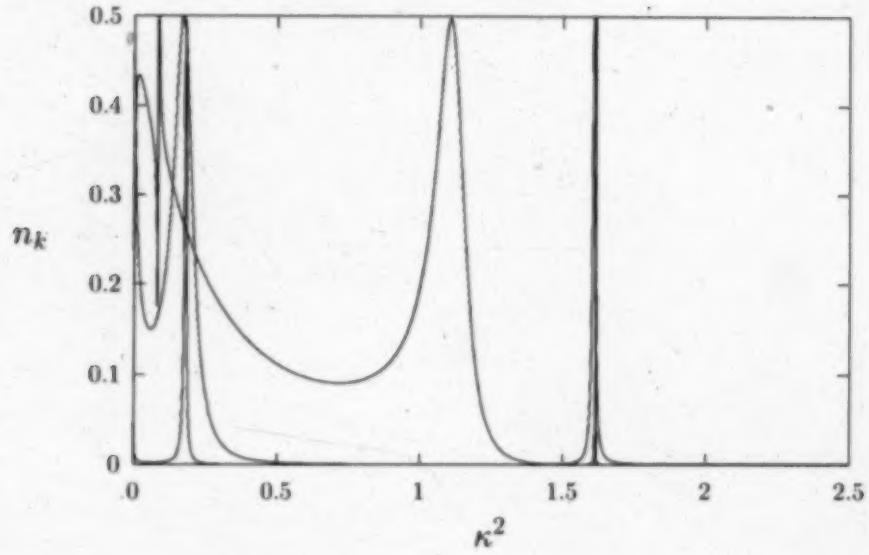

Figure 2.12: The envelope functions F_k for the occupation number n_k, showing bands of fermion excitation appearing for certain ranges of the conformal momentum parameter κ^2. The narrowest to broadest bands are the envelope functions for $q \equiv \frac{h^2}{\lambda} = 10^{-4}, 10^{-2}$, and 1.0, respectively. The band for $q = 10^{-2}$ deviates considerably from the perturbative expectation. Adapted from [4]; note that n_k should be twice as large as that depicted above.

where $X_k^{(1)}(T)$ is the value of the first fundamental (i.e., cosine-like) solution after one full oscillation, which is a function of k and q. Additionally, the modulation frequency ν_k satisfies

$$\cos \nu_k T = -\mathrm{Re} X_k^{(1)}(T). \tag{2.97}$$

Therefore, in order to find F_k and ν_k, it suffices to compute the (complex) value $X_k^{(1)}(T)$.

Greene and Kofman [4] carried out numerical calculations for $X_k^{(1)}(T)$, al-

lowing them to obtain the envelope function F_k plotted in Figure 2.12. Clearly, the spectrum of n_k differs considerably from the predictions of the calculation in the perturbative regime, which call for a narrowly peaked spectrum centred on $\kappa = \frac{\pi}{T} \approx 0.424$ with width $\Gamma^{-1}_{\phi \to \psi\psi}$. Figures 2.13–2.14 show the actual occupation of the fermionic resonance bands are filled after 10 oscillations of the inflaton.

The characteristic time scale for fermion excitation is determined by ν_k. The period of modulation $\frac{\pi}{\nu_k}$ is plotted as a function of κ^2 in Figure 2.15. We see the peaks of ν_k correspond to those points where F_k is peaked, so the modes with the largest possible occupation number n_k oscillate with the longest periods. For $q \gtrsim 1$, the modes in the principal peak have periods of about $20T$. When $q \ll 1$, on the other hand, the principal modes grow with periods on the order of $\frac{T}{\sqrt{q}}$. A curious aspect which deserves mention is that for modes well out of the peaks of the envelope function, the period is significantly shorter, and the integrated number of fermions rapidly saturates to its time-average value.

It turns out that the huge differences between the predictions of the perturbative regime and the theory considered here can be attributed to interference between various eigenmodes of the fermion fluctuations. We therefore have a *parametric excitation of fermions*, with q acting as the resonance parameter and the frequency ν_k acting as a fermionic conterpart of the bosonic characteristic exponent μ_k.[2] The amplitude of n_k is also reminiscent of the bosonic case, possessing a distinct sequence of resonance bands with widths that narrow significantly with increasing zone number. In the case where $q \ll 1$, it can be shown that the resonance bands are located at $\kappa = \frac{\pi}{T}(2l + 1)$, where $l = 0, 1, 2, \ldots$

Let us now consider the widths of the parametric excitations of fermions. In Figure 2.12, it is clear that for any q, the first, broadest zone has a width $\Delta\kappa \sim q^{1/4}$. This follows from the violation of the adiabaticity condition $\dot{\Omega}_k \geq$

[2]Notice that, in the bosonic case the modulating factor in (2.95) is replaced by $\sinh^2 \mu_k t$, leading to the familiar estimation $n_k \sim e^{2\mu_k t}$.

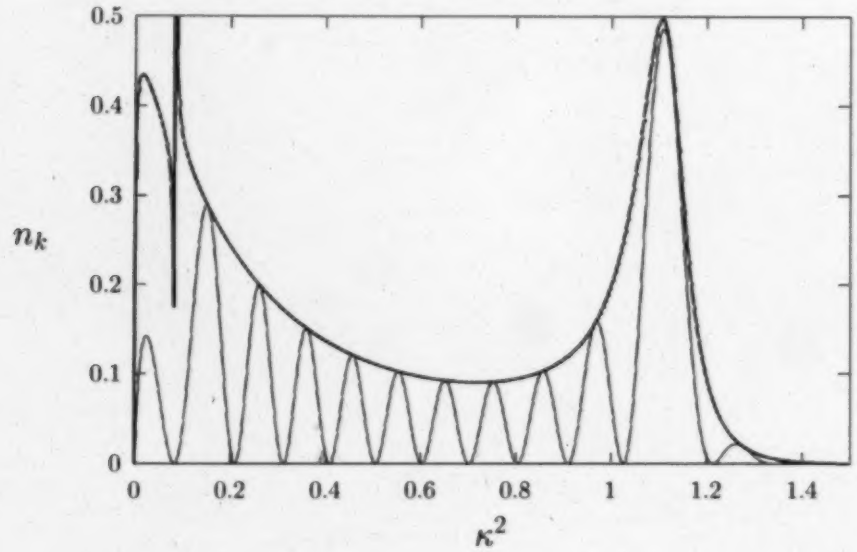

Figure 2.13: The resonance excitation band of fermions in $\lambda\phi^4$-inflation for $q \equiv \frac{h^2}{\lambda} = 1.0$. The heavy line shows the envelope F_k of maximum occupation number calculated from (2.96). The light curve is the actual occupation number n_k of each mode, calculated from (2.95), after 10 background oscillations. Adapted from [4]; note that n_k should be twice as large as that depicted above.

Ω_k^2, which gives us $\Delta k \leq q^{1/4}\sqrt{\lambda}\tilde{\varphi}$ in a manner completely analogous to our discussion of broad-band bosonic resonance in Section 2.3. While there are also some very narrow zones with higher momenta, they are quickly saturated. This has implications for the production of superheavy fermions with mass $m_\psi \sim q^{1/4}m_\phi = q^{1/4} \times (10^{13}\ \text{GeV})$.

We are able to estimate the energy that accumulates in our decay fermions—once more, we must average over the high-frequency oscillations, obtaining

$$\bar{\epsilon}_\psi = \frac{2}{\pi^2}\int dk\, k^2\, F_k\, \sin^2 \nu_k \tau. \tag{2.98}$$

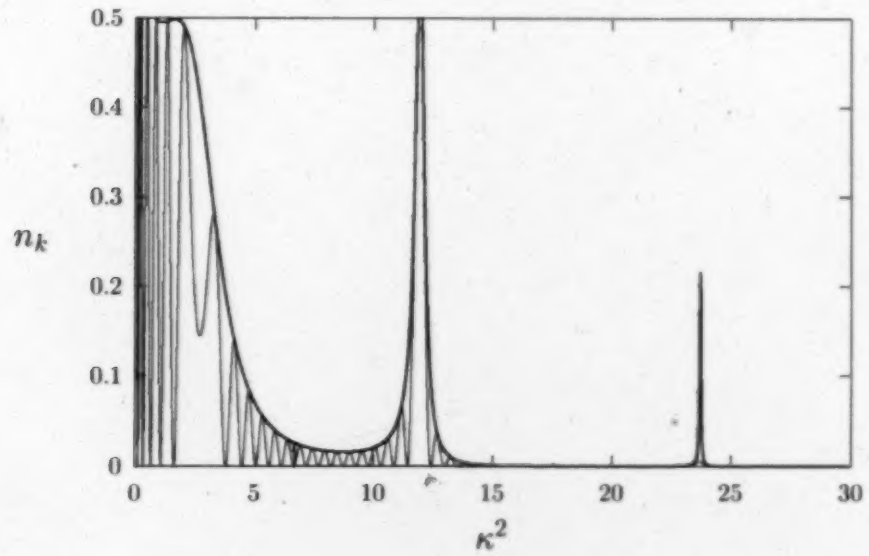

Figure 2.14: As in Figure 2.13, the resonance excitation band in $\lambda\phi^4$-inflation for $q \equiv \frac{h^2}{\lambda} = 100.0$. The heavy line shows the envelope F_k. The light curve is the actual occupation number of each mode n_k after 10 background oscillations. Adapted from [4]; note that n_k should be twice as large as that depicted above.

Broad-band fermionic resonance excitation occurs for $q \gg 1$; in this case, we get $\epsilon_\psi \sim 0.1 h^2 q^{1/4} \epsilon_\phi$, where the inflaton energy is $\epsilon_\phi = \frac{1}{4}\lambda\tilde{\phi}^4$. As previously mentioned, $\lambda \simeq 10^{-13}$ in chaotic $\frac{1}{4}\lambda\phi^4$ inflationary models. For q is large but $h \leq 0.1$, only a small fraction of the inflaton energy is transferred to fermions via this mechanism. Increasing the parameters such that $h \gtrsim 0.3$, $q \gtrsim 10^{12}$, on the other hand, allows for the transfer of substantial amounts of inflaton energy into fermions. Unfortunately, this turns out to be an rather extreme case, requiring SUSY cancellation of the radiative corrections $\sim h^4\phi^4$. However, hybrid inflationary models allow much more freedom in the choice of those model

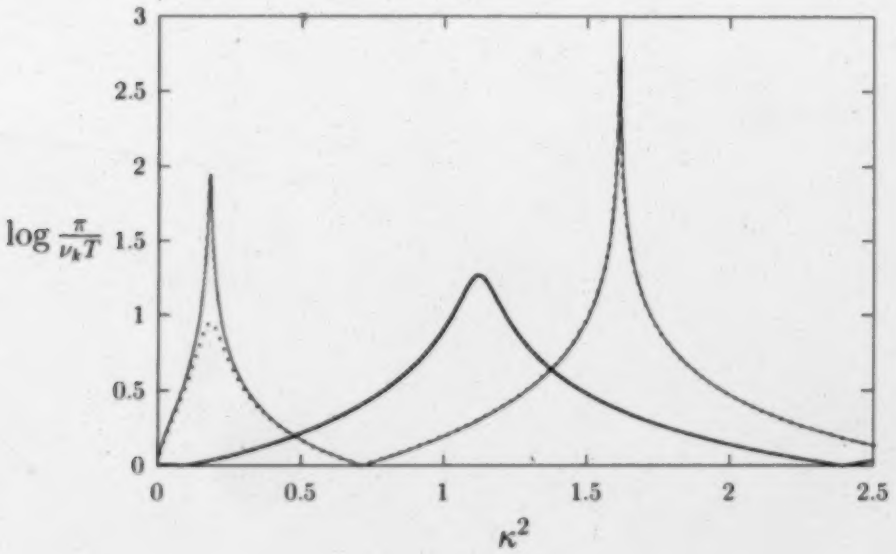

Figure 2.15: The log of the period of modulation $\frac{\pi}{\nu_k}$ (in units of T) as a function of κ^2 for $q \equiv \frac{h^2}{\lambda} = 10^{-4}, 10^{-2}$, and 1.0 for the light, dotted, and heavy curves respectively. Adapted from [4].

parameters which regulate preheating [35]. In such models, it may be possible to find a range of parameters for which the inflaton energy is fully converted into fermions before any bosonic resonance can develop.

2.7 Conclusion

Despite the many successes of various inflationary models from a theoretical standpoint, our understanding of the reheating epoch that follows inflation is still incomplete. For many years, it was believed that reheating proceeded exclusively by perturbative means; only recently have non-perturbative mechanisms been considered.

By reviewing the most important results of four of the most significant papers on preheating, we have laid the theoretical groundwork for the rest of this thesis. In particular, we have studied how the non-perturbative regime proceed in both $\frac{m^2\phi^2}{2}$ and $\frac{\lambda\phi^4}{4}$ theories, models of instant preheating, and models of preheating for fermions.

In the next chapter, we consider a refinement to the standard parametric resonance treatment of a toy $\frac{m^2\phi^2}{2}$ model—we introduce a complex inflaton field Φ as a replacement for the real scalar inflaton which has been used in all our considerations to this point. We wish to investigate what changes in the structure of the parametric resonance regime will result.

References

[1] L. A. Kofman, A. D. Linde, and A. A. Starobinsky, Phys. Rev. **D56** (1997), 3258.

[2] P. B. Greene, L. Kofman, A. D. Linde, and A. A. Starobinsky, Phys. Rev. **D56** (1997), 6175.

[3] G. Felder, L. Kofman, and A. D. Linde, Phys. Rev. **D59** (1999), 123523.

[4] P. B. Greene and L. A. Kofman, Phys. Lett. **B448** (1999), 6.

[5] A. D. Linde, *Particle Physics and Inflationary Cosmology* (Harwood, New York, 1990).

[6] A.D. Dolgov and A.D. Linde, Phys. Lett. **116B** (1982), 329.

[7] L.F. Abbott, E. Fahri and M. Wise, Phys. Lett. **117B** (1982), 29.

[8] M.E. Peskin and D.V. Schroeder, *An Introduction to Quantum Field Theory* (Addison-Wesley PC, New York, 1995).

[9] A. Albrecht, P. J. Steinhardt, M. S. Turner and F. Wilczek, Phys. Rev. Lett. **48** (1982), 1437.

[10] N. W. MacLachlan, *Theory and Application of Mathieu Functions* (Dover, New York, 1961).

[11] L.D. Landau and L. Lifshitz, *Mechanics* (Pergamon Press, New York, 1976).

[12] L. A. Kofman, A. D. Linde, and A. A. Starobinsky, Phys. Rev. Lett. **73** (1994), 3195.

[13] M. Yoshimura, Prog. Theor. Phys. **94** (1995), 873;
H. Fujisaki, K. Kumekawa, M. Yamaguchi, and M. Yoshimura, Phys. Rev. **D53** (1996), 6805.

[14] S. Khlebnikov and I. Tkachev, Phys. Lett. **B390** (1997), 80;
B.R. Greene, T. Prokopec and T.G. Roos, Phys. Rev. **D56** (1997), 6484;
I. Zlatev, G. Huey, P.J. Steinhardt, Phys. Rev. **D57** (1998), 2152.

[15] E.W. Kolb, A.D. Linde, and A. Riotto, Phys. Rev. Lett. **77** (1996), 4290;
E.W. Kolb, A. Riotto, and I.I. Tkachev, Phys. Lett. **B423** (1998), 348.

[16] S. Khlebnikov and I. Tkachev, Phys. Rev. Lett. **79** (1997), 1607.

[17] M.S. Turner, Phys. Rev. **D28** (1983), 1243.

[18] A. Erdelyi, ed. *Higher Transcendental Functions*, (Bateman Manuscript Project) Vol. 3 (NY: McGraw-Hill, 1955).

[19] D. Boyanovsky, H. J. de Vega, R. Holman, D. S. Lee, A. Singh, and J. F. J. Salgado, Phys. Rev. **D54** (1996), 7570.

[20] D.I. Kaiser, Phys. Rev. D56 (1997), 706.

[21] M. Abramowitz and I. Stegun, *Handbook of Mathematical Functions*, (Dover, New York, 1965), p. 685.

[22] A. D. Linde, Phys. Lett. **108B** (1982), 389.

[23] L. A. Kofman, A. D. Linde, and A. A. Starobinsky, Phys. Rev. Lett. **76** (1996), 1011;
I. I. Tkachev, Phys. Lett. **B376** (1996), 35;
S. Khlebnikov, L. Kofman, A. D. Linde, and I. I. Tkachev, Phys. Rev. Lett. **81** (1998), 2012;

I. I. Tkachev, S. Khlebnikov, L.A. Kofman, and A.D. Linde, Phys. Rev. Lett. **81** (1998), 2012.

[24] D. J. H. Chung, hep-ph/9809489.

[25] L. H. Ford, Phys. Rev. **D35** (1987), 2955;
B. Spokoiny, Phys. Lett. **B315** (1993), 40;
M. Joyce, Phys. Rev. **D55** (1997), 1875;
M. Joyce and T. Prokopec, Phys. Rev. **D57** (1998), 6022;
P. J. E. Peebles and A. Vilenkin, astro-ph/9810509.

[26] R.R. Caldwell, R. Dave, and P.J. Steinhardt, Phys. Rev. Lett. **80** (1998), 1582.

[27] J. Baacke, K. Heitmann, and C. Patzold, Phys. Rev. **D58** (1998), 125013.

[28] V. Berezinsky, M. Kachelriess, and A. Vilenkin, Phys. Rev. Lett. **79** (1997), 4302;
V. A. Kuzmin and V. A. Rubakov, Phys. Atom. Nucl. **61** (1998), 1028;
V. A. Kuzmin and V. A. Rubakov, Yad. Fiz. **61** (1998), 1122.

[29] D. J. H. Chung, E. W. Kolb, and A. Riotto, hep-ph/9802238;
V. A. Kuzmin and I. I. Tkachev, hep-ph/9802304;
V. A. Kuzmin and I. I. Tkachev, hep-ph/9809547.

[30] K. Greisen, Phys. Rev. Lett. **16** (1966), 748;
G.T. Zatsepin and V.A. Kuzmin, Pisma Zh. Eksp. Teor. Fiz. **4** (1966), 114.

[31] G. Felder, L. A. Kofman, A. D. Linde, and A. A. Starobinsky, in preparation.

[32] A. D. Dolgov and D. P. Kirilova, Sov. J. Nucl. Phys., **51** (1990), 172.

[33] N. B. Narozhnyi and A. I. Nikishov, Sov.Phys. JETP, **38** (1974), 427;
V. S. Popov, Sov. J. Nucl. Phys., **19** (1974), 1140.

[34] M. V. Mostepanenko and V. M. Frolov, Sov. J. Nucl. Phys., **19** (1974), 885.

[35] J. García-Bellido & A. Linde, Phys. Rev. **D57** (1997), 6065.

[36] J. Ellis & D.N. Nanopoulos, Phys. Lett. **116B**, 133 (1982);
K. Olive, Phys. Rep. **C190** (1990), 308.

[37] S. Khlebnikov & I. Tkachev, Phys. Rev. Lett. **77** (1996), 219.

Chapter 3

Parametric Resonance for Complex Fields

3.1 Introduction

As we have seen in the previous chapters, with the advent of inflationary theories of the early universe, it has been argued that the present stage of hot FRW "big-bang" cosmology was preceded by an epoch of cosmological evolution dominated by the dynamics of scalar fields [1]. The success of inflationary models in providing explanations for flat large-scale geometry (as suggested by the *location* of the acoustic peaks in the CMBR anisotropies), and for the origin of approximately scale-free adiabatic density perturbations (which can be used to simultaneously fit both the CMBR anisotropies and observations of cosmic structure formation), lends support to the idea of an early scalar-field dominated epoch. A crucial question in this picture is the nature of the transition from the scalar field dominated epoch to the hot FRW epoch, which is referred to as reheating. The nature of this transition also relates to other aspects of early universe dynamics necessary for a successful cosmology, such as mechanisms of baryogenesis, the resolution of

cosmological moduli problems, and possible sources for non-thermal dark matter.

The standard approach to reheating, which applies to sufficiently weakly coupled inflaton fields [2], is to treat quanta of the inflaton field as particles, which undergo independent single-particle decay; this treatment, if adequate, has the advantage that the post-inflation reheat temperature is determined by the microphysics of the model. This perturbative treatment is adaquate for inflaton fields possessing mass consistent with simple chaotic or supersymmetric models and decaying by gravitational strength interactions. Moderate reheat temperatures ($\lesssim$ O(10^{10}) GeV) result, which are consistent with the absence of GUT-scale defects such as monopoles, which are capable of incorporating a variety of (s)leptogenesis or electroweak mechanisms for generation of the baryon asymmetry of the universe (BAU), and which avoid, in the supersymmetric case, cosmological problems with thermal overproduction of gravitinos after reheating [3].

Recently it has been realized that the standard treatment of reheating in terms of single-particle inflaton decay may be seriously misleading in circumstances where there is coherent enhancement of the transition to bosonic decay products [4–16]. For large mode occupation numbers of the decay product field, we may treat its dynamics as being essentially classical. Mode by mode for the decay product field its coupling to the oscillating inflaton field induces a periodic time dependence in the mode mass (modulated by cosmic expansion which "sweeps" the time dependence of each comoving mode through the bands of the stability chart of the mode equations). This periodic modulation of the parameters of the oscillator associated with each mode of the decay product field can induce parametric resonance in bands of the mode parameters, leading to exponential growth in the decay mode amplitude. The resonant decay of the inflaton may have important cosmological implications like non-thermal symmetry

restoration and subsequent formation of topological defects [17, 18], revival of GUT baryogenesis scenarios [19, 20], supersymmetry breaking [21], superheavy particle production [16, 22], and gravitino production [23, 24].

The exponential growth in the mode occupation number may be modified or regulated by a number of physical processes. These include the decay of produced quanta to other particles [20, 25] or the rescattering of final state particles [9]. Another possibility, occurring in models with gauge-strength self-interactions between the produced final state particles, is the regulation of the parametric resonance by the self-interaction induced effective masses of the produced quanta, which can move these quanta out of the available resonance bands; in this case, resonance only proceeds as thermalization and Hubble dilution reduce the plasma masses of the final state quanta, resulting in a quasi-steady-state resonance conversion of inflaton oscillation energy to decay products [26]. This general scenario for the physically realistic case of decay products with gauge charge has been verified in explicit calculations in the narrow-band resonance case [26], and in numerical simulations in the broad-band case [10].

While to date analytical and numerical treatments of parametric resonance have considered oscillations of a single real field decaying to a single real decay product field, in realistic models the field content is often more extensive. In the case of supersymmetric theories this is unavoidably the case, as the physical scalars of simple (N=1) supersymmetry come as components of chiral multiplets and are complex. So for these types of theories, we should at the very least consider the nature of coherent decays when the fields involved are complex, though non-supersymmetric models with multiple real scalar fields may share some of the features of the simplest complex case.

Within supersymmetric models of particle physics, there are several different circumstances under which the decay of a homogeneous complex scalar conden-

sate may occur in the early universe. At the end of inflation one expects to have a spatially homogeneous inflaton scalar condensate, whose decay energy will ultimately be responsible for cosmic reheating and the initiation of hot big-bang cosmology. As well, in the supersymmetric standard model there are directions in the scalar field space of squarks and sleptons which are F-flat and D-flat, and which only gain a potential from supersymmetry breaking. In the early universe these directions may be populated with (very) large vev's after the end of the inflationary epoch; these vev's may carry enormous vev to mass ratios (Mathieu resonance parameter q) and couple to other directions in scalar field space with couplings capable of inducing resonant decay. Finally, supersymmetric models are generically plagued with gauge singlet scalar moduli, whose homogeneous oscillation poses grave cosmological difficulties which might be ameliorated by coherent decay of their oscillation amplitudes.

For self-interactions of complex scalars of the general form dictated by the F-term and D-term couplings arising in globally supersymmetric theories, the fields generally appear in complex conjugate pairs for the F-terms and diagonal D-terms. For example, let us consider a complex scalar field Φ in a chiral supermultiplet whose decay will be induced by a trilinear (renormalizable) coupling in a superpotential W to a chiral multiplet labelled by its scalar Ξ, where $W \simeq \Phi\Xi\Xi$. The resulting F-term coupling inducing the decay is then of the form $\Phi^*\Phi\Xi^*\Xi$, and is invariant under global phase redefinitions of either the Φ or the Ξ. We will see in the next section that in cases such as this the phase invariance of the resulting couplings implies that the equations for modes of the real and imaginary components of Ξ are decoupled and independent, and will allow us to simply analyze the resonant decay of a Φ condensate with out of phase oscillations for the real and imaginary components of Φ, into real and imaginary components of the decay product field Ξ.

We can always phase rotate our scalar field Φ to a basis such that its initial vev lies along the real axis. If there is no component of force along the direction of the imaginary axis (i.e. the scalar potential is phase invariant), the trajectory of the motion of Φ is limited to the real axis and the field hits the origin as it oscillates back and forth. In this case, provided that the coupling of the oscillating field to the final state field is also phase invariant, the situation is exactly that of a real oscillating field, and the same arguments apply for parametric resonance particle production. However, if the scalar potential is not phase invariant, i.e. depends on the phase of the oscillating field as well, a torque is exerted on the field. This leads to the deflection of the trajectory from a straight line and results in changing the trajectory into something that finally resembles an ellipsoid, after the torque in field space has effectively ceased its action. In this case the field no longer passes through the origin but rather has a finite distance of closest approach to it. This will have important implications for broad-band parametric resonance as we discuss below.

In supersymmetric models not only are complex scalar fields inherently involved, but also a phase dependent part of the scalar potential can arise naturally from supersymmetry breaking. Let us consider the simplest case with the following terms only involving the inflaton in the superpotential $W = \frac{1}{2}m\Phi^2 + \frac{1}{3}\lambda\Phi^3$. In supergravity models with broken supersymmetry, there is a corresponding phase dependent term (the "A-term") $Am_\Delta \frac{\partial W}{\partial \Phi}$ + h.c. in the scalar potential, where A is a dimensionless model-dependent constant and m_Δ is the scale of supersymmetry breaking in the sector in which Φ lies. There is also a phase dependent term $m\lambda^*\Phi\Phi^{*2}$ + h.c. in the F-term part of the scalar potential. This generically occurs in minimal supergravity models for inflation where the superpotential contains a series of $\lambda_n \frac{\Phi^n}{M^{n-3}}$ terms [27], and occurs even in "no scale" supergravity models after the inclusion of radiative corrections to the effective potential [28].

For $V \supset \Phi^m(\Phi^*)^n$ the potential along the angular direction is periodic with $m-n$ minima. In general, during inflation Φ rolls down to its minimum both along the radial and angular directions. In order to have a torque to deflect the trajectory, Φ must not be at the minimum along the angular direction at the onset of radial motion. This can happen in two ways: either there are several phase dependent parts of the potential with a non-adiabatic transition from the minimum of one to another, or Φ does not settle at the minimum along the angular direction. The first possibility happens when other supersymmetry breaking sources in the early universe (e.g. non-zero energy density of the universe or finite temperature effects) are dominant over the low energy one. In this case the minimum in the angular direction at early times is different from that at late times (due to independent phases for the coefficients of different A-terms). If the transition from one minimum to another one is non-adiabatic, Φ will not be at the minimum at late times regardless of its start at the minimum at early times. The second possibility happens when the potential along the angular direction is flat enough during inflation. In this case Φ will not roll down to its minimum and can start at any position at the onset of radial motion. In both cases, the further Φ is away from the minimum, the larger the deflection of its trajectory and the wider the ellipsoidal shape will be.

3.2 Complex Mathieu Resonance

As described in the previous section, the potential for complex scalar oscillations usually includes (as well as the scalar mass-squared terms) Hubble induced A-terms which are mainly effective during the first few cycles of oscillation. The A-terms provide a "torque" to the complex oscillation during the first few cycles, resulting in a net "elliptic" motion in the mass-term induced potential, after the A-terms have effectively ceased to be active. The resulting elliptic oscillation in

the mass term potential will be damped by the Hubble drag, resulting in the ellipse shrinking over time.

In order to introduce new considerations characteristic of resonance with complex fields, without getting involved in model dependent details, in most of this chapter we shall simply ignore the damping and consider complex, elliptic, constant amplitude oscillations. In particular, this means we do not need to specify which particular field is considered (e.g. inflaton versus SUSY standard model flat direction), nor do we need to determine the cosmological details involved in determining expansion and damping at the time that the oscillations of the field in question occur. In addition to presenting a tractable and interesting mathematical problem, consideration of the undamped oscillation should also provide the essential features of the full cosmological case including the effects of expansion, at least in the generic case of broad-band resonance. This follows from the key observation of [4, 5] that in the broad-band case the resonant excitation of the decay product field occurs over a tiny fraction of the cycle of the driving field, when the latter passes near the origin, as only here do the decay product field dynamics depart from the adiabatic regime. So mode number excitation proceeds by a series of abrupt jumps, and the dynamics of a given jump may be considered with the instantaneous value of the oscillator parameters, resulting in the picture of "stochastic resonance" analyzed in [5]. The present paper discusses the changes in the dynamics of decay mode excitation which arise from the complex nature of the driving field oscillation—the differences in question arise from suppression of the adiabaticity violations that induce the jump in mode occupation numbers of the decay product field, so we expect that considerations using the instantaneous value of the driving oscillation amplitude should give insight in the complex case, much as such considerations did in the real stochastic resonance case.

In any case, for the purposes of our present calculations we shall consider the parametric resonance production of decay product field modes Ξ, from phase-invariant coupling to constant-amplitude out of phase ("elliptic") oscillations of a driving field Φ. Detailed cosmological studies of applications to inflaton or moduli oscillations will be considered elsewhere.

With the couplings discussed in the previous section, after the A-terms cease to be effective, the equation of motion for the Ξ field is of the form:

$$\ddot{\Xi}_k + \left(\frac{k^2}{a^2} + m_\Xi^2 + g^2|\Phi|^2\right)\Xi_k = 0, \tag{3.1}$$

where Ξ_k is the decay product field mode with comoving wavenumber k, a is the FRW scale factor, m_Ξ the mechanical mass of the Ξ, and the superpotential coupling is as above. We note that both the real and imaginary piece of the Ξ field will separately obey this equation, and hereafter we use χ to denote either the real or imaginary piece of Ξ.

In our analysis, we will treat the physical momentum of the decay field mode and the relative phase and amplitude of the driving field oscillation as fixed parameters, and attempt to map out the regions of instability in their parameter ranges. As noted above, for the case of stochastic broad-band resonance, where the amplification occurs in small intervals while the field passes close to the origin, one should be able to approximate the instantaneous behaviour within each interval by the corresponding behaviour of a system of the type we analyze here.

We decompose the driving field Φ into real and imaginary pieces as follows:

$$\Phi = \phi_R + i\phi_I. \tag{3.2}$$

By a phase rotation we put the largest amplitude component of oscillation into the real piece, and so we write:

$$\phi_R = \phi \sin(m_\phi t) \tag{3.3}$$

$$\phi_I = f\phi\cos(m_\phi t), \tag{3.4}$$

where now ϕ is the constant amplitude of the real component of oscillation and $f \in [0,1]$ is the "out of phase" fractional component giving elliptic oscillation in the complex Φ plane; we will be particularly interested in the case where $f \ll 1$.

We wish to cast this into the canonical form of the (real) Mathieu equation:

$$y'' + (A - 2q\cos(2z))y = 0, \tag{3.5}$$

where $'$ denotes differentiation with respect to the independent variable z. We begin by substituting our definition of the Φ field into (3.1) above, giving

$$\ddot{\chi}_k + \left(\frac{k^2}{a^2} + m_\chi^2 + g^2\phi^2\left(\sin^2(m_\phi t) + f^2\cos^2(m_\phi t)\right)\right)\chi_k = 0. \tag{3.6}$$

We replace $\cos^2(m_\phi t)$ with $1 - \sin^2(m_\phi t)$ and collect terms, giving

$$\ddot{\chi}_k + \left(\frac{k^2}{a^2} + m_\chi^2 + f^2g^2\phi^2 + \left(1 - f^2\right)g^2\phi^2\sin^2(m_\phi t)\right)\chi_k = 0. \tag{3.7}$$

Using the half-angle formula $\sin^2\theta = \frac{1}{2}(1 - \cos 2\theta)$ we obtain the form

$$\ddot{\chi}_k + \left(\frac{k^2}{a^2} + m_\chi^2 + f^2g^2\phi^2 + \frac{1}{2}\left(1 - f^2\right)g^2\phi^2\left(1 - \cos(2m_\phi t)\right)\right)\chi_k = 0. \tag{3.8}$$

which may be rewritten in the form of the Mathieu equation

$$\chi_k'' + (A_k(f) - 2q(f)\cos 2z)\,\chi_k = 0 \tag{3.9}$$

with the following new identifications:

$$z = m_\phi t \tag{3.10}$$

$$A_k(f) = \frac{\frac{k^2}{a^2} + m_\chi^2 + f^2g^2\phi^2}{m_\phi^2} + 2q(f) \tag{3.11}$$

$$q(f) = \frac{(1 - f^2)g^2\phi^2}{4m_\phi^2}. \tag{3.12}$$

Notice that the coefficients of the Mathieu equation are now functions of the imaginary fraction f. This is an important feature, as it means that the characteristic behaviour of the parametric resonance as described by the Mathieu

equation takes the same form in the complex case as in the real case; however, *the relationship between the physical parameters of the process and the Mathieu coefficients is redefined.*

So we see that there is a mapping that takes the Mathieu equation for the complex modes of the decay field when driven by the complex parametric field with out of phase real and imaginary pieces in its oscillation amplitude, and maps it to a real Mathieu equation for the oscillations of the real and imaginary pieces of the decay product field with shifted parameters. There are several features of this mapping that simply encapsulate physical features of the original problem.

First we note that for the case where $f = 0$, where the oscillation of the parametric driving field is along the real axis, the coefficients A_k and q reduce to those previously considered in the literature for the case of purely real parametric oscillation [4, 5]. In the other extreme limit, when $f = 1$, we have $q(1) = 0$, meaning that one is restricted to be along the A_k axis on the Mathieu equation stability diagram, allowing only non-resonant particle production. This corresponds to the physical observation that because the decay couplings were phase invariant, our original equation for the complex oscillations involved only the magnitude of Φ in the oscillation equation. In the case that the real and imaginary pieces of the Φ oscillation have the same amplitude ($f = 1$), then the coefficients in the χ equation of motion become time independent and there can be no parametric amplification. We also note that the imaginary fraction f of the oscillations enters into the coefficients only as f^2, meaning that the effect is the same regardless of direction traveled around the ellipse (i.e. whether f is positive or negative). This reflects the fact that the original equation for the complex oscillations is second order and symmetric under time inversion, which corresponds to having the parametric field circulate about the oval in the Φ plane in the opposite sense, or reversing the sign of f.

Finally, in the intermediate regime $f \in (0,1)$, $q(f)$ is always lessened, while A_k is always increased (compared to $f = 0$), so increasing f never causes the system to leave the physical regime. As noted above, increasing f means moving "inland" on the stability diagram for the Mathieu equation. In general, this causes suppression of the resonant growth of the χ modes; however, it also allows one to explain the counterintuitive observation that in certain cases the resonant band exponential growth parameter μ_k may actually increase as one turns on the out of phase component f. To understand this, imagine that for oscillations with no imaginary fraction f one is sitting in parameter space at the lower border of one of the instability bands (where μ_k is zero). Now slowly increase f. The parameter mapping derived above implies that you start to move in a "northwest" direction on the band chart into the instability band. As such, your μ_k begins to increase. As you continue to increase f, you will eventually hit the maximum possible μ_k along your trajectory, after which your μ_k begins to drop again. Eventually you will leave the instability band altogether for sufficiently large f. For very high order instability bands, it should be possible to encounter many bands along one trajectory of increasing f.

From a different point of view, were one to look at the instability diagram as a function of the the A_k and q of standard real Mathieu parametric resonance (i.e., as a function of our $A_k(0)$ and $q(0)$, for different values of f), the effect of turning on f would be seen to manifest itself as both a narrowing and a downwards shift of the instability bands as f increased. In addition, isocontours of μ_k would be seen to "flow out" of the bands as f increases. For $f = 1$ each instability band collapses to a line with $\mu_k = 0$, as with a phase independent coupling of the parameter field to the mode field there would be no time dependence in the mode field equation of motion, and the system would be stable for all A_k and q. Figure 3.1 illustrates in detail both the bending of the bands and the decrease

of μ_k for the first resonance band as we turn on the imaginary fraction f of our oscillations. We expect that the suppression of resonance for fixed non-zero imaginary fraction f is stronger in higher resonance bands, as at larger q the resonance proceeds by violation of adiabaticity in the decay mode evolution, and for large q at fixed f the induced decay mode field mass is always large. This is illustrated in Figure 3.2 where we show the quenching of resonance for the first 7 resonance bands, as f is turned on. We see that there is more severe suppression for the higher bands, in accord with our physical intuition; in the next section we will analytically estimate the extent of the domain of surviving resonant bands, for fixed imaginary fraction f.

3.3 Parameter Domain For Broad-Band Resonance

Let us first briefly discuss the effect of mixing in the narrow-band regime. The narrow-band resonance in the case of a real oscillating field is efficient for $(\frac{m}{g})^{\frac{1}{3}} \leq \phi \leq \frac{m}{g}$ [6]. In the case of a complex field with mixing parameter f this reads as

$$\left(\frac{m^2+f^2g^2\phi^2}{(1-f^2)g^2}\right)^{\frac{1}{3}} \leq \phi \leq \left(\frac{m^2+f^2g^2\phi^2}{(1-f^2)g^2}\right)^{\frac{1}{2}}, \tag{3.13}$$

where m and g are replaced with $\sqrt{m^2+f^2g^2\phi^2}$ and $\sqrt{1-f^2}g$, respectively. It is easily seen that the condition for an efficient narrow-band resonance remains almost unchanged in the complex case, unless f is close to 1. Therefore, in physically interesting situations the narrow-band resonance will not be substantially affected by the mixing. Of course, in the extreme case with $f = 1$, there is no time variation in the Mathieu equation and, hence, no narrow-band resonance.

In the case of real broad-band parametric resonance, Kofman, Linde, and Starobinski [4, 5] argue that the requirement of adiabaticity violation for broad-

band parametric amplification implies that it only occurs with significant μ_k for $A_k - 2q \lesssim \sqrt{q}$. Their argument presupposes that the decay terminates after it has entered an "explosive" phase, where the effective mass of the decaying ϕ is dominated by the coupling to the plasma of decay product χ modes which has been built up by parametric resonance decay. The effective physical 3-momentum of the quasi-relativistic decay χ modes is of order their energy, which is no more than of order the induced mass of the decaying ϕ; this is of order $g\chi_{\rm end}$ which in turn is of order $g\phi_{\rm end}$ which can also be written $\sqrt{gm_\phi^{\rm eff}\phi_{\rm end}}$. So $(k^2_{\rm phys}/m^2_\phi) \lesssim (g\phi_{\rm end}/m^{\rm eff}_\phi)$, which can be rewritten as $A_k - 2q \lesssim \sqrt{q}$. For a detailed discussion we refer to the treatment in [5].

We have seen in the preceding section that the case of complex oscillation with imaginary fraction f can be mapped onto a Mathieu equation with shifted resonance parameters. By substituting the "shifted" parameters induced by the non-zero imaginary component of oscillation, we should thus be able to determine what range of q supports broad-band resonance for oscillation with a given fraction of out of phase imaginary component for the oscillation of the driving parameter.

Recall the expressions for the equivalent shifted $A_k(f)$ and $q(f)$ from equations (3.11) and (3.12) respectively. Substituting these expressions into the relation $A_k - 2q \lesssim \sqrt{q}$ allows us to write it as

$$\frac{\frac{k^2}{a^2} + m_\chi^2 + f^2g^2\phi^2}{m_\phi^2} \lesssim \frac{\sqrt{(1-f^2)}g\phi}{2m_\phi}. \tag{3.14}$$

This leads us to the relation

$$A_k(0) - 2q(0) + 4f^2q(0) \lesssim \sqrt{1-f^2}\sqrt{q(0)}, \tag{3.15}$$

or, defining $E_k \equiv A_k(0) - 2q(0)$, we have

$$E_k + 4f^2q(0) \lesssim \sqrt{1-f^2}\sqrt{q(0)}. \tag{3.16}$$

If we recall that physical values of E_k are positive semi-definite, we find that for a fixed non-zero imaginary fraction f there is an upper bound on the parameter $q(0)$ for which resonance occurs, and the allowed range of resonant $q(0)$ is bounded above as $\frac{1-f^2}{16f^4}$. (For the small imaginary fractions f of physical interest, however, the weaker approximate bound of $\frac{1}{16}f^{-4}$ will suffice). So instead of an ever widening resonance region above the $A_k = 2q$ line, with thickness of order $\sqrt{q}$, as one has in the real case, in the complex case with fixed non-zero imaginary fraction f, one instead has a region above the $A_k = 2q$ line of finite extent, with an upper bound on the values of the q parameter which can result in resonance. This is qualitatively reasonable, as a fixed imaginary fraction f for the oscillation means that as we scale up q the ellipse of Φ broadens as it lengthens, preserving its shape; so throughout the Φ oscillation $|\Phi|$ has a large value, inducing a large mass for the modes of the decay field Ξ, which in turn leads to adiabatic evolution of the Ξ, and suppression of broad-band parametric resonance production of the Ξ.

3.4 Complex Resonance in "Instant Preheat"

Recently, a simpler method of efficient scalar field decay has been proposed, called "instant preheat" [16]. Within models of this type the decaying field rolls once through the origin, at which point the mass of the decay product field to which it is coupled passes through zero, and modes of the decay product field experience non-adiabatic excitation. As the decaying field rolls away from zero (perhaps monotonically) the modes of the decay product field grow in mass; they drain energy from the decaying field through their mass. As the mass of the modes of the decay product field grows, so does their decay width; their subsequent decay, after their mass and decay width have grown sufficiently, then releases the energy they have taken from the original decay field, and dumps it

into their final decay products, which thermalize the resulting energy.

It is interesting to note that while final state effects such as rescattering, backreaction, or plasma masses can prevent preheating from occurring, they are unimportant in the instant preheating scenario. The reason is that for these effects to become important, (at least) several oscillations are needed to build up a large enough occupation number for the final state field. In the instant preheating, on the other hand, the energy drain from the oscillating field occurs during each half of an oscillation. In fact, instant preheating can be efficient even if the adiabaticity condition is violated only during the first half of the first oscillation. Therefore, instant preheating is essentially unaffected by the final state effects. The mixing of the real and imaginary parts of the oscillating field, on the other hand, has the same effect in the instant preheating case as in the standard preheating scenario. We recall that the torque from A-terms deflects the trajectory of the oscillating field from that of a straight line. The Hubble induced A-terms have their largest value at the beginning of the oscillations, and rapidly decrease with Hubble expansion. This means that the deflection is largest during the initial oscillations. Thus, a large enough f to restore adiabaticity in the preheating case could do the same for the instant preheating case.

3.5 Non-Convex Potentials

Another possibility to achieve rapid decay of a homogeneous condensate occurs in the case that the potential governing the evolution of the condensate scalar has non-convex behaviour over some region of field space [12, 29]. In this circumstance, it becomes energetically favorable for a scalar condensate in the non-convex region to decompose into inhomogeneous modes; provided the inhomogeneity occurs over long enough wavelengths, the price one pays in kinetic energy for the inhomogeneity is more than compensated by the decreased aver-

age potential energy of the regions of field excess and deficit compared to the average field value. This produces a wavenumber band for exponential growth of the mode amplitudes. This has been considered in both the case of inflaton decay [12], and in the case of the growth of inhomogeneities in scalar condensates corresponding to F-flat and D-flat directions of the standard model with non-convex potentials of the type arising from gauge-mediated supersymmetry breaking [29]. It is clear that this is one type of instability which is not vitiated by having the scalar order parameter complex or involving multiple scalar fields. If there is a region in field space with respect to which the potential is non-convex in some direction, then fluctuations corresponding to modes of the field variation in that field direction, of sufficiently long wavelength, will win on the potential versus kinetic energy budget, and grow exponentially. Indeed the treatment of (complex) flat directions in the supersymmetric standard model in [29] explicitly analyzes the conditions for instability of a complex field with a potential which is a non-convex function of the field modulus, and exhibits the resulting instability bands.

3.6 Other Couplings

Here, we briefly comment on the situation for another type of coupling between Φ and Ξ fields which is also of interest and application. This is the coupling $g^2(\phi_R\chi_R + \phi_I\chi_I)^2$, where its simplest manifestation is for the potential $V(\Phi) = \frac{1}{4}\lambda|\Phi|^4$, with Φ and Ξ being the same field. It also arises in supersymmetric models from the D-term part of the scalar potential. This type of coupling leads to the mixing of χ_R and χ_I mode equations:

$$\ddot{\chi}_{R,k} + \left(\frac{k^2}{a^2} + {m_\chi}^2 g^2 {\phi_R}^2\right)\chi_{R,k} + g^2\phi_R\phi_I\chi_{I,k} = 0 \qquad (3.17)$$

$$\ddot{\chi}_{I,k} + \left(\frac{k^2}{a^2} + {m_\chi}^2 g^2 {\phi_I}^2\right)\chi_{I,k} + g^2\phi_R\phi_I\chi_{R,k} = 0. \qquad (3.18)$$

In this case the mass eigenstates are $\frac{\phi_R\chi_R+\phi_I\chi_I}{\phi}$ and $\frac{\phi_I\chi_R-\phi_R\chi_I}{\phi}$ instead of ϕ_R and ϕ_I themselves. For oscillatory motion of ϕ_R and ϕ_I with a phase difference, there are two periodic changes that may lead to resonance: change in the mass eigenvalues (the usual parametric resonance) and change in the mass eigenstates. They can't be simply superimposed and it is not very easy to give rough arguments for the instability bands and the respective value of μ_k's. The important point is that for such a coupling, even in the $f = 1$ case there is still time variation in mode equations. This variation is present in both the mass eigenstates and mass eigenvalues.

3.7 Cosmic Expansion and Complex Resonance

So far, we have considered modifications to parametric resonance decay which arise in complex field oscillations in the absence of effects of Hubble expansion. As we noted above, since broad-band resonance is induced by non-adiabaticity of the χ evolution during small intervals of the ϕ oscillation, instantaneous approximation of the χ excitation should be a useful guide during each of the jumps in mode number. Cosmic expansion then functions to shift the parameters of the oscillator between episodes of mode excitation as ϕ passes near zero. We now examine the implications of this in both the narrow- and broad-band cases.

Implications for the narrow-band case are simple; as we have seen, the introduction of a phase difference between real and imaginary components of our complex inflaton field Φ only kills narrow-band resonance for phase differences approaching $\frac{\pi}{2}$, or, in the language of this chapter, for $f \cong 1$. Therefore, the resonance should be qualitatively the same in the static approximation and with the Hubble expansion included.

For broad-band resonance the situation is completely different. According to equation (3.16), the broad-band resonance is shut off for $q > \frac{1}{16}f^{-4}$. In the

static limit f and q are both constant and resonance is either suppressed, or viable. In an expanding universe, f eventually becomes approximately constant as the Hubble induced A-terms turn off (indeed, as pointed out earlier, after several Hubble times the motions along the real and imaginary directions are decoupled and free), while, on the other hand, $q(t) = \left(\frac{g\phi(t)}{2m}\right)^2$ is redshifted as a^{-3}. This implies that even if the resonance is suppressed initially, it may be initiated after a sufficient time such that $q(t) < \frac{1}{16}f^{-4}$. The right-hand side is less than 1 (or very close to it) for $f \gtrsim \frac{1}{2}$. Therefore, in the case of large out of phase components of oscillation, the broad-band resonance is killed and resonance may resume only in the narrow-band regime at a later time. In most physically interesting cases, however, $f < \frac{1}{2}$ and the right-hand side is considerably greater than 1. In such cases, the broad-band resonance is not eliminated in an expanding universe, but rather delayed. The parameter f is determined by the action of the scalar potential (including A-terms) for the oscillating field, and after the initial oscillations it often becomes effectively time-independent. Depending on the dimensionality of the A-term, it may be a function of q_i, the value of q at the start of oscillations. If $q_i < \frac{1}{16}f^{-4}$, the onset of broad-band resonance will be unaffected. For $q_i > \frac{1}{16}f^{-4}$, resonance is delayed initially, but will resume after sufficient expansion such that $q < q_{\rm eq} = \frac{1}{16}f^{-4}$. A larger f leads to a smaller $q_{\rm eq}$, for $f \gtrsim \frac{1}{2}$ we have $q_{\rm eq} < 1$ and resonance can only occur in the narrow-band regime. For $f = 1$ resonance is eliminated.

Even though the broad-band resonance (for interesting cases) is only delayed in an expanding universe, the mixing still has important consequences. Perhaps the most notable example relates to the production of superheavy particles during resonance. In the standard preheating, Ξ's with a mass up to $q^{\frac{1}{4}}m_\phi$ can be produced. A reduction in q at the onset of resonance implies a reduction in the maximum mass of produced particles. This is even more pronounced in the

instant preheating case. Here Ξ decay products Ψ with masses up to $q^{\frac{1}{2}}m_\phi$, and which have a large enough coupling h to Ξ, can be produced [16]. A smaller $q_{\rm eq}$ has a two-fold effect in this case. First, the allowable masses are smaller, and second, the decay rate $\Gamma_d = \frac{h^2}{8\pi}g\phi$ may not be large enough (compared to the frequency of oscillations m_ϕ) for efficient production of Ψ's. It is easily seen that $\Gamma_d \leq m_\phi$ for $h \lesssim 4\pi^{\frac{1}{2}}f$. Therefore, Ψ production is not efficient if $h \lesssim 4\pi^{\frac{1}{2}}f$. Even for $h \gg 4\pi^{\frac{1}{2}}f$, only Ψ's with a mass $m_\psi \lesssim \frac{1}{4f^2}m_\phi$ can be produced.

3.8 Conclusions

In this chapter, we have considered the changes to the standard picture of parametric resonance decay of a real homogeneous cosmological scalar field which arise if the field is instead complex, with out of phase oscillation of its real and imaginary components and a phase invariant decay coupling. For the case of complex Mathieu type resonance, we give an explicit mapping to a corresponding real Mathieu resonance with shifted parameters that encode the effects of the out of phase components of the oscillating decay field. We showed the resulting effects on the instability bands, demonstrating how they shift and shrink as the out-of-phase ("elliptic") component of the driving field motion increases, limiting the swath of instability to a finite area on the A_k-q chart, and eliminating broad-band resonance in the higher modes. We argued that similar effects may be present in the case of complex field models of "instant preheating," but that instabilities due to regions in field space with non-convex potentials are qualitatively the same in the complex case. Finally, in the context of an expanding FRW universe, we noted that the presence of a fraction of out of phase oscillation would usually delay the onset of parametric resonance, but not eliminate it entirely.

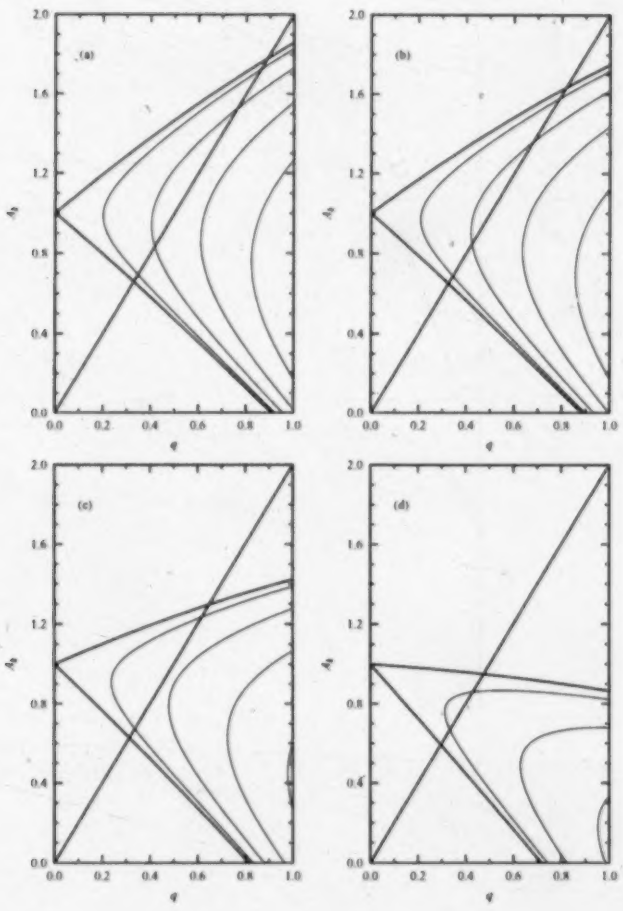

Figure 3.1: The Mathieu equation stability diagram for the first resonance band. The physical region lies above and to the left of the diagonal line $A_k = 2q$. Contour lines represent isocontours of μ starting from $\mu = 0$ (band boundary) and increasing by units of 0.1 as one moves from left to right in the band. Different panels represent different imaginary fractions f: (a) $f = 0$; (b) $f = 0.2$; (c) $f = 0.4$; (d) $f = 0.6$.

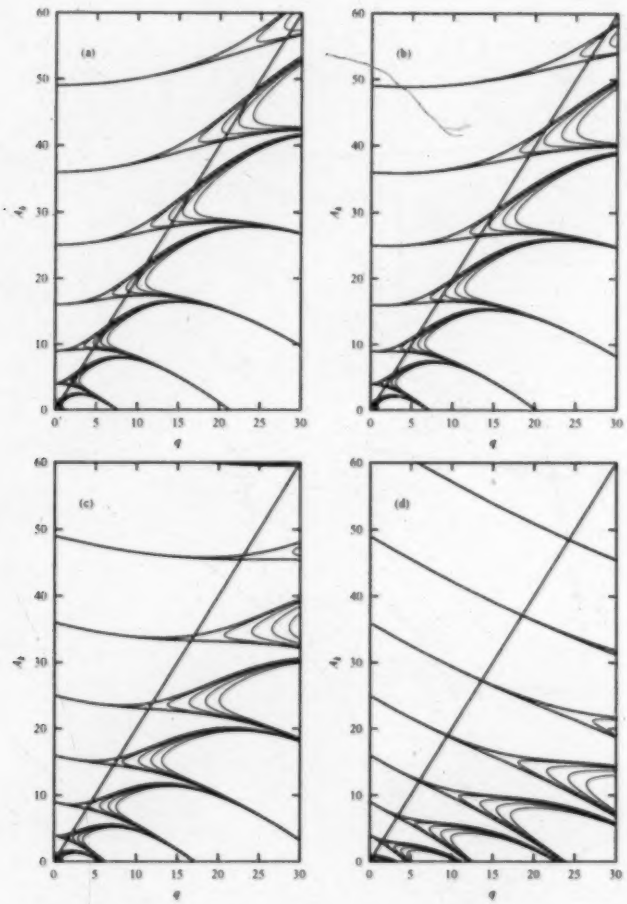

Figure 3.2: The Mathieu equation stability diagram for the first 7 resonance bands. The physical region lies above and to the left of the diagonal line $A_k = 2q$. Contour lines represent isocontours of μ starting from $\mu = 0$ (band boundary) and increasing by units of 0.1 as one moves from left to right in the bands. Different panels represent different imaginary fractions f: (a) $f = 0$; (b) $f = 0.2$; (c) $f = 0.4$; (d) $f = 0.6$.

References

[1] For reviews see: A. D. Linde, *Particle Physics And Inflationary Cosmology* (Harwood, New York, 1990);
K. A. Olive, Phys. Rep. **C190** (1990), 307.

[2] A. Dolgov and A. Linde, Phys. Lett. **116B** (1982), 329;
L. F. Abbott, E. Farhi, and M. Wise, Phys. Lett. **117B** (1982), 29.

[3] J. Ellis, J. E. Kim, and D. V. Nanopolous. Phys. Lett. **B145** (1984), 181;
M. Kawasaki and T. Moroi, Prog. Theor. Phys. **93** (1995), 879;
for a review see: S. Sarkar, Rept. Prog. Phys. **59** (1996), 1493.

[4] L. Kofman, A. D. Linde, and A. A. Starobinski, Phys. Rev. Lett. **73** (1994), 3195.

[5] L. Kofman, A. D. Linde, and A. A. Starobinski, Phys. Rev. **D56** (1997), 3258.

[6] Y. Shtanov, J. Traschen, and R. Brandenberger, Phys. Rev. **D51** (1995), 5438.

[7] D. I. Kaiser, Phys. Rev. **D 53** (1996) 1776;
D. I. Kaiser, Phys. Rev. **D56** (1997), 706.

[8] S. Yu. Khlebnikov and I. I. Tkachev, Phys. Rev. Lett **77** (1996), 219;
S. Yu. Khlebnikov and I. I. Tkachev, Phys. Lett. **B390** (1997), 80. (1997).

[9] S. Yu. Khlebnikov and I. I. Tkachev, Phys. Rev. Lett **79** (1997), 1607.

[10] T. Prokopec and T. Roos, Phys. Rev. **D55** (1997) 169.

[11] P. B. Green, L. Kofman, A. D. Linde, and A. A. Starobinski, Phys. Rev. **D56** (1997), 6175;
D. I. Kaiser, Phys. Rev. **D57** (1998), 702.

[12] B. Greene, T. Prokopec, and T. Roos, Phys. Rev. **D56** (1997), 6484.

[13] I. Zlatev, G. Heuy, and P. J. Steinhardt, Phys. Rev. **D57** (1998), 2152.

[14] P. B. Greene and L. Kofman, Phys. Lett. **B44** (1999), 6.

[15] P. B. Greene, L. Kofman, and A. A. Starobinski, Nucl. Phys. **B543** (1999), 423.

[16] G. Felder, L. Kofman, and A. D. Linde, Phys. Rev. **D59** (1999), 123523;
G. Felder, L. Kofman, and A. D. Linde, hep-ph/9903350.

[17] L. Kofman, A. D. Linde, and A. A. Starobinski, Phys. Rev. Lett. **76** (1996), 1011;
I. I. Tkachev, Phys. Lett. **B376** (1996), 35.

[18] S. Yu. Khlebnikov, L. Kofman, A. D. Linde, and I. I. Tkachev, Phys. Rev. Lett. **81** (1998), 2012;
I. I. Tkachev, S. Yu. Khlebnikov, L. Kofman, and A. D. Linde, Phys. Lett. **B440** (1998), 262;
S. Kasuya and M. Kawasaki, Phys. Rev. **D58** (1998), 083516.

[19] E. W. Kolb, A. D. Linde, and A. Riotto, Phys. Rev. Lett. **77** (1996), 4290.

[20] E. W. Kolb, A. Riotto, and I. I. Tkachev, Phys. Lett. **B423** (1998), 348.

[21] G. Anderson, A. D. Linde, and A. Riotto, Phys. Rev. Lett **77** (1996), 3716;
G. Dvali and A. Riotto, Phs. Lett. **B388** (1996), 247.

[22] D. J. H. Chung, E. W. Kolb, and A. Riotto, Phys. Rev. Lett. **81** (1998), 4048;
D. J. H. Chung, E. W. Kolb, and A. Riotto, Phys. Rev. **D59** (1999), 023501.

[23] H. Fujisaki, K. Kumekawa, M. Yamguchi, and M. Yoshimura, Phys. Rev. **D54** (1996), 2494.

[24] A. L. Maroto and A. Mazumdar, hep-ph/9904206;
R. Kallosh, L. Kofman, A. D. Linde, and A. Van Proeyen, hep-th/9907124;
G. Giudice, I. I. Tkachev, and A. Riotto, hep-ph/9907510.

[25] S. Kasuya and M. Kawasaki, Phys. Lett. **B388** (1996), 686.

[26] R. Allahverdi and B. A. Campbell, Phys. Lett. **B395** (1997), 169.

[27] M. Dine, L. Randall, and S. Thomas, Nucl. Phys. **B458** (1996), 291.

[28] M. K. Gaillard, H. Murayama, and K. A. Olive, Phys. Lett. **B355** (1995), 71.

[29] A. Kusenko and M. Shaposhnikov, Phys. Lett. **B418** (1998), 46.

Chapter 4

Conclusions

The nature of the transition which occurs at the end of the inflationary epoch has many important ramifications for the subsequent evolution of the universe, affecting such diverse areas as structure formation, heavy relics, dark matter, and baryogenesis. Several recent papers have demonstrated that the structure of the reheating epoch is significantly more complicated than originally thought. In particular, there exist numerous mechanisms by which the inflaton can experience a phase of parametric resonance decay, known as preheating, during which certain modes of the product fields experience exponential growth.

In Chapter 3, we investigated the effects of replacing the real inflaton field ϕ with a complex inflaton field Φ with out of phase oscillation of its real and imaginary components and a phase invariant decay coupling in the standard treatment of preheating. Using a toy $m^2|\Phi|^2$ model of complex Mathieu type resonance, we were able to compute an explicit mapping to a corresponding real Mathieu resonance with parameters that were functions of the imaginary fraction f. As f is turned on, the instability bands cant over and shrivel up, and the swath of instability is limited to an ever smaller region on the A_k-q chart. In this manner, broad-band resonance is rapidly eliminated in the higher modes. As the

torque due to the action of the A-terms is maximal for the first oscillations of the inflation field, similar effects may be present in the case of complex field models of "instant preheat;" however, instabilities due to regions in field space with non-convex potentials are qualitatively the same in the complex case. Finally, in the context of an expanding FRW universe, the presence of a fraction of out-of-phase oscillation would usually delay the onset of parametric resonance, but not eliminate it entirely.

Although our considerations were restricted to a toy $m^2|\Phi|^2$ model of chaotic inflation, our results are applicable (at the very least in a qualitative sense) to a broad range of inflation models incorporating complex scalar fields—the presence of a sufficiently large elliptic component of oscillation prevents the violations of adiabaticity which are crucial to broad-band resonance. However, detailed study of particular supersymmetric models of inflation is now required, in order to assess more fully the extent to which out of phase mixings can arise and the resulting effects on the reheat temperature T_r and particle abundances. It is also of interest to reconsider the preheating of fermions in the context of complex driving fields, as it is unclear from our treatment exactly how the production of fermions will be affected.

Appendix A

Notation and Sign Conventions

In this thesis, the following notation and sign conventions are used:

1. Greek indices μ, ν, ρ, σ, ... are used to label Lorentz four-vectors.
2. The Einstein summation convention is used throughout—repeated upper and lower indices are summed over unless explicitly specified otherwise.
3. Three-vectors are denoted by boldface letters, thus: $\mathbf{k}$.
4. The "particle physics" signature for metric tensors $(+,-,-,-)$ is used throughout.
5. For the Ricci tensor, we use the convention

$$R_{\mu\nu} = R^{\sigma}_{\mu\sigma\nu} = \Gamma^{\sigma}_{\mu\nu,\sigma} - \Gamma^{\sigma}_{\sigma\mu,\nu} + \Gamma^{\sigma}_{\mu\nu}\Gamma^{\rho}_{\sigma\rho} - \Gamma^{\sigma}_{\rho\mu}\Gamma^{\rho}_{\sigma\nu} \qquad \text{(A.1)}$$

Appendix B

Source Code

B.1 Introduction

In the course of this research, about ten different C programs were used to explore various aspects of the resonance and the resulting particle production. While each program may have had a different purpose, they all drew upon nearly identical subroutines; therefore, this appendix gives the annotated source code for one sample program which embodies most of the characteristics of the software package developed. (It is hoped that in the near future, the many disparate programs may be combined into one comprehensive package.)

B.2 A Typical Program

The source code for the progam `contourroot.c` is given below. It was written to solve for the locations of the contours in Figures 3.1 and 3.2. This represents a somewhat brute force method; however, the output generated from conventional contour-plotting programs was unsatisfactory—many of the fine details on the Mathieu equation stability diagram were either washed out or incorrectly

represented.

Conventional algorithms require a regularly spaced grid of values; the desired contours are then determined through interpolation. Unfortunately, the resolution of the generated contour plots is strongly dependent on the grid size. In our particular case, the narrow band regime was missed completely by conventional algorithms, as were the areas where the instability bands "grow into" one another. Reducing the grid size to a level sufficient to resolve such fine details led to time prohibitive computer runs; indeed, to cover the entire stability diagram at that resolution is unnecessary.

After a few unsuccessful experiments with non-uniformly spaced grids, a solution was found. In `contourroot.c`, the algorithm is as follows. For particular values of q, the critical exponent μ_k is determined as a (numerical) function of A_k. For the desired contour value μ_k^*, all roots of the equation

$$\mu_k(A_k) - \mu_k^* = 0 \tag{B.1}$$

within a specified range of A_k are found. The final contour plots may then be assembled in any plotting program. In this manner, multiple runs at different resolutions may be combined without problem.

This method is not without weaknesses. Most prominently, for contours which loop back on themselves, the turning point cannot easily be determined. In such cases, two succesive trials at progressively higher resolution are run in the region of "the gap;" however, the contours must eventually be joined through the introduction (by hand) of a linearly interpolated turning point. Additionally, the program's tabulation routine does not properly handle contours that exit from the area being considered. Once again, the data file must be reformatted (by hand) before it can be passed to a plotting program.

B.2.1 Libraries

To start with, we load in the standard libraries. These contain various function definitions not included in the basic C inplementation. For example, loading in `math.h` provides such functions as `sin()` and `exp()`.

```
#include <stdlib.h>
#include <stddef.h>
#include <math.h>
#include <time.h>
```

B.2.2 Parameters and Macros

In this portion of the code, we set various global parameters and macros. The standard syntax is `#define arg value`. Any time that the compiler encounters the term `arg`, it replaces it with `value`. This is useful for setting global parameters in the program, such as $\pi = 3.14159265\ldots$. Alternatively, one may use the same syntax to create macros (simple functions). As these functions are not called in the code, merely substituted at compile time, this leads to a somewhat more efficient program.

Let us now turn to the first set of parameters given below. `MAXSTP` is a cutoff used in the routine `odeint` which sets the maximum number of steps to be used in integrating an ODE to avoid infinitely long runs in the event of certain pathological equations. `TINY` is a *very* small number which is used in a number of routines to avoid occasional division by zero errors caused by roundoff within the machine.

```
#define MAXSTP 100000001
#define TINY 1.0e-301
```

The following parameters are used in the routine `stiff` in assessing whether the next step size should be increased or decreased.

```
#define SAFETY 0.91
#define GROW 1.51
#define PGROW -0.251
#define SHRINK 0.51
#define PSHRINK (-1.01/3.01)
#define ERRCON 0.12961
#define MAXTRY 5001
```

The next set of parameters are the Kaps-Rentrop parameters used in the Rosenbrock (generalized Runge-Kutta-Fehlberg) algorithm [1] employed by the function **stiff** in integrating a stiff set of ODE's.

```
#define GAM 0.2311
#define A21 2.01
#define A31 4.524708207361
#define A32 4.163528788601
#define C21 -5.071675338771
#define C31 6.020152728651
#define C32 0.1597506846731
#define C41 -1.8563436186771
#define C42 -8.505380858191
#define C43 -2.084075136021
#define B1 3.957503746631
#define B2 4.624892388361
#define B3 0.6174772638731
#define B4 1.2826129452681
#define E1 -2.302155402921
#define E2 -3.073634485391
#define E3 0.8732808018021
#define E4 1.2826129452681
#define C1X GAM
#define C2X -0.396296677520e-011
#define C3X 0.5507789395791
```

```
#define C4X -0.553509845700e-011
#define A2X 0.4621
#define A3X 0.8802083333331
```

The next set of parameters is used in the routine **stifbs** for two purposes: for controlling the extrapolation to the solution and for determining the size of the next step.

```
#define KMAXX 7
#define IMAXX (KMAXX + 1)
#define SAFE1 0.251
#define SAFE2 0.71
#define REDMAX 1.0e-51
#define REDMIN 0.71
#define SCALMX 0.11
```

The following parameters are used in the root finding algorithm **zbrent**, setting limits on how many iterations will be attempted before returning an error message if a root still has not been found.

```
#define ITMAX 100
#define EPS 3.0e-8
#define FPMIN 1.0e-30
```

The next two parameters are used in the error and memory allocation routines discussed in Sections B.2.5 and B.2.6 below.

```
#define FREE_ARG char *
#define NR_END 11
```

MAXROOT is a parameter which limits the maximum number of roots which our root solving algorithms can store.

```
#define MAXROOT 25
```

We now include a set of four macros. These are simple functions with simple purposes: **DSQR** returns the square of whatever value it is given, **DMAX** compares two arguments and returns the larger, **DMIN** compares two values and returns the smaller, and **SIGN** forces the sign of its first argument to be the same as that of its second.

```
static double dsqrarg;
#define DSQR(a) ((dsqrarg=(a)) == 0.0 ? 0.0 : dsqrarg*dsqrarg)

static double dmaxarg1,dmaxarg2;
#define DMAX(a,b) (dmaxarg1=(a),dmaxarg2=(b),(dmaxarg1)>(dmaxarg2) ?\
                   (dmaxarg1) : (dmaxarg2))

static double dminarg1,dminarg2;
#define DMIN(a,b) (dminarg1=(a),dminarg2=(b),(dminarg1)<(dminarg2) ?\
                   (dminarg1) : (dminarg2))

#define SIGN(a,b) ((b) >= 0.0 ? fabs(a) : -fabs(a))
```

The final two parameters are included for the user's convenience: **NVAR** specifies the number of variables in the system under consideration, while **PI** gives a value of π to 10 decimal places.

```
#define NVAR 21
#define PI 3.14159265351
```

B.2.3 Function Prototypes

Any program written in C requires the definition of function prototypes. Essentially, this informs the compiler of the structure of the particular function—what information it returns, how many and what type of arguments does it take, and the particular calling sequence which will be employed. This information is then

used by the compiler to check for errors in function calls, but does not impact on any of the algorithms themselves. Below we list all the function prototypes required for this program.

```
double *vector(long, long);
long *ivector(long, long);
double **matrix(long, long, long, long);
void free_vector(double *, long, long);
void free_ivector(long *, long, long);
void free_matrix(double **, long, long, long, long);
void nrerror(char []);

void odeint(double [], long, double, double, double,
        double, double, long *, long *,
        void (*)(double, double[], double[]),
        void (*)(double[],double[],long,double *,double,double,
                double[],double *, double *, void (*)(double,
                double[],double[])));
void stiff(double [], double [], long, double *, double, double, double [],
        double *, double *,
        void (*)(double, double [], double[]));
void stifbs(double [], double [], long, double *, double, double, double [],
        double *, double *,
    void (*)(double, double [], double []));
void simpr(double [], double [], double [], double **, long,
        double, double, long, double [],
   void (*)(double, double [], double []));
void ludcmp(double **, long, long *, double *);
void lubksb(double **, long, long *, double []);

void zbrak(double (*)(double), double, double, long, double [], double [],
        long *);
double zbrent(double (*)(double), double, double, double);
```

```
void derivs(double,double [],double []);
void jacobn(double,double [],double [],double **,long);

double wk2(double);
double muk(double);

void output(long,long);
```

B.2.4 Global Variables

While generally regarded as poor programming practice, global variables do have some useful aspects as well. In this case, multiple functions require access to the same information. As several of these functions, in turn, make calls to various other functions, the number of arguments which would have to be passed between functions starts to become unwieldy. As a result, a few key variables are set up here as global variables, to minimize the number of variables which have to be explicitly passed.

Some of the more important variables given below are `*xp` and `**yp`, the intermediate results of the integrated ODE, in addition to `Akf`, `q`, `qf`, `f`, which are the variables $A_k(f)$, $q(0)$, $q(f)$, and f of Chapter 3, respectively.

```
long kmax,kount;
double *xp,**yp,*params,dxsav;

double **d, *x;

double Akf,q,qf,f,con;
```

B.2.5 Error Handling

A simple routine to handle potential known problems with algorithms, adapted from one given in [2]. The function `nrerror(error message)` prints a diagnostic message to the screen and gracefully terminates the program in the event that the program encounters a known problem. For example, if an ODE requires more steps to solve than `MAXSTP` allows, `nerror` is invoked, informing the user and terminating the program.

```
void nrerror(char error_text[])
{
   fprintf(stderr,"Numerical Recipes run-time error...\n");
   fprintf(stderr,"%s\n",error_text);
   fprintf(stderr,"...now exiting to system...\n");
   exit(1);
}
```

B.2.6 Memory Allocation and Deallocation

Unlike other languages, such as FORTRAN, arrays in C cannot be given arbitrary ranges of indices. All arrays in C must have indices running from 0 to $n-1$. Unfortunately, many algorithms are written with sums from 1 to n, and making conversions back and forth between the two systems, while trivial, opens up many possibilities for programming errors which are usually hard to detect.

Fortunately, C allows for the creation of custom data structures, which we use to create arrays with arbitrary index ranges. The routines `*vector`, `*ivector`, and `**matrix`, which are adapted from [2], allocate, respectively, double precision vectors, long integer vectors, and double precision matrices with arbitrary ranges on indices. The functions `free_vector`, `free_ivector` and `free_matrix` are used to deallocate these data structures when they are no longer needed.

```
double *vector(long nl, long nh)
{
   double *v;

   v=(double *)malloc((size_t) ((nh-nl+1+NR_END)*sizeof(double)));
   if (!v) nrerror("allocation failure in vector()");
   return v-nl+NR_END;
}

long *ivector(long nl, long nh)
{
   long *v;

   v=(long *)malloc((size_t) ((nh-nl+1+NR_END)*sizeof(long)));
   if (!v) nrerror("allocation failure in vector()");
   return v-nl+NR_END;
}

double **matrix(long nrl, long nrh, long ncl, long nch)
{
   long i, nrow=nrh-nrl+1, ncol=nch-ncl+1;
   double **m;

   /* allocate pointers to rows */
   m=(double **) malloc((size_t)((nrow+NR_END)*sizeof(double *)));
   if (!m) nrerror("allocation failure 1 in matrix()");
   m+=NR_END;
   m-=nrl;

   /* allocate rows and set pointers to them */
   m[nrl]=(double *) malloc((size_t)((nrow*ncol+NR_END)*sizeof(double)));
   if (!m[nrl]) nrerror("allocation failure 2 in matrix()");
   m[nrl]+=NR_END;
```

```
    m[nrl]-=ncl;

    for(i=nrl+1; i<=nrh;i++) m[i]=m[i-1]+ncol;

    /* return pointer to array of pointers to rows */
    return m;
}

void free_vector(double *v, long nl, long nh)
{
    free((FREE_ARG) (v+nl-NR_END));
}

void free_ivector(long *v, long nl, long nh)
{
    free((FREE_ARG) (v+nl-NR_END));
}

void free_matrix(double **m, long nrl, long nrh, long ncl, long nch)
{
    free((FREE_ARG) (m[nrl]+ncl-NR_END));
    free((FREE_ARG) (m+nrl-NR_END));
}
```

B.2.7 The Main Routine

At long last, we have finally reached the main routine of our program. Here we initialise the variables, and collect the input from the user regarding the contour that we are searching, as well as the ranges of A_k and q in which we are interested. We then increment through various values of q, and use the root-finding algorithm **zbrak** to find the values of A_k at which μ_k takes on the value of the contour being searched for. We then export the results in tabular form.

```
main()
{
   long i,j,k,nq,num,maxroot,maxroot0;
   double resq,q0,mu,x,minAk,maxAk,*Ak1,*Ak2;

   kmax = 50000001;
   dxsav = 0.0011;

   xp = vector(1,kmax);
   yp = matrix(1,NVAR,1,kmax);
   params = vector(1,kmax);


   fprintf(stderr,"Please input resolution along q axis: ");
   scanf("%lf",&resq);

   fprintf(stderr,"Please input the initial q value: ");
   scanf("%lf",&q0);

   fprintf(stderr,"Please input number of steps along q axis: ");
   scanf("%ld",&nq);

   fprintf(stderr,"Please input a value for the imaginary fraction: ");
   scanf("%lf",&f);

   fprintf(stderr,"Please input a value for the minimum Ak: ");
   scanf("%lf",&minAk);

   fprintf(stderr,"Please input a value for the maximum Ak: ");
   scanf("%lf",&maxAk);

   fprintf(stderr,"Please input the contour being searched for: ");
   scanf("%lf",&con);
```

```
fprintf(stderr,"What is the maximum # of roots to find: ");
scanf("%ld",&maxroot0);

fprintf(stderr,"Please input a number of intervals in Ak: ");
scanf("%ld",&num);


Ak1 = vector(1,MAXROOT);
Ak2 = vector(1,MAXROOT);


for(i=0;i<=nq;i++) {

   maxroot = maxroot0;

   q = q0 + i*reso;
   qf = (1.0l-f*f)*q;

   printf("%14.10f",q);

   zbrak(muk,minAk,maxAk,num,Ak1,Ak2,&maxroot);

   for(j=1;j<=maxroot;j++){
      printf("%14.10f",zbrent(muk,Ak1[j],Ak2[j],1e-12));
   }

   printf("\n");
}


free_vector(xp,1,kmax);
free_matrix(yp,1,NVAR,1,kmax);
```

```
    free_vector(parame,1,kmax);
    free_vector(Ak1,1,MAXROOT);
    free_vector(Ak2,1,MAXROOT);

    return 0;
}
```

B.2.8 ODE Integration Routines

Perhaps the most important part of the code is the package of routines for the numerical integration of ordinary differential equations. Let us therefore look at all the routines which we use in this program.

The key routine is the controller, **odeint**. This is an adaptation of a routine given in [2]. It is an adaptive method, meaning that it has built in error estimation, and adjusts the step sizes taken to keep the total numerical error below a specified target value. It does not actually do the integration itself; instead, it calls a "stepper" routine which integrates the solution one step forward.

As **odeint** is one of the more important functions in the program, it is of some use to see what each of its arguments are. **ystart[]** is the set of initial conditions for the set of first order differential equations, with **nvar** telling the routine the number of variables in the system. **x1** and **x2** are the starting and ending times, respectively, for the system of equations. The desired error target is passed as **eps**. **h1** and **hmin** are user-specified values for the initial step size and the minimum allowed step size, respectively. The remaining two arguments, ***derivs** and ***stiff**, are pointers to functions—the system of differential equations to be solved and the "stepper" routine to be used, respectively.

```
void odeint(double ystart[], long nvar, double x1, double x2, double eps,
            double h1, double hmin, long *nok, long *nbad,
            void (*derivs)(double, double[], double[]),
```

```
        void (*stiff)(double[],double[],long,double *,double,double,
                      double[],double *, double *, void (*)(double,
                      double[],double[]))
{
   long nstp,i;
   double xsav,x,hnext,hdid,h;
   doubIe *yscal,*y,*dydx;

   yscal=vector(1,nvar);
   y=vector(1,nvar);
   dydx=vector(1,nvar);
   x=x1;
   h=SIGN(h1,x2-x1);
   *nok = (*nbad) = kount = 0;
   for (i=1;i<=nvar;i++)  y[i]=ystart[i];
   if (kmax > 0) xsav=x-dxsav*2.0;
   for (nstp=1;nstp<=MAXSTP;nstp++){
      (*derivs)(x,y,dydx);
      for (i=1;i<=nvar;i++){
         yscal[i]=DMAX(0.11,fabs(y[i]));
      }
      if (kmax > 0 && kount < kmax-1 && fabs(x-xsav) > fabs(dxsav)){
         xp[++kount]=x;
         for (i=1;i<=nvar;i++)  yp[i][kount]=y[i];
         xsav=x;
      }
      if ((x+h-x2)*(x+h-x1) > 0.0)  h=x2-x;
      (*stiff)(y,dydx,nvar,&x,h,eps,yscal,&hdid,&hnext,derivs);
      if (hdid == h) ++(*nok); else ++(*nbad);
      if ((x-x2)*(x2-x1) >= 0.0) {
         for (i=1;i<=nvar;i++) ystart[i]=y[i];
         if (kmax) {
            xp[++kount]=x;
```

```
            for (i=1;i<=nvar;i++)  yp[i][kount] = y[i];
        }
        free_vector(dydx,1,nvar);
        free_vector(y,1,nvar);
        free_vector(yscal,1,nvar);
        return;
      }
      if (fabs(hnext) <= hmin) nrerror("Step size too small in odeint");
      h=hnext;
    }
    nrerror("Too many steps in routine odeint");
}
```

As we are dealing with exponentially increasing solutions of the Mathieu equation in this program, we require routines that are suitable for so-called "stiff" differential equations. In essence, the local error inherent in any algorithm, if left unchecked, becomes exponentially amplified, and the algorithm becomes unstable. In such cases, the forward differencing scheme breaks down except for prohibitively small step sizes; therefore, we must use some form of *implicit* or backwards differencing scheme. (For a review of various differencing schemes, see, e.g., [3])

The function **stiff** given below is an version of the Kaps-Rentrop implementation of a Rosenbrock method [1] which has been adapted from [2]. In practice, this method is very reliable (avoiding problems with singular solutions which cause many other methods to fail), although not as fast as some other routines.

```
void stiff(double y[], double dydx[], long n, double *x, double htry,
           double eps, double yscal[], double *hdid, double *hnext,
           void (*derivs)(double, double [], double[]))
{
    void jacobn(double x, double y[], double dydx[], double **dfdy, long n);
    void lubksb(double **a, long n, long *indx, double b[]);
```

```
void ludcmp(double **a, long n, long *indx, double *d);

long i,j,jtry,*indx;
double d,errmax,h,xsav,**a,*dfdx,**dfdy,*dysav,*err;
double *g1,*g2,*g3,*g4,*ysav;

indx=ivector(1,n);
a=matrix(1,n,1,n);
dfdx=vector(1,n);
dfdy=matrix(1,n,1,n);
dysav=vector(1,n);
err=vector(1,n);
g1=vector(1,n);
g2=vector(1,n);
g3=vector(1,n);
g4=vector(1,n);
ysav=vector(1,n);
xsav=(*x);
for (i=1;i<=n;i++) {
   ysav[i]=y[i];
   dysav[i]=dydx[i];
}
jacobn(xsav,ysav,dfdx,dfdy,n);
h=htry;
for (jtry=1;jtry<=MAXTRY;jtry++) {
   for (i=1;i<=n;i++) {
      for (j=1;j<=n;j++) a[i][j] = -dfdy[i][j];
      a[i][i] += 1.01/(GAM*h);
   }
   ludcmp(a,n,indx,&d);
   for (i=1;i<=n;i++) {
      g1[i]=dysav[i]+h*C1X*dfdx[i];
   }
```

```
lubksb(a,n,indx,g1);
for (i=1;i<=n;i++) {
   y[i]=ysav[i]+A21*g1[i];
}
*x=xsav+A2X*h;
(*derivs)(*x,y,dydx);
for (i=1;i<=n;i++) {
   g2[i]=dydx[i]+h*C2X*dfdx[i]+C21*g1[i]/h;
}
lubksb(a,n,indx,g2);
for (i=1;i<=n;i++) {
   y[i]=ysav[i]+A31*g1[i]+A32*g2[i];
}
*x=xsav+A3X*h;
(*derivs)(*x,y,dydx);
for (i=1;i<=n;i++) {
   g3[i]=dydx[i]+h*C3X*dfdx[i]+(C31*g1[i]+C32*g2[i])/h;
}
lubksb(a,n,indx,g3);
for (i=1;i<=n;i++) {
   g4[i]=dydx[i]+h*C4X*dfdx[i]+(C41*g1[i]+C42*g2[i]+C43*g3[i])/h;
}
lubksb(a,n,indx,g4);
for (i=1;i<=n;i++) {
   y[i]=ysav[i]+B1*g1[i]+B2*g2[i]+B3*g3[i]+B4*g4[i];
   err[i]=E1*g1[i]+E2*g2[i]+E3*g3[i]+E4*g4[i];
}
*x=xsav+h;
if (*x == xsav) nrerror("Stepsize not significant in stiff");
errmax=0.0;
for (i=1;i<=n;i++) errmax=DMAX(errmax,fabs(err[i]/yscal[i]));
errmax /= eps;
if (errmax <= 1.0) {
```

```
            *hdid=h;
            *hnext=(errmax > ERRCON ? SAFETY*h*pow(errmax,PGROW) : GROW*h);
            free_vector(ysav,1,n);
            free_vector(g4,1,n);
            free_vector(g3,1,n);
            free_vector(g2,1,n);
            free_vector(g1,1,n);
            free_vector(err,1,n);
            free_vector(dysav,1,n);
            free_matrix(dfdy,1,n,1,n);
            free_vector(dfdx,1,n);
            free_matrix(a,1,n,1,n);
            free_ivector(indx,1,n);
            return;
        } else {
            *hnext=SAFETY*h*pow(errmax,PSHRINK);
            h=(h >= 0.0 ? DMAX(*hnext,SHRINK*h) : DMIN(*hnext,SHRINK*h));
        }
    }
    nrerror("Exceeded MAXTRY in stiff");
}
```

The function **stifbs** is our other "stepper" routine for stiff ODEs. It is an implementation of a Bulirsch-Stoer method [4] which has been modified for use with stiff ODEs as suggested by Bader and Deuflhard [5]. The particular version used here has been adapted from [2]. In practice, this method turns out to be extremely fast compared to **stiff**; however, due to the mechanics of the algorithm itself, it is expected to be less rugged in the event of pathological systems of equations.

As the two routines **stiff** and **stifbs** are implementations of two completely different algorithms, they act as a check on each other. For every set of initial conditions, two runs were performed—one with each of the "stepper" routines.

If the two give equivalent results, we can be confident that we have the actual solution to the system.

The Bulirsch-Stoer method relies upon an interesting extrapolation technique, and so calls two additional routines, **simpr** and **pzextr**. We will discuss these at a later point in the text.

```
void stifbs(double y[], double dydx[], long nv, double *xx, double htry,
            double eps, double yscal[], double *hdid, double *hnext,
    void (*derivs)(double, double [], double []))
{
   void jacobn(double x, double y[], double dfdx[], double **dfdy, long n);
   void simpr(double y[], double dydx[], double dfdx[], double **dfdy,
              long n, double xs, double htot, long nstep, double yout[],
      void (*derivs)(double, double [], double []));
   void pzextr(long iest, double xest, double yest[], double yz[],
               double dy[],long nv);

   long i,iq,k,kk,km;
   static long first=1,kmax,kopt,nvold=-1;
   static double epsold = -1.01,xnew;
   double eps1,errmax,fact,h,red,scale,work,wrkmin,xest;
   double *dfdx,**dfdy,*err,*yerr,*ysav,*yseq;
   static double a[IMAXX+1];
   static double alf[KMAXX+1][KMAXX+1];
   static long nseq[IMAXX+1]={0,2,6,10,14,22,34,50,70};
   long reduct, exitflag=0;

   d=matrix(1,nv,1,KMAXX);
   dfdx=vector(1,nv);
   dfdy=matrix(1,nv,1,nv);
   err=vector(1,KMAXX);
   x=vector(1,KMAXX);
   yerr=vector(1,nv);
```

```
ysav=vector(1,nv);
yseq=vector(1,nv);

if(eps !=epsold || nv != nvold) {
   *hnext = xnew = -1.0e291;
   eps1=SAFE1*eps;
   a[1]=nseq[1]+1;
   for (k=1;k<=KMAXX;k++)  a[k+1]=a[k]+nseq[k+1];
   for (iq=2;iq<=KMAXX;iq++) {
      for (k=1;k<iq;k++) {
 alf[k][iq]=pow(eps1,((a[k+1]-a[iq+1])/
            ((a[iq+1]-a[1]+1.01)*(2*k+1))));
      }
   }
   epsold = eps;
   nvold = nv;
   a[1] += nv;
   for (k=1;k<=KMAXX;k++)  a[k+1]=a[k]+nseq[k+1];
   for (kopt=2;kopt<KMAXX;kopt++) {
      if (a[kopt+1] > a[kopt]*alf[kopt-1][kopt])  break;
   }
   kmax=kopt;
}
h=htry;
for (i=1;i<=nv;i++)  ysav[i] = y[i];
jacobn(*xx,y,dfdx,dfdy,nv);
if (*xx != xnew || h!= (*hnext)) {
   first = 1;
   kopt = kmax;
}
reduct=0;
for(;;) {
   for (k=1;k<=kmax;k++) {
```

```
        xnew=(*xx)+h;
if (xnew == (*xx))  nrerror("Step size underflow in stifbs");
simpr(ysav,dydx,dfdx,dfdy,nv,*xx,h,nseq[k],yseq,derivs);

xest=DSQR(h/nseq[k]);
pzextr(k,xest,yseq,y,yerr,nv);
if (k != 1) {
   errmax = TINY;
   for (i=1;i<=nv;i++)  errmax=DMAX(errmax,fabs(yerr[i]/yscal[i]));
   errmax /= eps;
   km = k-1;
   err[km]=pow(errmax/SAFE1,1.0/(2*km+1));
}
if (k != 1 && (k >= kopt-1 || first)) {
   if (errmax < 1.0) {
      exitflag=1;
      break;
   }
   if (k == kmax || k == kopt+1) {
      red=SAFE2/err[km];
      break;
   }
   else if (k == kopt && alf[kopt-1][kopt] < err[km]) {
      red = 1.01/err[km];
      break;
   }
   else if (kopt == kmax && alf[km][kmax-1] < err[km]) {
      red = alf[km][kmax-1]*SAFE2/err[km];
      break;
   }
   else if (alf[km][kopt] < err[km]) {
      red=alf[km][kopt-1]/err[km];
      break;
```

```
    }
  }
      }
      if (exitflag)  break;
      red=DMIN(red,REDMIN);
      red=DMAX(red,REDMAX);
      h*=red;
      reduct=1;
    }
    *xx=xnew;
    *hdid=h;
    first=0;
    wrkmin=1.0e351;
    for (kk=1;kk<=km;kk++) {
      fact=DMAX(err[kk],SCALMX);
      work=fact*a[kk+1];
      if (work < wrkmin) {
        scale=fact;
wrkmin=work;
kopt=kk+1;
      }
    }
    *hnext=h/scale;
    if (kopt >= k && kopt !=kmax && !reduct) {
      fact=DMAX(scale/alf[kopt-1][kopt],SCALMX);
      if (a[kopt+1]*fact <= wrkmin) {
        *hnext=h/fact;
kopt++;
      }
    }
    free_vector(yseq,1,nv);
    free_vector(ysav,1,nv);
    free_vector(yerr,1,nv);
```

```
   free_vector(x,1,KMAXX);
   free_vector(err,1,KMAXX);
   free_matrix(dfdy,1,nv,1,nv);
   free_vector(dfdx,1,nv);
   free_matrix(d,1,nv,1,KMAXX);
}
```

The **simpr** function implements a *semi-implicit midpoint rule.* This is a scheme by which the partitioning of the interval under consideration can be carried out in such a way as to minimize function calls and to ensure the success of the extrapolation scheme in the Bulirsch-Stoer method.

```
void simpr(double y[], double dydx[], double dfdx[], double **dfdy, long n,
           double xs, double htot, long nstep, double yout[],
   void (*derivs)(double, double [], double []))
{
   void lubksb(double **a, long n, long *indx, double b[]);
   void ludcmp(double **a, long n, long *indx, double *d);

   long i,j,nn,*indx;
   double d,h,x,**a,*del,*ytemp;

   indx=ivector(1,n);
   a=matrix(1,n,1,n);
   del=vector(1,n);
   ytemp=vector(1,n);
   h=htot/nstep;
   for (i=1;i<=n;i++){
      for (j=1;j<=n;j++)  a[i][j] = -h*dfdy[i][j];
      ++a[i][i];
   }
   ludcmp(a,n,indx,&d);
   for (i=1;i<=n;i++) {
```

```
        yout[i]=h*(dydx[i]+h*dfdx[i]);
    }
    lubksb(a,n,indx,yout);
    for (i=1;i<=n;i++) {
        ytemp[i]=y[i]+(del[i]=yout[i]);
    }
    x=xs+h;
    (*derivs)(x,ytemp,yout);
    for (nn=2;nn<=nstep;nn++) {
        for (i=1;i<=n;i++) {
            yout[i]=h*yout[i]-del[i];
        }
        lubksb(a,n,indx,yout);
        for (i=1;i<=n;i++) {
            ytemp[i] += (del[i] += 2.01*yout[i]);
        }
        x += h;
        (*derivs)(x,ytemp,yout);
    }
    for (i=1;i<=n;i++) {
        yout[i]=h*yout[i]-del[i];
    }
    lubksb(a,n,indx,yout);
    for (i=1;i<=n;i++) {
        yout[i] += ytemp[i];
    }
    free_vector(ytemp,1,n);
    free_vector(del,1,n);
    free_matrix(a,1,n,1,n);
    free_ivector(indx,1,n);
}
```

The polynomial extrapolation used in the Bulirsch-Stoer method is imple-

mented in the routine **pzextr**. Given a set of data, which comprises a set of results for various values of the step size h, it extrapolates to the data value which should appear for $h = 0$, which corresponds to the theoretical maximum accuracy of the algorithm.

```
void pzextr(long iest, double xest, double yest[], double yz[], double dy[],
            long nv)
{
   long k1,j;
   double q,f2,f1,delta,*c;

   c=vector(1,nv);
   x[iest]=xest;
   for (j=1;j<=nv;j++) dy[j]=yz[j]=yest[j];
   if (iest == 1) {
      for (j=1;j<=nv;j++) d[j][1]=yest[j];
   } else {
      for (j=1;j<=nv;j++) c[j]=yest[j];
      for (k1=1;k1<iest;k1++) {
         delta=1.01/(x[iest-k1]-xest);
 f1=xest*delta;
 f2=x[iest-k1]*delta;
 for (j=1;j<=nv;j++) {
    q=d[j][k1];
    d[j][k1]=dy[j];
    delta=c[j]-q;
    dy[j]=f1*delta;
    c[j]=f2*delta;
    yz[j] += dy[j];
 }
      }
      for (j=1;j<=nv;j++)  d[j][iest]=dy[j];
   }
```

```
    free_vector(c,1,nv);
}
```

B.2.9 Matrix Algebra

The implicit differencing schemes used in integration of stiff differential equations require the solution of matrix equations. This is most successfully accomplished by decomposing the matrix **A** in question into lower and upper triangular matrices **L** and **U** such that

$$\mathbf{L} \cdot \mathbf{U} = \mathbf{A}. \tag{B.2}$$

Then the matrix equation $\mathbf{A} \cdot \mathbf{x} = \mathbf{b}$ becomes

$$(\mathbf{L} \cdot \mathbf{U}) \cdot \mathbf{x} = \mathbf{L} \cdot (\mathbf{U} \cdot \mathbf{x}) = \mathbf{b}. \tag{B.3}$$

It is then possible to proceed by solving first for the vector **y** such that

$$\mathbf{L} \cdot \mathbf{y} = \mathbf{b}, \tag{B.4}$$

and then solving

$$\mathbf{U} \cdot \mathbf{x} = \mathbf{y}, \tag{B.5}$$

as both of the preceding equations are triangular and can be solved rather simply through a prodecure called *(forward) backward substitution.*

The first of the two routines in this section, **ludcmp**, decomposes any nonsingular matrix into the product of a upper triangular and a lower triangular matrix. It is an adaptation of a routine given in [2].

```
void ludcmp(double **a, long n, long *indx, double *d)
{
    long i,imax,j,k;
    double big,dum,sum,temp;
    double *vv;
```

```
vv=vector(1,n);
*d=1.01;
for (i=1;i<=n;i++) {
   big=0.01;
   for (j=1;j<=n;j++) {
      if ((temp=fabs(a[i][j])) > big)  big=temp;
   }
   if (big == 0.01)  nrerror("Singular matrix in routine ludcmp");
   vv[i]=1.01/big;
}
for (j=1;j<=n;j++) {
   for (i=1;i<j;i++) {
      sum=a[i][j];
      for (k=1;k<i;k++)  sum -= a[i][k]*a[k][j];
      a[i][j] = sum;
   }
   big=0.01;
   for (i=j;i<=n;i++) {
      sum=a[i][j];
      for (k=1;k<j;k++) {
         sum -= a[i][k]*a[k][j];
      }
      a[i][j] = sum;
      if ( (dum=vv[i]*fabs(sum)) >= big) {
         big=dum;
         imax=i;
      }
   }
   if (j != imax) {
      for (k=1;k<=n;k++) {
         dum=a[imax][k];
         a[imax][k]=a[j][k];
```

```
            a[j][k]=dum;
          }
          *d = -(*d);
          vv[imax]=vv[j];
        }
        indx[j]=imax;
        if (a[j][j] == 0.01)  a[j][j]=TINY;
        if (j != n) {
          dum = 1.01/(a[j][j]);
          for (i=j+1;i<=n;i++) a[i][j] *= dum;
        }
      }
      free_vector(vv,1,n);
}
```

The second routine, **lubksb**, handles the backsubstitution portion of the process of solving a matrix equation. As with **ludcmp**, it is adapted from a routine given in [2].

```
void lubksb(double **a, long n, long *indx, double b[])
{
    long i,ii=0,ip,j;
    double sum;

    for (i=1;i<=n;i++) {
      ip=indx[i];
      sum=b[ip];
      b[ip]=b[i];
      if (ii) {
        for (j=ii;j<=i-1;j++) sum -= a[i][j]*b[j];
      } else if (sum) ii=i;
      b[i]=sum;
    }
```

```
    for (i=n;i>=1;i--) {
        sum=b[i];
        for (j=i+1;j<=n;j++)  sum -= a[i][j]*b[j];
        b[i]=sum/a[i][i];
    }
}
```

B.2.10 Root Finding Algorithms

In this particular portion of the code, we consider how to find the roots of the equation $\mu_k - \mu_k^* = 0$, where μ_k^* is the particular value of the contour which we wish to locate.

The first routine, **zbrak**, looks at a particular range of value for the variable in question. It divides the region into a set of equally sized bins, and identifies the ones which contain roots of the equation by taking the products of the endpoints of each bin and noting those which are negative.

```
void zbrak(double (*fx)(double), double x1, double x2, long n, double xb1[],
           double xb2[], long *nb)
{
    long nbb, i;
    double x,fp,fc,dx;

    nbb=0;
    dx=(x2-x1)/n;
    fp=(*fx)(x=x1);
    for (i=1;i<=n;i++) {
        fc=(*fx)(x += dx);
        if (fc*fp <=0.0) {
            xb1[++nbb] = x-dx;
  xb2[nbb] = x;
  if (*nb == nbb) return;
```

```
      }
      fp=fc;
   }
   *nb=nbb;
}
```

The function **zbrent** solves for a root within a certain interval via Brent's method [6]. This routine is an adaptation of one given in [2].

```
double zbrent(double (*func)(double), double x1, double x2, double tol)
{
   long iter;
   double a=x1, b=x2, c=x2, d, e, min1, min2;
   double fa=(*func)(a),fb=(*func)(b),fc,p,q,r,s,tol1,xm;

   if ((fa > 0.0 && fb > 0.0) || (fa < 0.0 && fb < 0.0))
      nrerror("Root must be bracketed in zbrent");
   fc=fb;
   for (iter=1;iter<=ITMAX;iter++) {
      if ((fb > 0.0 && fc > 0.0) || (fb < 0.0 && fc < 0.0)) {
         c=a;
fc=fa;
e=d=b-a;
      }
      if (fabs(fc) < fabs(fb)) {
         a=b;
b=c;
c=a;
fa=fb;
fb=fc;
fc=fa;
      }
      tol1=2.0*EPS*fabs(b)+0.5*tol;
      xm=0.5*(c-b);
```

```
      if (fabs(xm) <= tol1 || fb == 0.0) return b;
      if (fabs(e) >=tol1 && fabs(fa) > fabs(b)) {
         s=fb/fa;
if (a == c) {
   p=2.0*xm*s;
   q=1.0-s;
} else {
   q = fa/fc;
   r=fb/fc;
   p=s*(2.0*xm*q*(q-r)-(b-a)*(r-1.0));
   q=(q-1.0)*(r-1.0)*(s-1.0);
}
if (p > 0.0) q = -q;
p = fabs(q);
min1=3.0*xm*q-fabs(tol1*q);
min2=fabs(e*q);
if (2.0*p < (min1 < min2 ? min1 : min2)) {
   e=d;
   d=p/q;
} else {
   d=xm;
   e=d;
}
     } else {
        d=xm;
e=d;
     }
     a=b;
     fa=fb;
     if (fabs(d) > tol1)
        b += d;
     else
        b += SIGN(tol1,xm);
```

```
        fb=(*func)(b);
    }
    nrerror("Maximum number of iterations exceeded in zbrent");
    return 0.0;
}
```

B.2.11 User-Defined System Equations

Here's where the user finally tells the program what the system of interest is. These are user-supplied functions with specific purposes.

The first routine, **derivs**, states the differential equation in terms of a coupled system of first order ODEs.

```
void derivs(double x,double y[],double dydx[])
{
    dydx[1] = y[2];
    dydx[2] = -y[1]*(Akf - 2.01*qf*cos(2.01*x));
}
```

The next routine, **jacobn**, gives the Jacobian matrix for the system of differential equations. This is necessary for our case, as we are dealing with a set of stiff differential equations, so a standard forward-differencing scheme will not work. Instead, we use an implicit diffencing scheme, in which case, we require the Jacobian to solve the resulting matrix equation.

```
void jacobn(double x,double y[],double dfdx[],double **dfdy,long n)
{
    long i;

    dfdx[1] = 0.01;
    dfdx[2] = -y[1]*4.01*qf*sin(2.01*x);
```

```
    dfdy[1][1] = 0.01;
    dfdy[1][2] = 1.01;
    dfdy[2][1] = -(Akf - 2.01*qf*cos(2.01*x));
    dfdy[2][2] = 0.01;
}
```

The function **wk2** computes the value of ω_k^2. This is of particular use in computing various other quantities in the system, such as n_k, the number of particles in the particular Fourier mode χ_k. In this particular program, it is not used.

```
double wk2(double t)
{
    double result;

    result = Akf - 2.01 * qf * cos(2.01 * t);

    return result;
}
```

Our last routine, **muk**, computes the value of the critical exponent μ_k of a given solution of the Mathieu equation. To do this, we exploit a useful result which follows from Floquet's theorem (see, e.g., [7]). Given the "cosine-like" solution of the Mathieu equation, $w_1(z)$, where

$$w_1(z) = 1, \qquad w_1'(z) = 0, \tag{B.6}$$

then we have the result [8]

$$\cosh \mu\pi = w_1(\pi). \tag{B.7}$$

Our plan of attack is therefore clear: we numerically integrate the Mathieu equation, selecting $w_1(z)$ through the appropriate choice of initial conditions, and obtain the value $w_1(\pi)$. We then use (B.7) to find the value of the critical

exponent μ_k. Note that in the regions of the stability diagram where the solutions are stable, μ_k is complex. Therefore, in dealing with these regions, we simply solve for the imaginary component. The above algorithm is implemented in the function **muk** given below.

```
double muk(double arg)
{
   long nok,nbad;
   double mu,x,*y0;

   y0 = vector(1,NVAR);

   y0[1] = 1.01;
   y0[2] = 0.01;

   Akf = arg + 4.01*f*f*q - 2.01*q + 2.01*qf;

   odeint(y0,NVAR,0.01,PI,1.0e-141,1.0e-61,0.01,&nok,&nbad,derivs,stifbs);

   x = fabs(yp[1][kount]);

   if (x > 1.01)  {
      mu = log(x+sqrt(x*x - 1.0))/PI;
   } else {
      mu = -acos(x)/PI;
   }
   free_vector(y0,1,NVAR);

   return mu - con;
}
```

B.2.12 Output Routines

The routine output given below is only used in this particular code for diagnostic purposes. It allows for the visualisation of the numerical solutions to the differential equation being considered, in addition to providing some information about how many steps the ODE integrator was required to go back and correct. The latter information can help in setting appropriate error value targets for various runs.

```
void output(long nok, long nbad)
{
   long i,j;

   printf("Integration accomplished with %ld steps (%ld bad steps rejected)"
          ,nok+nbad,nbad);
   printf("\n\nParameters\n\n");
   printf("Ak = %6.3f, q = %6.3f, f = %6.3f\n",Akf,qf,f);

   printf("There are %ld sets of data points.\n",kount);

   for (i=1;i<=kount;i++)
   {
      printf("\n %10.6f %15.6e %15.6e", xp[i],yp[1][i],params[i]);
   }
   printf("\n");
}
```

References

[1] P. Kaps and P. Rentrop, Numerische Mathematik **33** (1979), 55.

[2] W. H. Press, S. A. Teukolsky, W. T. Vetterling, and B. P. Flannery, *Numerical Recipes in C: The Art of Scientific Computing*, 2nd ed., (Cambridge Univ. Press, Cambridge, 1992).

[3] D. Kincaid and W. Cheney, *An Introduction to Numerical Analysis*, 2nd ed., (Brooks/Cole, Pacific Grove, California, 1996).

[4] J. Stoer and R. Bulirsch, *Introduction to Numerical Analysis*, (Springer Verlag, New York, 1980).

[5] G. Bader and P. Deuflhard, Numerische Mathematik **41** (1983), 373.

[6] R. P. Brent, *Algorithms for Minimization without Derivatives*, (Prentice Hall, Englewood Cliffs, New Jersey, 1973).

[7] E. L. Ince, *Ordinary Differential Equations*, (Dover, New York, 1956).

[8] F. M. Arscott, *Periodic Differential Equations*, (MacMillan, New York, 1964).